HOT HYDROGEN TESTING OF REFRACTORY METALS AND CERAMICS

Ralph Zee, Bryan Chin and Jon Cohron
Materials Engineering Program
Auburn University
Auburn, AL 36849

Table of Contents

HOT HYDROGEN TESTING OF REFRACTORY METALS AND CERAMICS

Ralph Zee, Bryan Chin and Jon Cohron
Materials Engineering Program
Auburn University
Auburn, AL 36849

I. Abstract of the Investigation

The objective of this investigation is to develop a technique with which refractory metal carbide samples can be exposed to hydrogen containing gases at high temperatures, and to use various microstructural and analytical techniques to determine the chemical and rate processes involved in hydrogen degradation in these materials. Five types of carbides were examined including WC, NbC, HfC, ZrC and TaC. The ceramics were purchased and were all monolithic in nature. The temperature range investigated was from 850 to 1600°C with a hydrogen pressure of one atmosphere. Control experiments, in vacuum, were also conducted for comparison so that the net effects due to hydrogen could be isolated. The samples were analyzed prior to and after exposure. Gas samples were collected in selected experiments and analyzed using gas chromography. Characterization of the resulting microstructure after exposure to hydrogen was conducted using optical microscopy, x-ray diffraction, scanning electron microscopy and weight change. The ceramics were purchased and

were all monolithic in nature. It was found that all samples lost weight after exposure, both in hydrogen and vacuum. Results from the microstructure analyses show that the degradation processes are different among the five types of ceramics involved. In addition, the apparent activation energy for the degradation process is a function of temperature even within the same material. This indicates that there are more than one mechanism involved in each material and that the mechanisms are temperature dependent.

II. Introduction

Advanced propulsion systems for space exploration will require materials to perform at ultra high temperatures and in hostile environments. In many applications, temperatures in excess of 2000°C in combination with corrosive hydrogen gas are required. As a result, interest in high temperature materials has grown in the past decade. The degradation behavior and various mechanical and electrical properties of refractory metals (such as W, Ta and Mo) and ceramics (carbides, oxides and nitrides) has been the subject of numerous investigations. An extensive data base exists for the interaction of hydrogen with materials at temperatures below 1000°C. These studies investigated the diffusivity, hydride formation, and weight loss during hydrogen exposure. However, a literature survey of the subject reveals that little effort has been devoted to the higher temperature interaction of hydrogen with metals and ceramics. This is due to the experimental difficulty involved in the heating and control of specimens at these high temperatures. Consequently there is an urgent need for a fundamental study of the degradation mechanism of materials in hydrogen at ultra high temperatures.

Much of the understanding of the effects of hydrogen in materials has been obtained from experiments conducted at lower temperatures than those proposed here. Most of the research in high temperature has been limited to thermodynamic calculations based on data extrapolated from low temperature regimes. Results from these studies can be effectively used to design the experiments needed at ultra high

temperatures and to interpret the data obtained from these experiments.

Hydrogen degradation is a complex process and it strongly depends on temperature. Hydrogen can exist in a solid in three forms: solution, hydride and gas. At concentration levels below the solubility limit, hydrogen atoms occupy the interstitial sites of the matrix and solution strengthen the material. At supersaturation levels, hydride may be formed and most metal hydrides are very brittle leading to hydrogen embrittlement. Under irradiation environment, the presence of hydrogen (in supersaturated levels) may also result in gas bubble formation which has been observed experimentally under ion irradiation.

One particular feature of hydrogen is that it is extremely mobile. Activation energy for diffusion of hydrogen atom in most metals is on the order of 10 kcal/mole with a pre-exponential coefficient of approximately 10^{-2} cm^2/s. At 3000 K, this corresponds to a diffusion length of greater than 3 mm in 1 minute. This implies that diffusion is not the rate limiting step in the ultrahigh temperature range of interest in this study. It is therefore appropriate to assume that no concentration gradient exists in the bulk throughout the experiment making interpretation of the results much simplified.

The diatomic hydrogen gas (H_2) in the environment does not react directly with the material due to its chemical stability. Even at 4000°C, the fraction of atomic hydrogen in the hydrogen gas is negligible due to the high binding energy of H_2 (104 kcal/mole or 4.5 eV/bond) which is much larger than the thermal energy available.

This means that the first interactive process must be the dissociation of the molecules into atomic hydrogen at the surface. This is followed by the rapid diffusion into the bulk as discussed in the last paragraph.

Hydrogen degradation at low and intermediate temperatures occurs mainly as a result of hydride formation due to low hydrogen solubility. However, at the ultra high temperature of interest here, the solubility is extremely high and no hydrides will be formed even at considerable hydrogen concentrations. This is a reasonable assumption if the hydrogen pressure is not very high. Under this condition, the hydrogen atoms will occupy the interstitial sites of the material and their effect will be to alter the atomic bond strength which in term affects the stability of the materials. However when the material cools, hydrogen may become trapped. Depending on the cooling rate and conditions, the system will either hydride or be supersaturated with hydrogen which is thermodynamically unstable. Both conditions can lead to material degradation. In ceramics especially where carbon, nitrogen and oxygen are present, hydrogen may also react with these elements to form hydrocarbons which will then evolve as gases resulting in a large weight loss.

This research addresses both the physical and chemical aspects of the interaction of hydrogen with ceramic materials. The study is designed to provide a basic understanding of the forces that govern the hydrogen degradation in materials at high temperatures. The main objectives are to develop a system which can expose ceramic materials to hydrogen at high temperatures and to determine the governing

mechanisms for hydrogen degradation based on microstructural analyses using electron spectroscopy, scanning electron microscopy, x-ray diffraction and other techniques.

III. Research

A. Materials Selection

The materials chosen for this research were ceramics and were acquired from two main sources. Sixty grams of HfC and 150 grams of ZrC were obtained from Pure-Tech Inc. Also 29 grams of NbC, 4.5 grams of WC and 20 grams of TaC were secured from the High Temperature Materials Laboratory (HTML) of Oak Ridge National Laboratory (ORNL). The three materials obtained from ORNL were 60%, 86% and 94% of the theoretical density respectively. Due to the high porosity of the samples, in particular NbC and WC, the optical microscopy of the as-received samples was impaired. However, with the use of the x-ray diffraction (XRD) and energy dispersion spectroscopy (EDS) the as-received specimens were positively identified and used as a reference for the post reaction analysis.

B. Experimental System Development

The ultrahigh temperatures needed combined with the potential for uncontrolled detonation of the hydrogen gas required careful design and operation of experiments in this investigation. A short description of the method used for heating, the experimental chamber, the sample preparation and the experimental procedure are as

follows:

B.1. Heating System: The 50kW induction generator at Auburn University was used for this purpose. Because of the range of susceptibility in the ceramics that where investigated in this study, direct induction heating of specimens was not feasible. Furthermore at the temperatures of interest, reaction of the specimens with any crucible or support would occur readily. It is therefore imperative that the experimental geometry minimizes physical contact of the specimens with the surrounding. A Nb-1Zr tube was used as the susceptor which was heated by the induction field. The thickness of the tube was approximately 0.01" which was sufficient to absorb most of the RF power. The specimens were in the form of small pieces and were placed inside the tube. Efforts were made to keep the shape of the samples cubical and relatively the same size. This is important to ensure that proper comparison can be made based on volume and areal normalization. The specimens were then heated by radiation, convection and conduction of the heat generated in the susceptor. Heating of the Nb-1Zr susceptor instead of direct induction heating of the specimens also provided a direct correlation between RF power and temperature which was independent of specimen properties. This direct correlation facilitates a simple means for temperature calibration. Temperature during hot hydrogen exposures was determined using pyrometry and tungsten-rhenium thermocouples. With the pyrometer a correction was made for surface emissivity.

B.2. Experimental Chamber: A double wall vacuum chamber was used to carry out the experiments. Figures 1 and 2 respectively show a photograph and a schematic drawing of the system. The inner chamber was a 3/4 inch diameter Nb-1Zr tube and was also used as the susceptor for the induction field. The tube was typically seven to eight inches long and was tungsten inert gas (TIG) welded at one end. The tube was replaced periodically because of degradation due to thermal and hydrogen embrittlement and oxidation. The use of the TIG weld eliminated the necessity to produce a vacuum tight swage-lock at one end. The other end was connected to a stainless steel gas/exit line using a swage-lock connection. The inner chamber was enclosed in a stainless steel containment vessel (outer chamber) which was significantly larger. Since hydrogen was only introduced into the inner chamber, this chamber was kept small compared to the outer chamber due to safety considerations. The outer chamber was basically a large stainless steel "tee". On the outer chamber the three ports were designated back, front and top. Each port was 16 inches in diameter. The back port contained the vacuum line to the main pumping system. The front port contained the feedthroughs for the induction coils, thermocouples, pressure sensor, hydrogen gas line, and the venting line to the chamber. The top port was removable and was used to place the samples inside the inner chamber. It also contained the viewport which was utilized by the pyrometer. The viewport also served as a safety device. The viewport was a flat circular piece of quartz that was slightly larger than the port hole in the top plate. The quartz was sealed against the

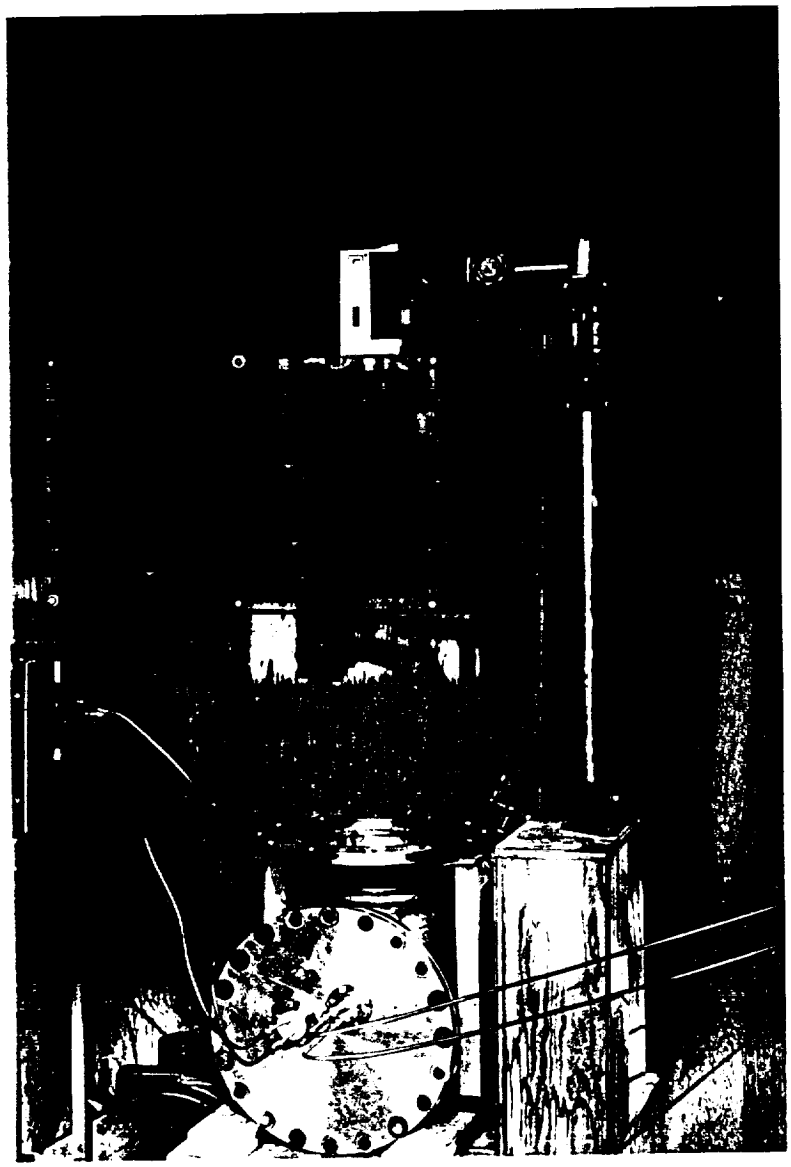

Figure 1. Photograph of hydrogen exposure system.

Schematic of Chamber

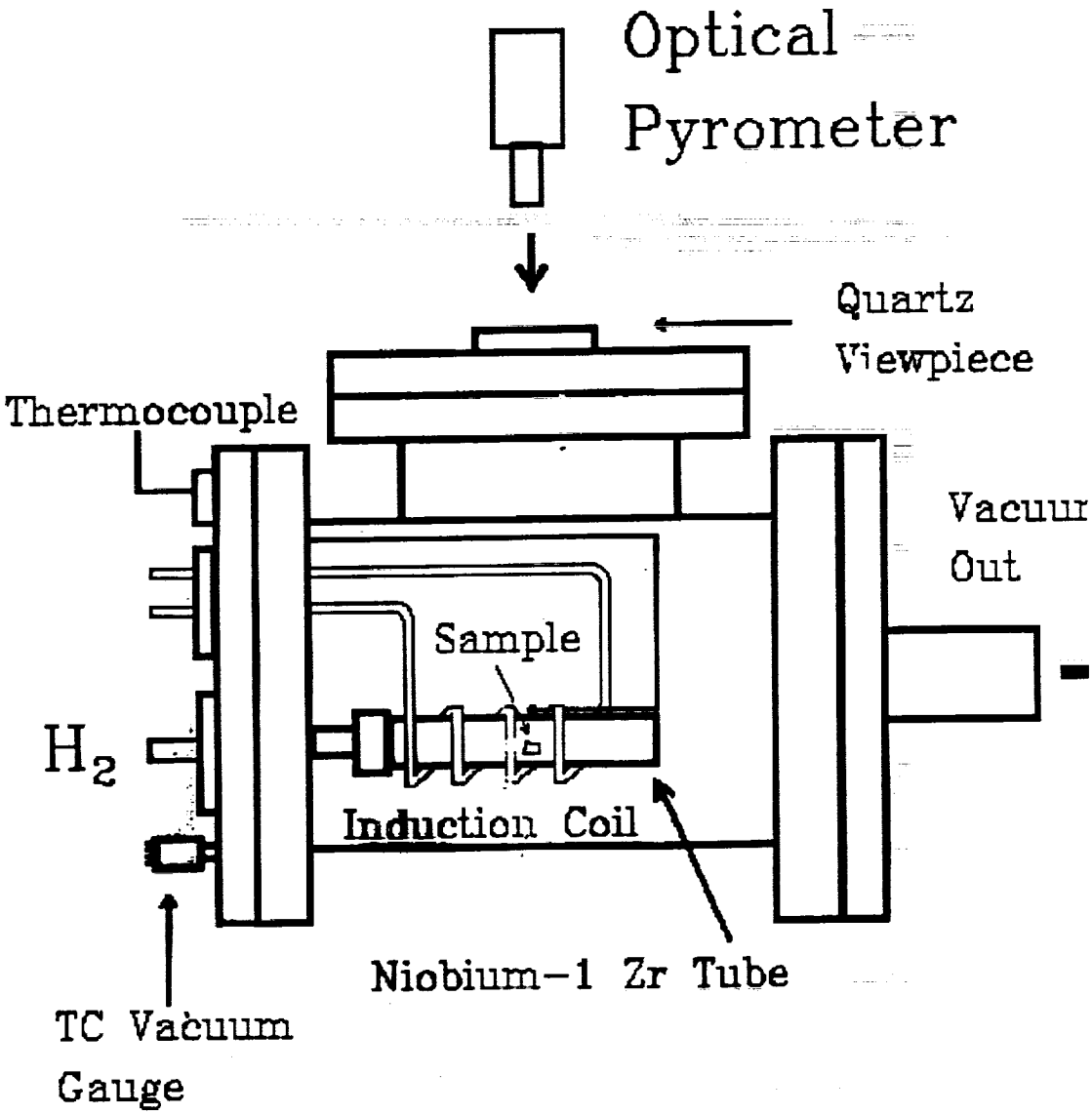

Figure 2. Schematic drawing of the hydrogen exposure system showing all the essential components.

face plate by the vacuum inside the chamber and vacuum grease. This viewport also served as a pressure relief device, if there was an undesirable pressure buildup in the outer chamber.

B.3. Sample Preparation: The samples were first cut into small pieces of the desired shape using an electro-discharge machine (EDM). The samples were then cleaned in acetone ultrasonically and then dried in a vacuum of one millitorr for 24 hours. This procedure insures that there no trapped liquid which would outgas during the reaction remains. The outgassing would cause false readings on weight change measurements. Once the sample was dry, its weight was precisely measured using an electrobalance. The color and shape of the specimens were also documented.

B.4. Experimental Procedures: Once the samples were properly prepared, they were placed in the inner chamber. The inner chamber was then secured to the hydrogen gas line, via swage-lock fittings, inside the larger outer chamber. When fitting the Nb-1Zr tube inside the outer chamber, care was taken to insure that the samples remained in the hot zone. The hot zone is the region along the tube which is inside the induction field and is approximately 4 inches in length. The temperature of this zone was monitored during the coarse of the experiments and assumed to be the temperature of the specimens. There were two devices used to monitor this temperature. The first device was a C-type thermocouple (W-Re). It was attached to

the outside of the Nb-1Zr tube in the hot zone. The thermocouple leads passed through the front plate of the outer chamber and was connected to a digital readout externally. The second device used to monitor the temperature was an optical pyrometer. The pyrometer camera was focused to the same region as the thermocouple. The pyrometer was interfaced with a computer so that the continuous temperature readings can be permanently recorded. Two devices were used in case of failure by one or the other and to enhance the accuracy of the temperature measured.

After the inner chamber was secured, it was tested for leaks using a Varian helium leak detector. Once the inner chamber had been leak checked and found to be safe, the top plate was mounted and bolted shut. The outer chamber was also leak checked using the Varian detector. Both the inner and outer chamber pressure was measured continuously throughout the experiment to insure that no significant hydrogen leakage was present for safety reasons. After both chambers were secured and found to be safe and free from leaks, the system was purged and then heated.

The purging procedure consisted of obtaining the best possible vacuum on the outer and inner chambers. Once a good vacuum was attained, the inner chamber was pressurized with hydrogen and re-evacuated. This was done to minimize the amount of residual oxygen in the inner chamber. After the inner chamber had been sufficiently purged, it was filled with hydrogen to one atmospheric pressure. The inner chamber was then ready to be heated. Heating to the desired temperature was accomplished with care (with slow controlled rates) so as not to thermally shock the

system. Thermal shock to the system can cause rupture of the Nb-1Zr tube which in turn causes premature termination of the experiment.

C. Experimental Results

To ensure proper interpretation of the effects of hydrogen on microstructures, it is imperative to first determine the structure of the as-received materials so that meaningful comparisons can be made. The analyses used for verification and initial condition were x-ray diffraction (XRD), energy dispersion spectroscopy (EDS) and optical microscopy. The XRD confirmed, from the Joint Community of Pattern Diffraction Standards (JCPDS) files, that the materials were indeed what had been ordered and purchased. The SEM (using the EDS option) also confirmed the material compositions. Results from optical microscopy show high porosity in all materials received in accord with the density measurements conducted by the suppliers (figures 3, 4 and 5). High porosity is inherent to the hot isostatic pressing process that was used for the fabrication of these ceramics.

Theoretical Ellingham diagrams were generated which will be used to interpret the possible reactions involving the ceramics and the atmosphere of interest (which includes oxygen and hydrogen). This energy information is shown in figures 6 thru 10.

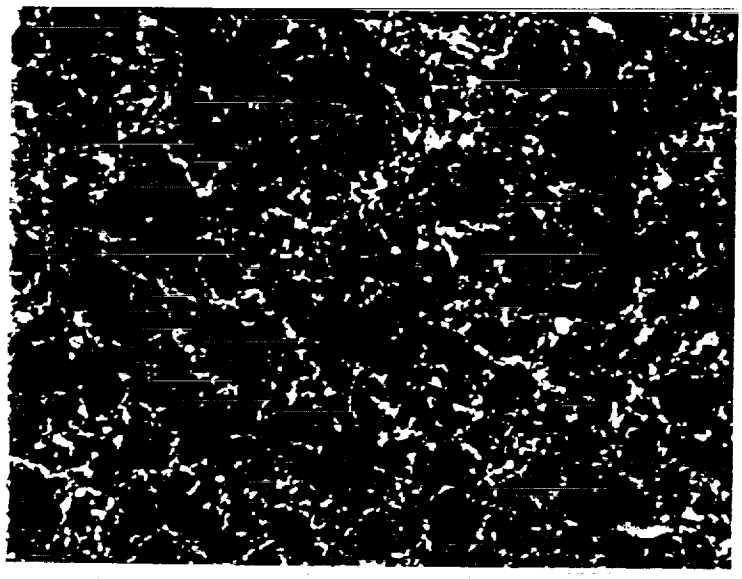

NbC 200X

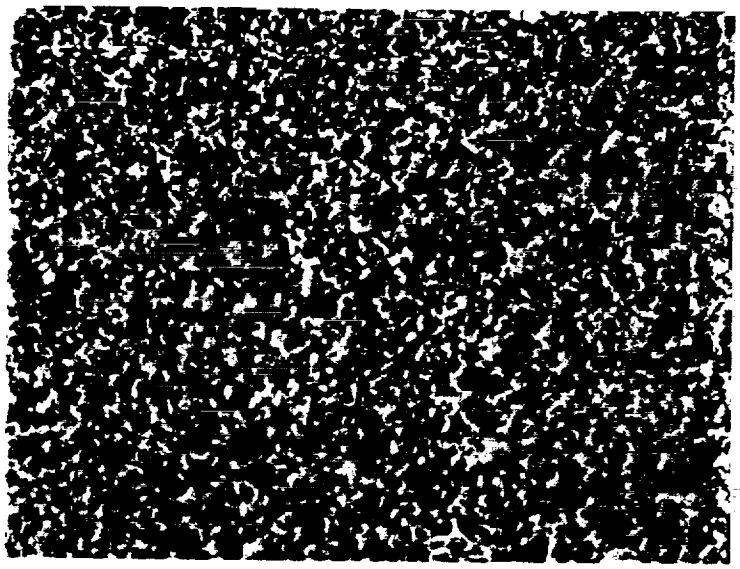

TaC 200X

Figure 3. Microstructure of NbC and TaC in the as-received condition obtained using an optical microscope.

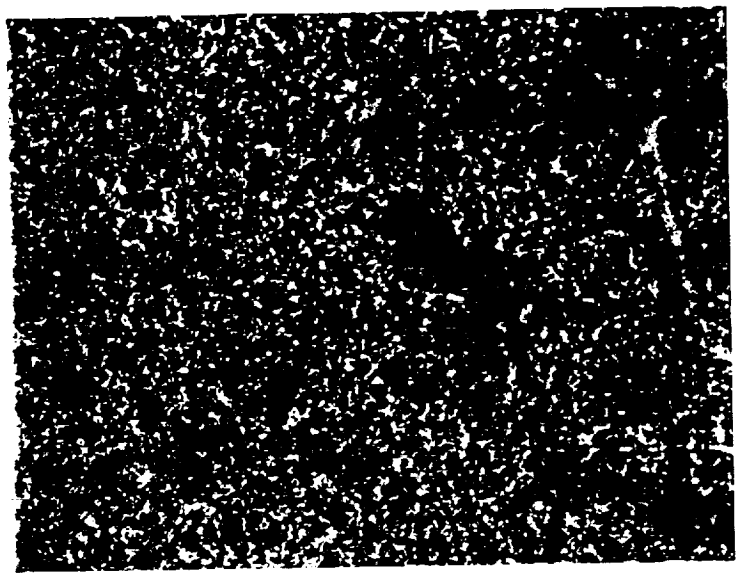

WC 200X

Figure 4. Microstructure of WC in the as-received condition obtained using an optical microscope.

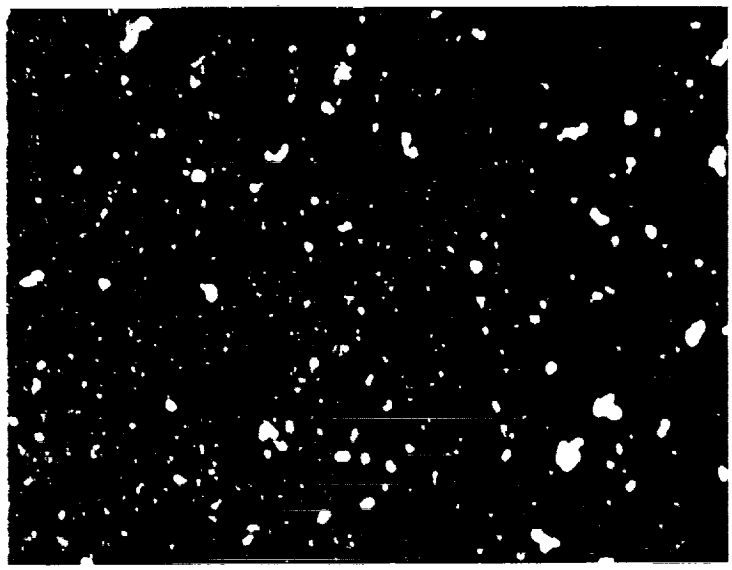

ZrC 200X

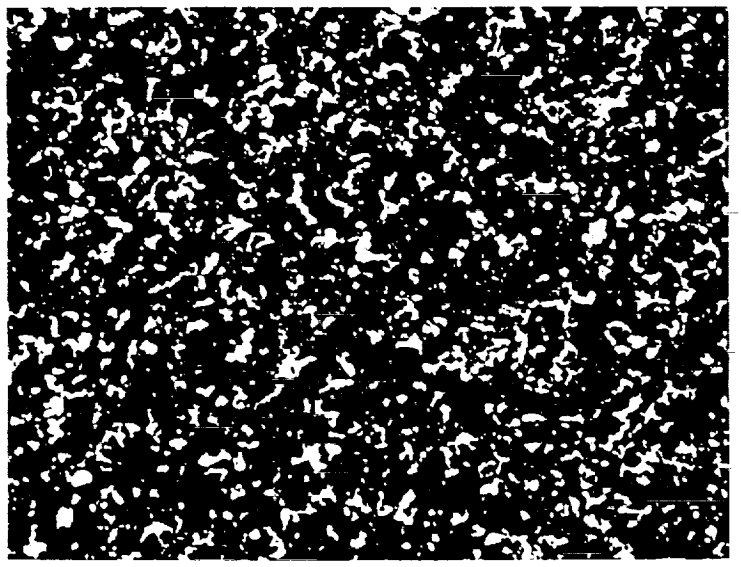

HfC 200X

Figure 5. Microstructure of ZrC and HfC in the as-received condition obtained using an optical microscope.

Ellingham Diagram

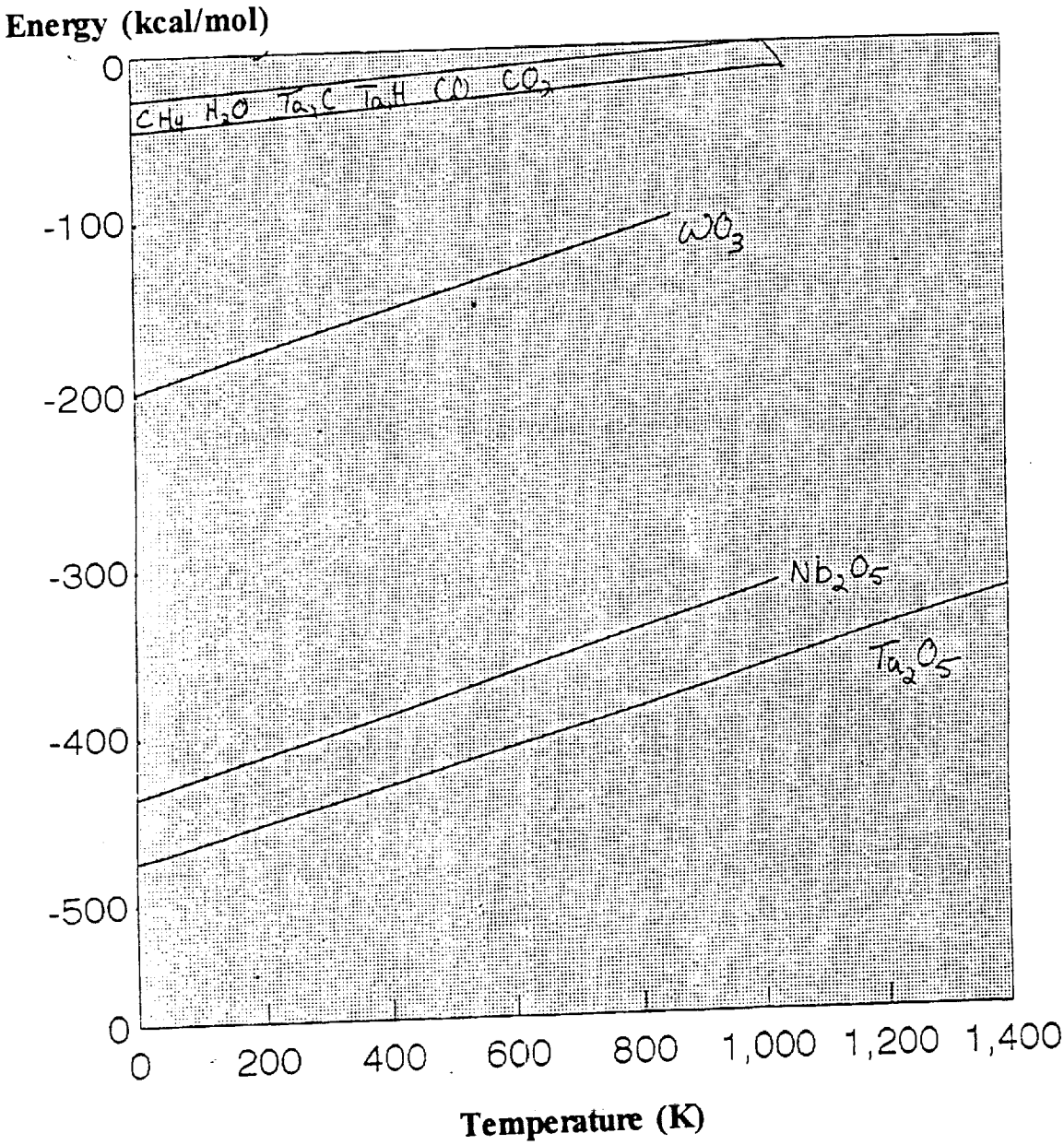

Figure 6. Ellingham diagram for the formation of relevant compounds.

Ellingham Diagram

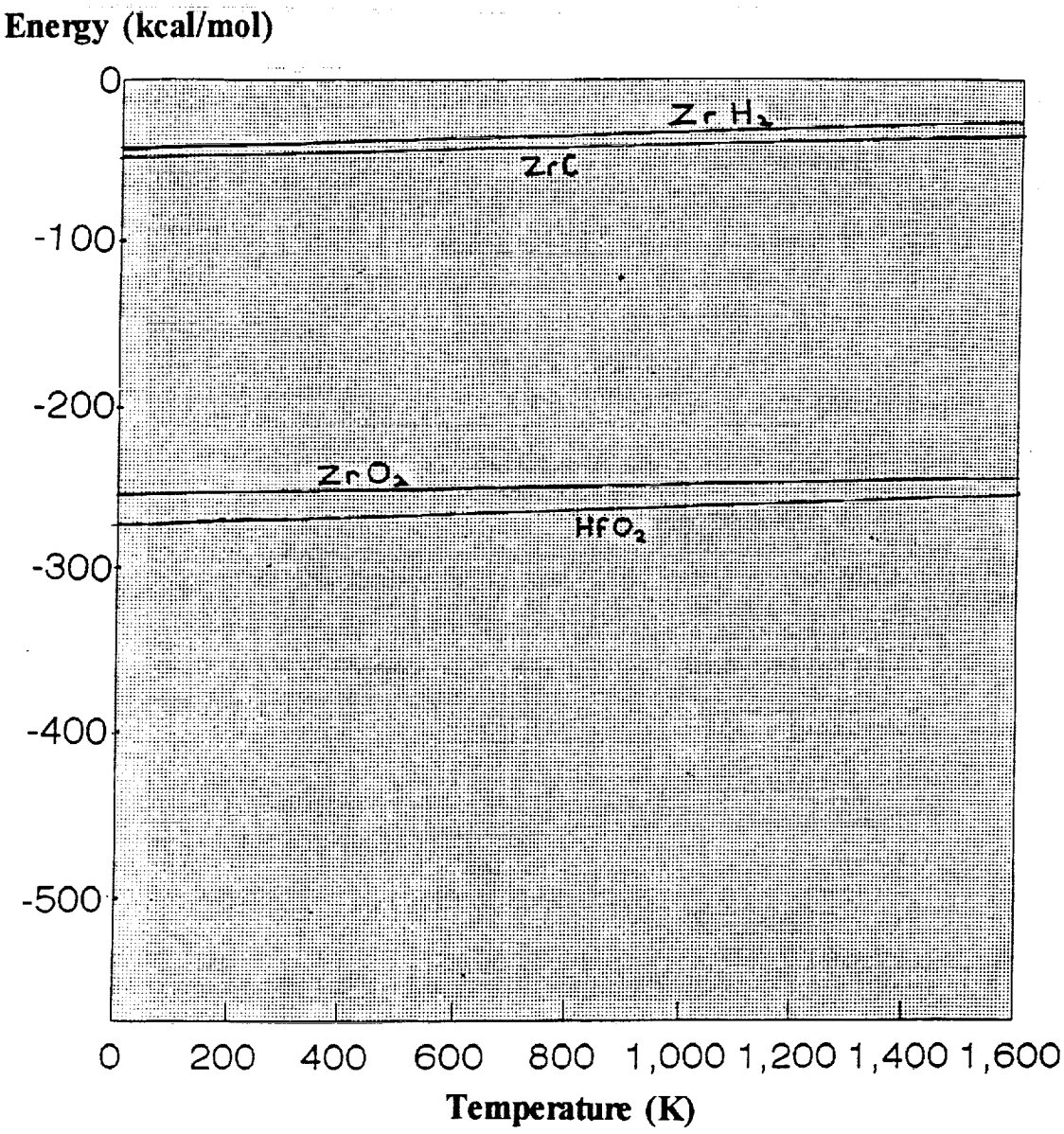

Figure 7. Ellingham diagram for the formation of relevant compounds.

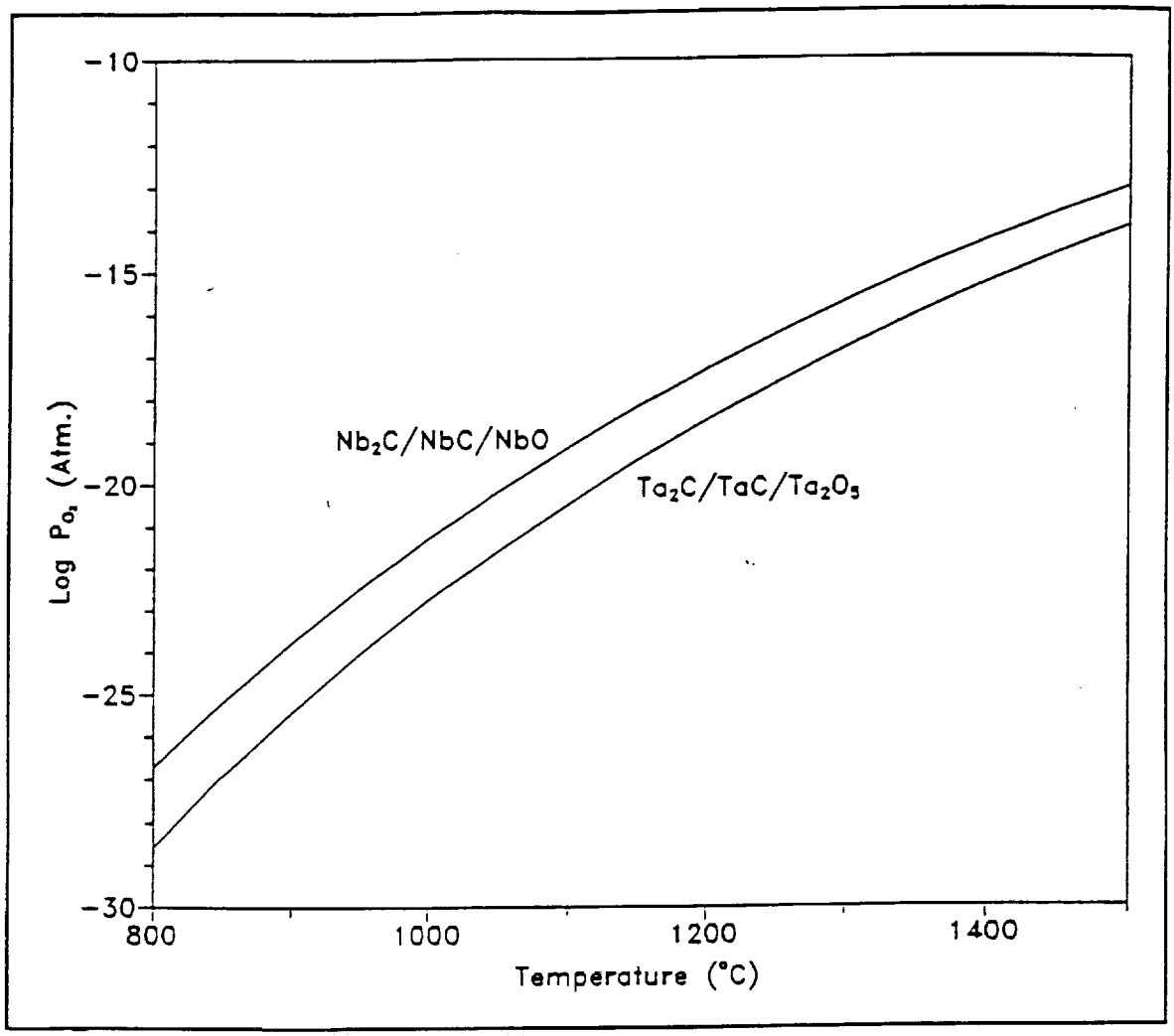

Figure 8. Equilibrium oxygen partial pressure for the oxidation of Nb_2C/NbC and Ta_2C/TaC.

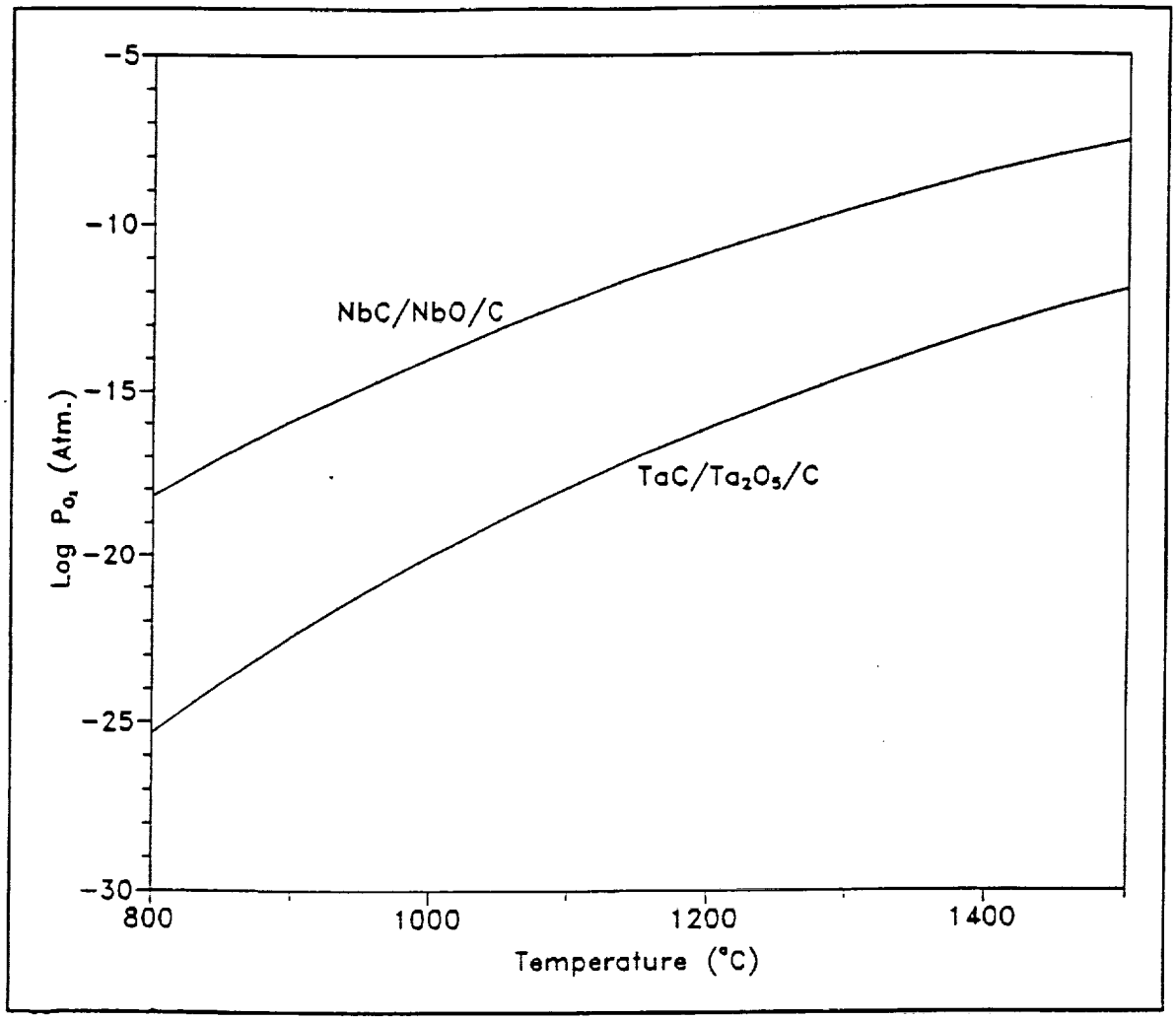

Figure 9. Equilibrium oxygen partial pressure for the oxidation of NbC and TaC.

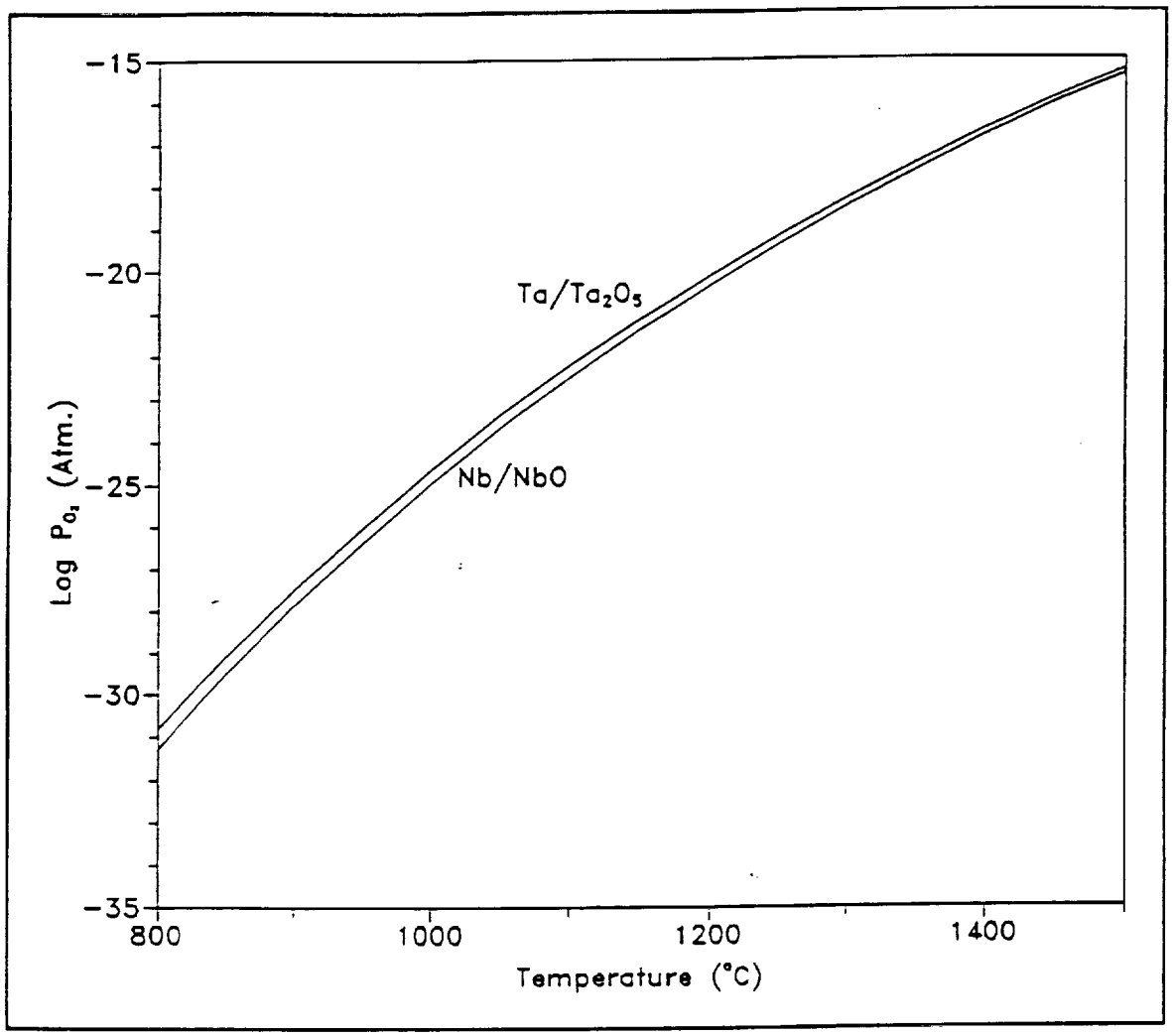

Figure 10. Equilibrium oxygen partial pressure for the oxidation of Nb and Ta.

Experimental research in this study can be divided into two primary forms. The first was for isochronal experiments and the other was for isothermal studies, both of which were conducted at one atmospheric pressure of hydrogen. In all cases, controlled experiments were also conducted without hydrogen. These experiments are referred to as dry runs. The dry runs were made so that direct comparison can be made with hydrogen runs to elucidate the exact role of hydrogen on the degradation process at elevated temperatures. Tables 1a and 1b summarize the experimental conditions of all the samples processed in this study. Extensive x-ray diffraction analysis was conducted on all the samples process. The spectra obtained are given in the Appendix section of this report. The figure numbers are chosen in such a way that the first entry refers to the type of material investigated and the second entry refers to the run number (cross reference with Tables 1a and 1b). For example, figure TaC.1 refers to the spectrum obtained from the TaC sample processed at 1165 K for 1 hour in a hydrogen atmosphere. The figure numbers are given at the top of the spectra for each specimen.

Table 1.a. Summary of Experimental Conditions

Group One	Temperature(K)	Time(hrs)	Atmosphere
TaC, NbC, WC			
Run #1	1165	1	Hydrogen
Run #2	1147	1	Vacuum
Run #3	1457	1	Hydrogen
Run #4	1555	1	Hydrogen
Run #5	1534	1	Vacuum
Run #6	1326	1	Hydrogen
Run #7	1273	1	Vacuum
Run #8	1221	1	Hydrogen
Run #9	1390	1	Hydrogen
Run #10	1289	1	Hydrogen
Run #11	1364	1	Hydrogen
Run #12	1536	2	Hydrogen
Run #13	1330	2	Hydrogen
Run #14	1320	8	Vacuum
Run #15	1333	8	Hydrogen
Run #16	1355	16	Hydrogen
Group Two			
HfC, ZrC			
Run #6	1427	1	Hydrogen
Run #7	1273	1	Vacuum
Run #8	1223	1	Hydrogen
Run #9	1443	1	Hydrogen
Run #10	1523	1.5	Hydrogen
Run #11	1613	1	Hydrogen
Run #12	1428	1	Vacuum
Run #13	1420	1	Hydrogen
Run #14	1492	8	Hydrogen
Run #15	1420	1	Hydrogen

Table 1.b. Percent Weight Loss

Group One	TaC	NbC	WC
Run #1	.03104	.19500	.07780
Run #2	.06221	.39640	.10315
Run #3	.02383	.81400	.04815
Run #4	.06720	1.1410	.04340
Run #5	.06086	.55000	.04440
Run #6	.04390	1.6700	.26100
Run #7	.01948	1.8190	.24100
Run #8	.12116	1.8800	.26870
Run #9	.05150	.50100	.03478
Run #10	.03369	1.9009	.44350
Run #11	.02845	.19300	.21490
Run #12	------	1.5020	.26280
Run #13	.08675	.45780	.16010
Run #14	.02451	.14070	.28920
Run #15	.01449	.31508	.93990
Run #16	.12650	.38412	.13630
Group Two	**HfC**	**ZrC**	
Run #6	2.3080	2.6990	
Run #7	1.9220	4.2140	
Run #8	1.8490	2.6810	
Run #9	.51700	.07200	
Run #10	.31000	.37000	
Run #11	.50500	1.1060	
Run #12	0.0000	.03600	
Run #13	4.8260	-.1280 (gain)	
Run #14	.43500	-1.055 (gain)	
Run #15	1.1140	.70700	

C.1. Isochronal Experiments: All the initial experiments were conducted for a period of one hour. The variable in the experiment was the temperature at which the reaction was carried out. The temperature of the experiments ranged from 850 to 1600°C. The samples were subdivided into two groups; one consisting of NbC, TaC, and WC the other HfC and ZrC. Samples in the first group (TaC, NbC and WC) were received prior to those of the second group (HfC and ZrC). Therefore, more extensive experiments were conducted for the former. Nevertheless, both groups were analyzed in the same manner.

After each experiment, the first data collected was the weight change. The weight in the samples from the first group all decreased (lost weight). In the second group two samples experienced a weight increase whereas all the others lost weight. The two samples that gained weight were the first two samples exposed in the study and were dried in an air oven prior to exposure. It is believed that this process led to the formation of an oxide layer on the surface which resulted in the anomleous behavior of weight gain. Results from these two samples will not be included in the analyses. All other samples were dried in vacuum.

Figures 11 to 14 show the weight change of the samples as a function of temperature for the two groups of materials. These figures were replotted in the Arrhenius manner in order to determine if the processes were thermally activated. These are shown in figures 15 to 18 for the five specimens in the two groups of

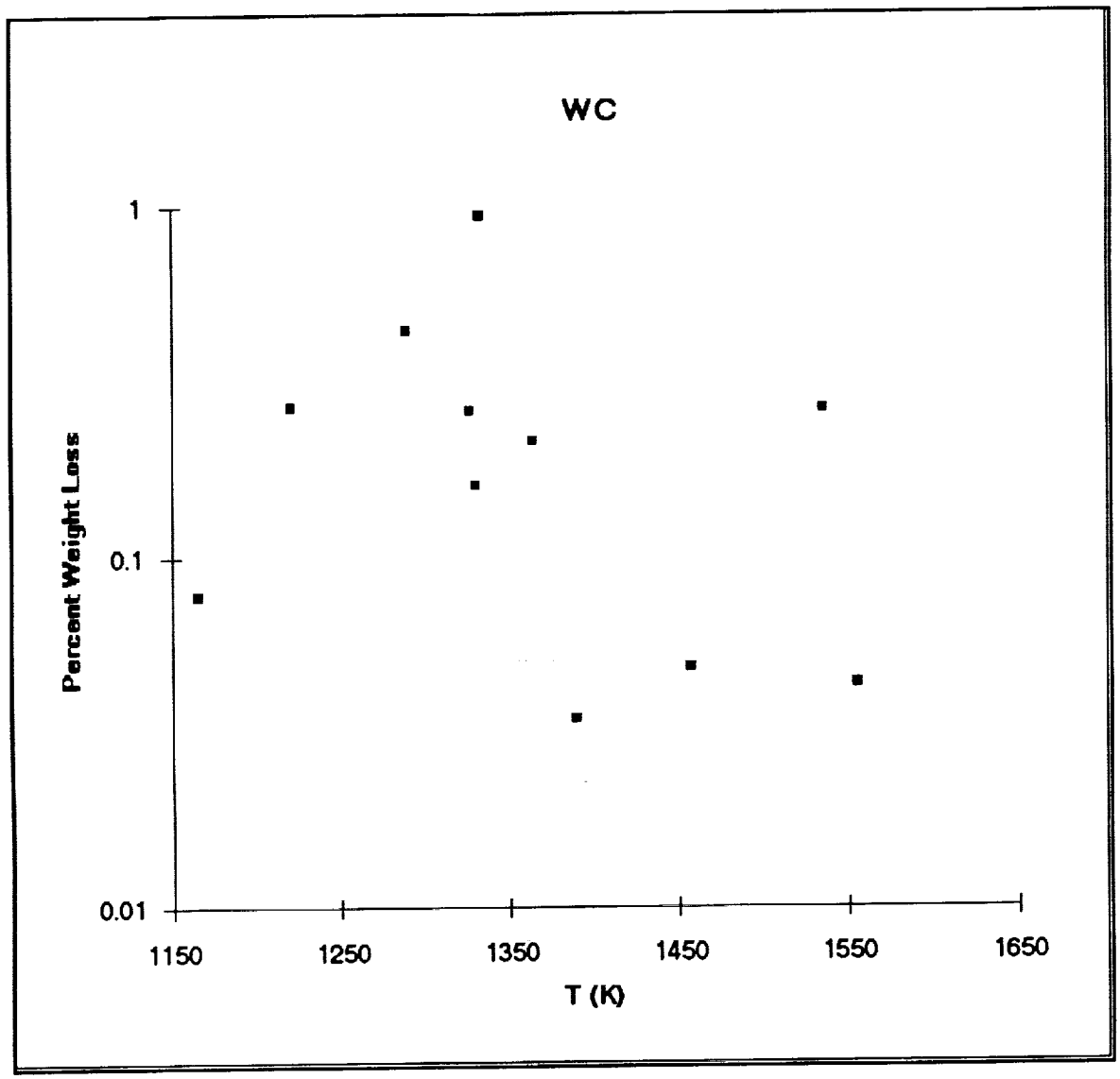

Figure 11. Percent weight loss as a function of temperature for WC.

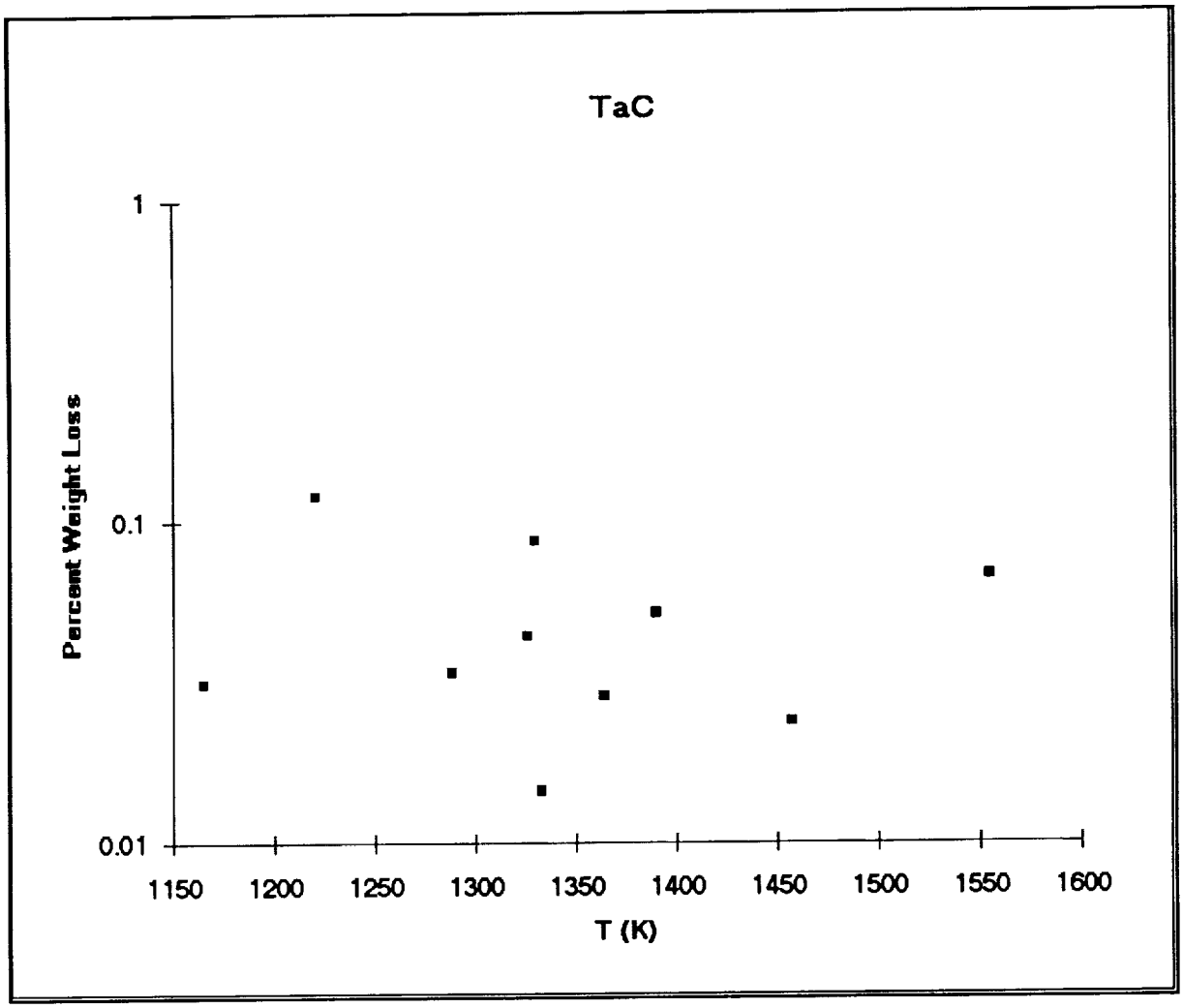

Figure 12. Percent weight loss as a function of temperature for TaC.

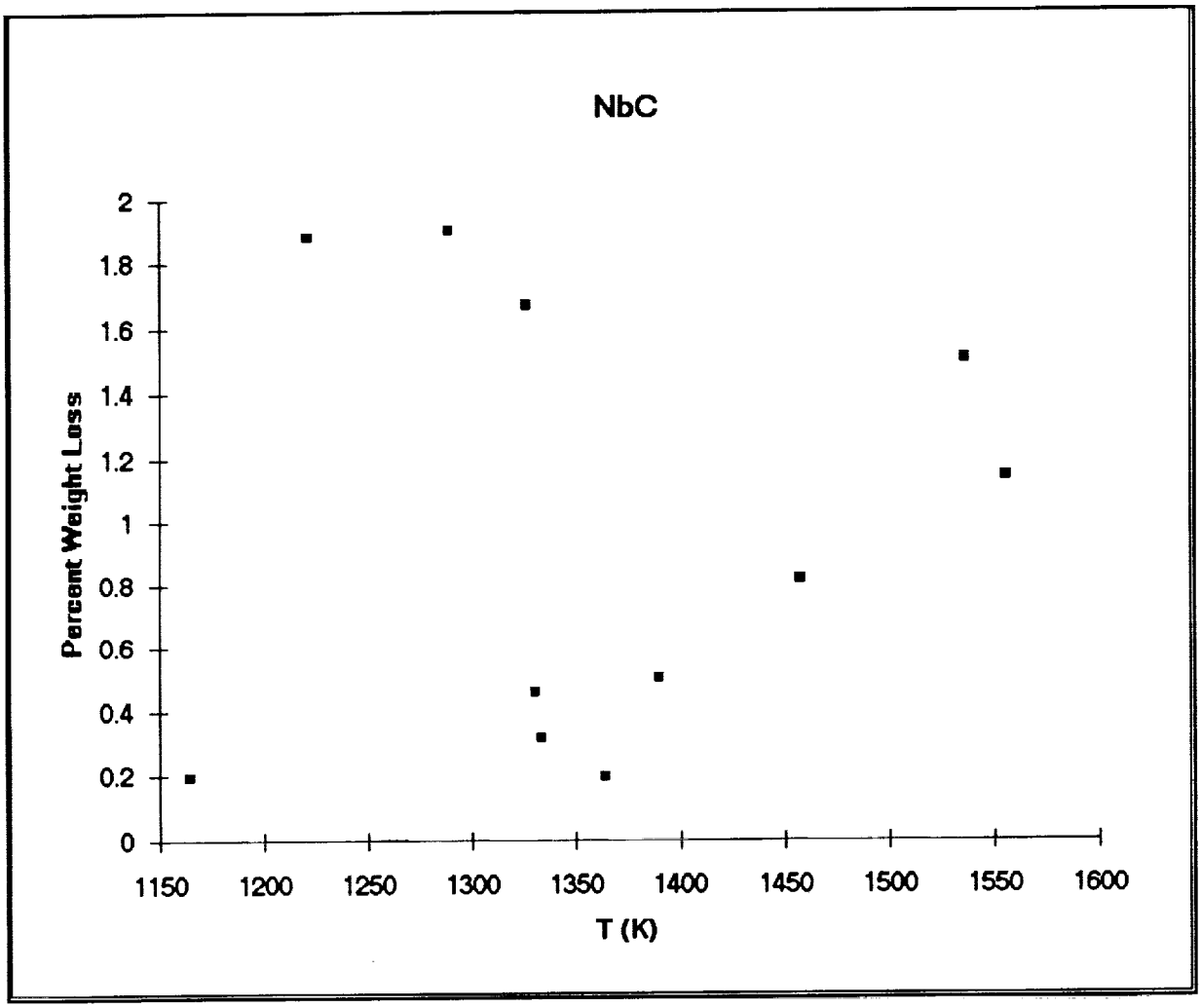

Figure 13. Percent weight loss as a function of temperature for NbC.

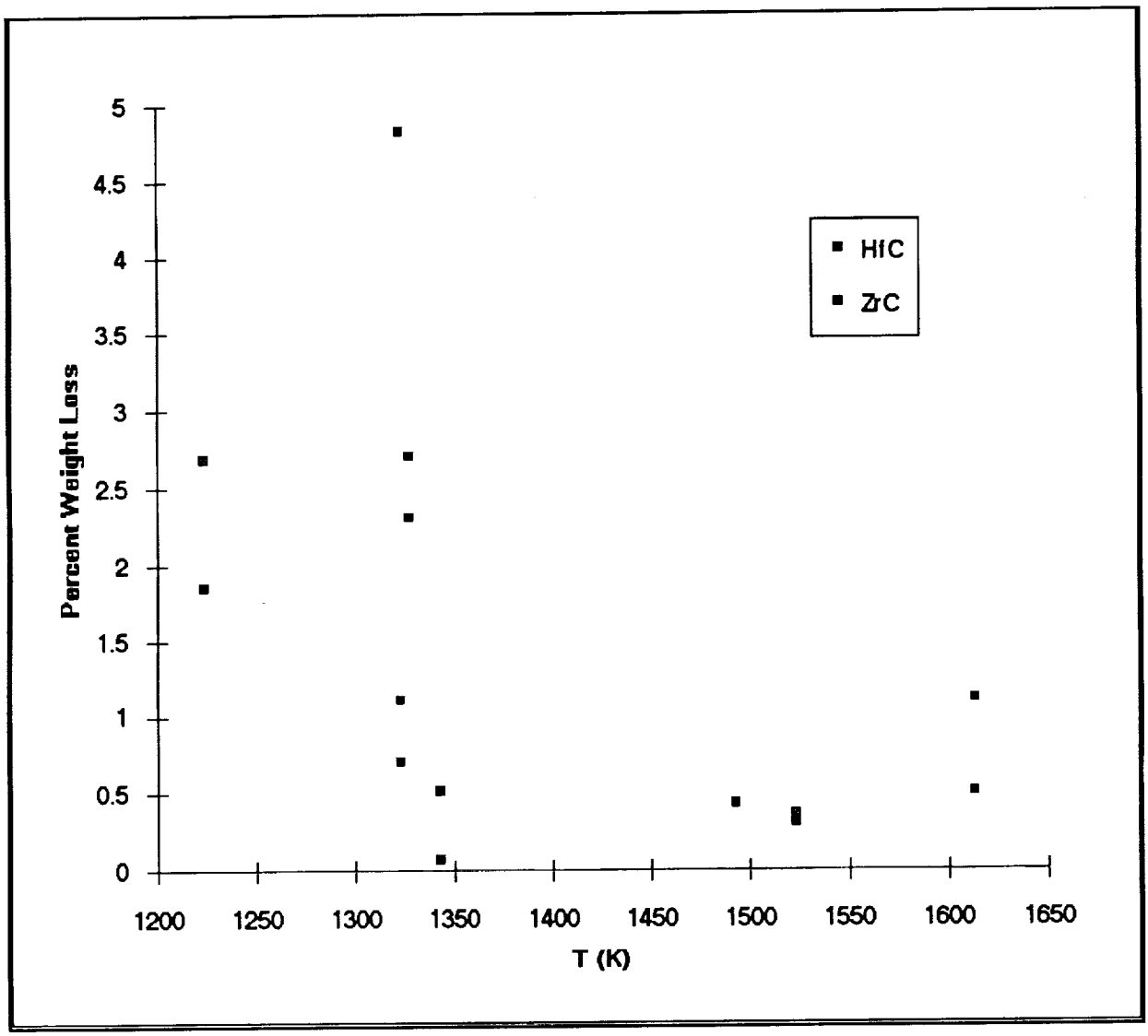

Figure 14. Percent weight loss as a function of temperature for HfC and ZrC.

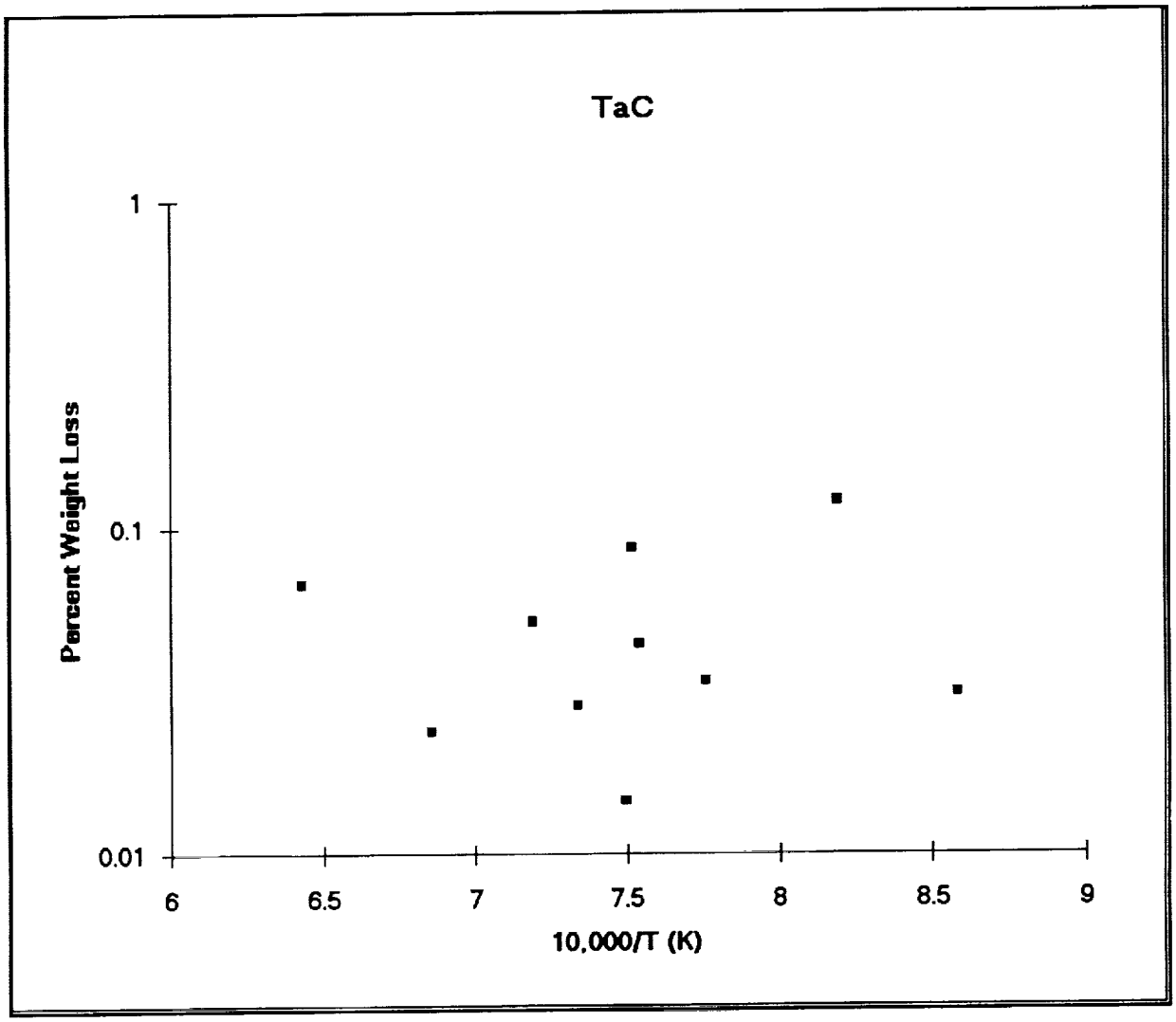

Figure 15. Arrhenius plot for the weight loss in TaC.

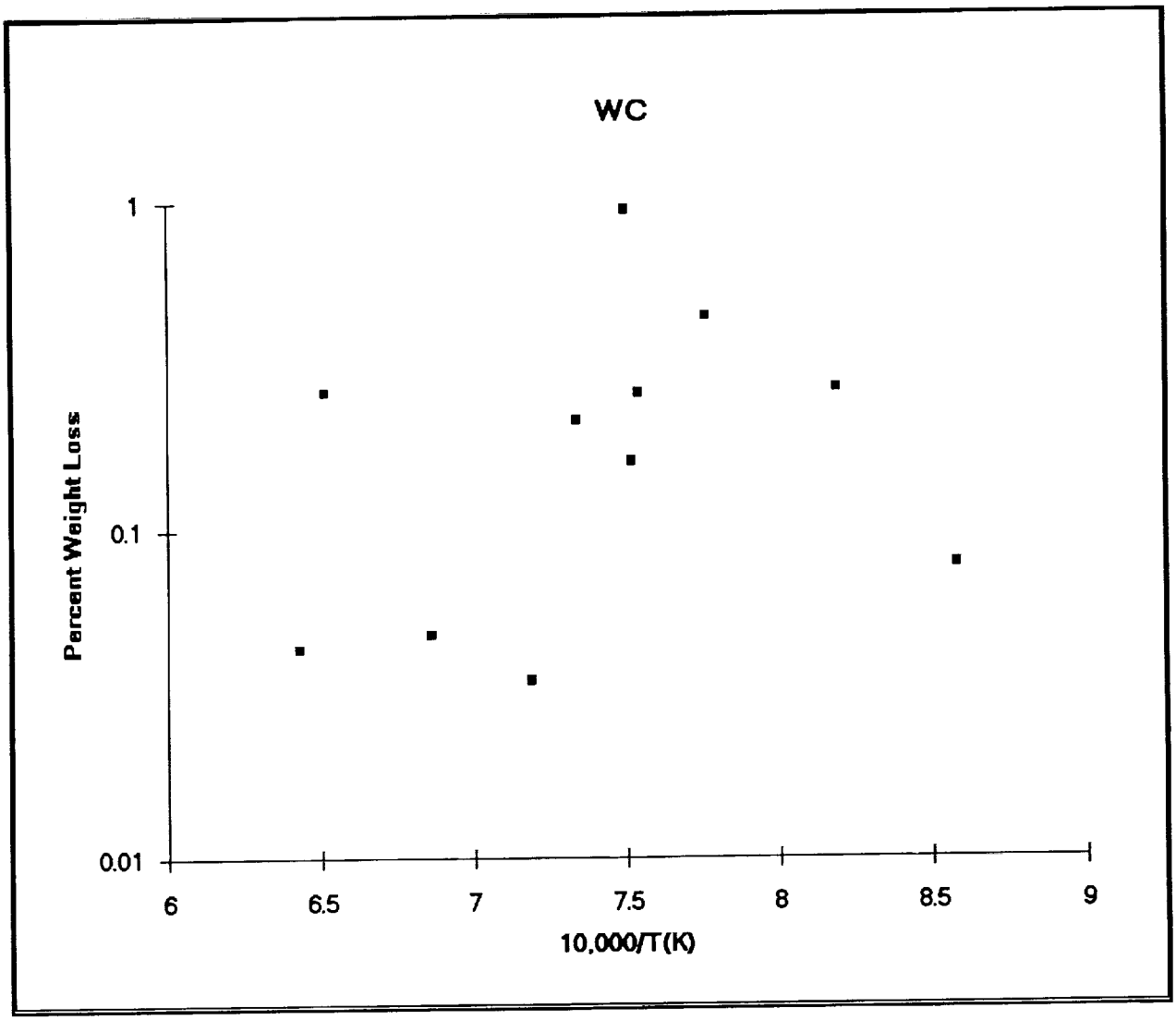

Figure 16. Arrhenius plot for the weight loss in WC.

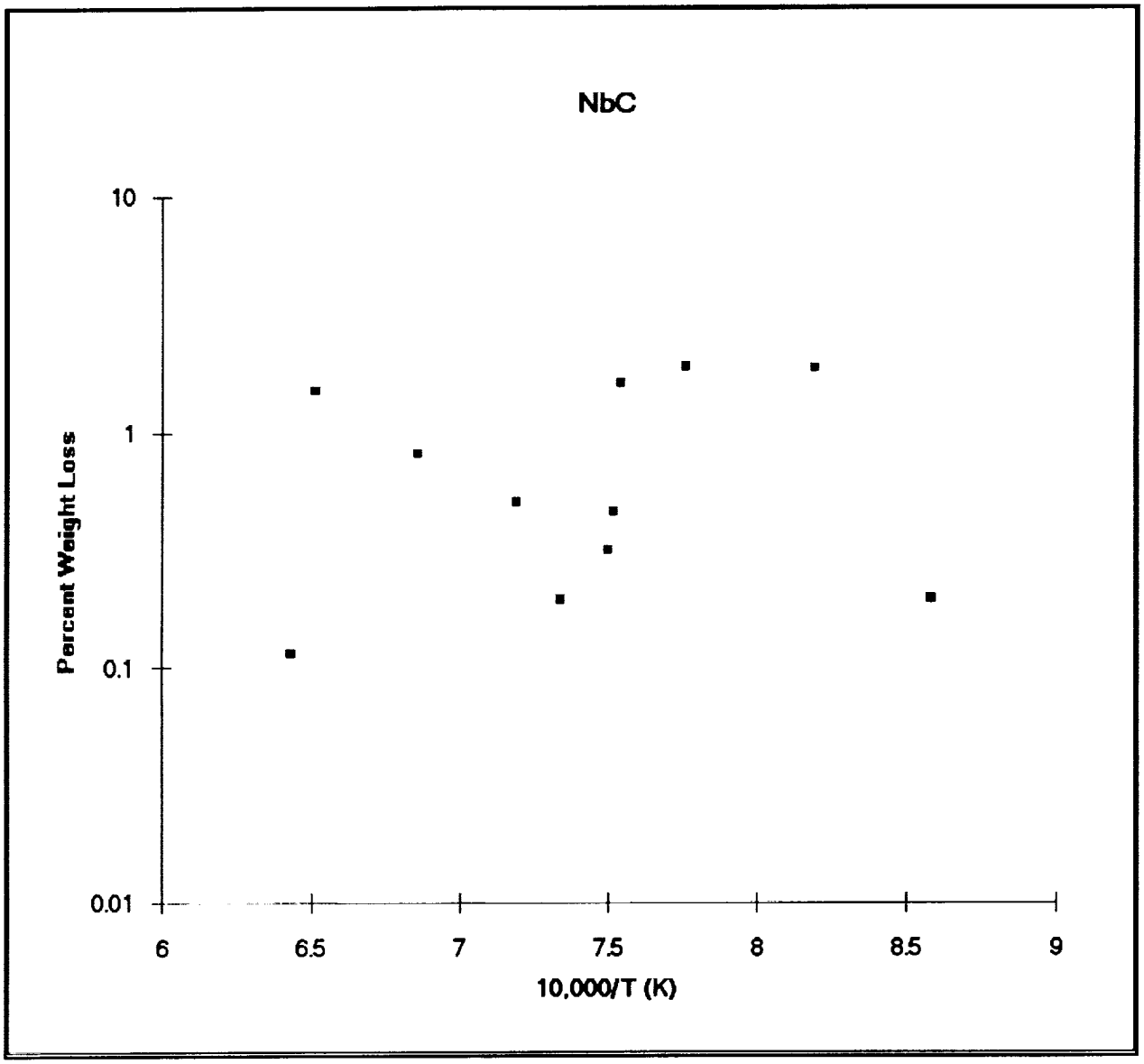

Figure 17. Arrhenius plot for the weight loss in NbC.

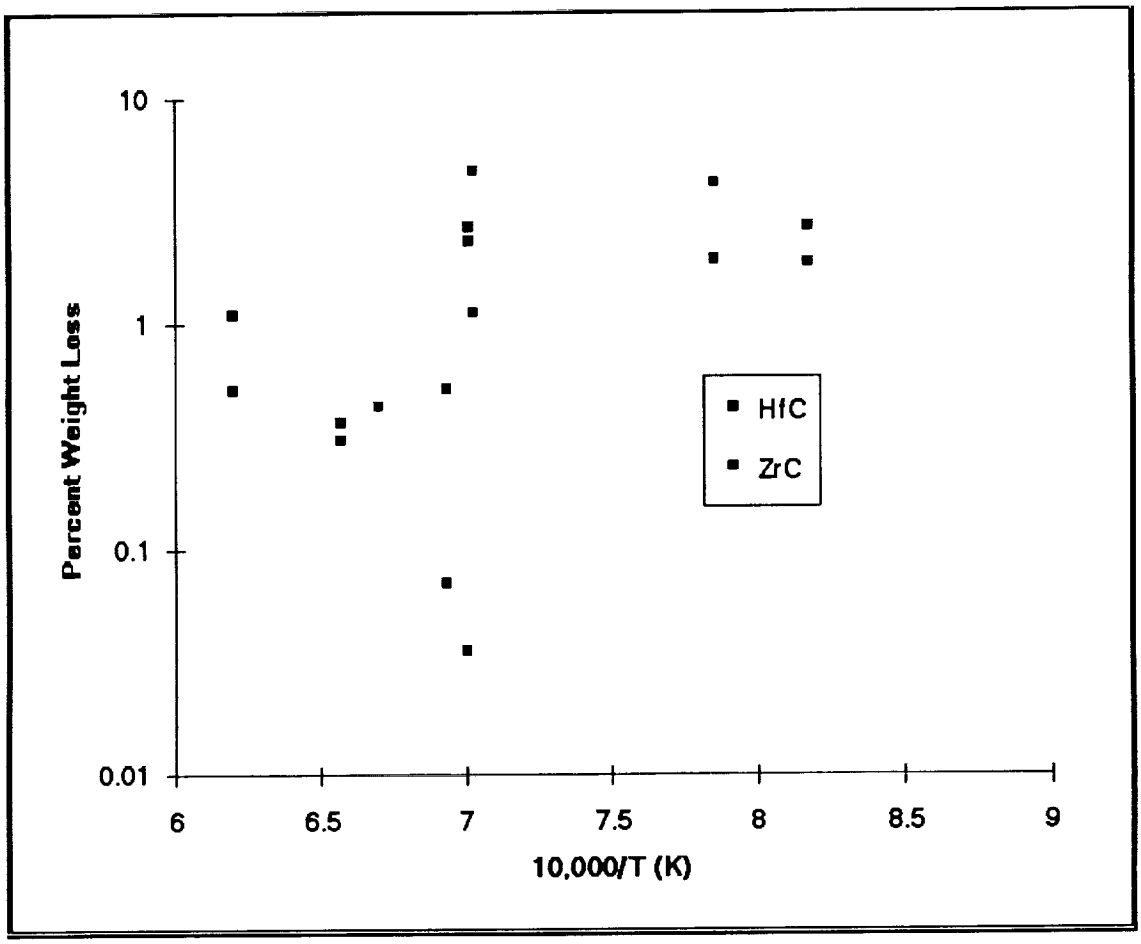

Figure 18. Arrhenius plot for the weight loss in ZrC and HfC.

samples. It is important to note the difference in the y-axis scale between the different samples.

After weighing the exposed sample, XRD analysis was performed immediately. This was done in order to determine if any metastable phases were formed. Such metastable phases would transform to more stable phases as a function of time. The data were analyzed using the JCPDS files for phase identification. The Fink index was also utilized which provided information on d-spacing and their intensity in the XRD spectra. Detailed microstructure and EDS chemical analyses were conducted on all the samples processed. The microstructure of the surface in all cases had not been modified as a result of exposure to hydrogen as well as in vacuum. The micrographs shown in figures 3, 4 and 5, taken from the as-received materials, are representative of their respective materials after exposure. EDS chemical analysis results also confirm that the composition of the materials has not been altered by the exposure, at least not beyond the detection sensitivity of the analysis, which is on the order of one percent.

C.1.1. The First Group:

NbC: In the first group, NbC was found to be the most resistant one to hydrogen exposure. However, this was not the initial impression of the results obtained from NbC. After the first few reactions, NbC was believed to be the most affected due to the larger weight loss that it had over the other two specimens. But,

as more experiments and XRD analyses were performed, it was realized that the NbC was the more resistant. It is believed that due to the high porosity of NbC, some of the weight loss may have been due to excessive outgassing in the initial experiments during exposure. The large weight loss in the initial runs was not as noticeable in the later and, more importantly, longer runs. This fact was not confirmed until longer exposure times were preformed. This will be discussed in more detail in the isothermal section. For the most part, only traces of oxides were formed in any of the NbC samples. The oxides were noticeable in the XRD spectra when the as-received specimen was compared to the post experiment spectra of some of the experiments. The XRD spectra for all of the samples and their corresponding experimental runs will be presented later in this report. Results from the SEM and EDS analyses do not show any compositional variation due to hydrogen or vacuum exposure for NbC, or any of the samples. This was due to the low amounts of oxides or hydrides that may have formed in the test specimens which are below the detection limits of the instruments.

TaC: TaC was initially believed to be the least affected by hydrogen. This was due to the almost non-existing weight change that was observed. However, results from XRD analysis show that TaC contains what is believed to be traces of hydrides and oxides after exposure (figure TaC 15 in the Appendix). In terms of thermodynamics, NbC and TaC should both form oxides if there is sufficient residual oxygen present (figure 6 thru 10). When considering just the aspect of weight loss,

TaC was the most stable compound amongst the five types of materials investigated as evidence from the weight change verse temperature figures.

WC: WC showed an intermediate weight change between TaC and NbC. Although WC lost more weight than TaC, it did not show any hydride or oxide formation. However, results from XRD analysis showed that the WC was transforming to pure tungsten. Therefore, based on thermodynamic considerations shown in the Ellingham diagrams, it was assumed that methane or some form of hydrocarbons would be produced. Gas chromography (GC) was done on selected experimental runs in hopes of proving the presence of methane (or other CH's). But the results showed only the presence of hydrogen. There is a great difficulty in detecting methane in small quantities and it is believed that the methane present in the gas samples was below the detection limits of the GC.

C.1.2. The Second Group:

HfC and ZrC: The HfC and ZrC had similar results from the hydrogen experiments. With the exception of the first two specimens, all the samples lost weight in a similar manner to the samples from the first group. The first two samples were oven dried in air and gained weight during exposure due to the formation of oxides prior to exposure. Some of the ZrC and HfC samples formed oxides. This oxide formation was found to be associated with the higher temperature hydrogen exposures and can therefore be attributed to a thermally activated process. Although

both types of samples lose weight, ZrC tends to lose the most weight which is evident in the weight loss figure 15. Neither the ZrC nor the HfC showed any signs of hydride formation. Again, the XRD spectra for all the samples and their corresponding experimental runs are presented later.

C.2. Isothermal: Initially all the experiments were done for the same duration of time. However, only minimal changes were observed as a result of the one hour experiments. It was then decided to extend the experiment time. The first extended time was for two hours, then for eight hours, and eventually 16 hours. There was a dry run made for the two hour and eight hour runs but not for the 16 hour run. As in the isochronal experiments, the hydrogen was maintained at one atmosphere of pressure while the time became the variable in these experiments. The first group of experiments were conducted at approximately 1330K while the second group of experiments were run at approximately 1470K.

C.2.1. The First Group:

NbC: For the first extended experiments with a long duration of two hours, both the dry and the hydrogen runs, the NbC continued to show the greatest weight loss from the first group (NbC, TaC, WC). Although the weight change observed in the NbC was the largest among the three types of carbides in this group, hydrogen exposure did not lead to the formation of new phases as revealed by the XRD spectra.

Only minor traces of the oxide were ever detected in various experimental spectra. This indicates that the relatively large weight loss observed is due to the direct degradation of the NbC rather than the forming of oxides. This can be explained by higher concentration of residual oxygen in some of the experiments. As the exposure time was increased to eight hours, the XRD patterns changed little and the weight loss of NbC for the hydrogen was surpassed by that of WC. This can be seen in the XRD spectra and weight change verses temperature plots of the two samples. However, results from the dry run at eight hours showed that the NbC has greater loss than the WC. This observation suggests that the degradation of the NbC is not greatly influenced by the presence of the hydrogen and that degradation is more thermally controlled. When the 16 hour run was completed, the NbC again had the largest weight change.

TaC: The TaC material was found to be the most resistant to weight loss. Whether it was a dry run or a hydrogen run, the TaC always retained the largest percentage of its original weight. However, there were traces of oxide formation in most of the extended runs and possibly the formation of hydride s in some of the samples. The above observation is confirmed by the appearance of the oxide and hydride peaks in XRD spectra for the TaC as a result of the exposure. TaC samples tend to be effected by the presence of hydrogen and not the temperature at which the experiment was run. This suggests that the degradation process of TaC is not entirely thermally dependent and is influenced by the concentration or pressure of hydrogen.

WC: Among the three types of samples in this group (NbC, TaC, WC) the XRD spectra obtained from the WC exhibited the most significant change after extended runs. After the two-hour experiment, the WC material started to show more distinct changes in the XRD patterns than that observed in the isochronal experiments. After the eight hour run, the spectra was completely altered (at least for a given depth of penetration). This was later found to be a transformation of WC to pure tungsten. Again, GC was used to detect the presence of methane (or other CH's). But no convincing evidence was found. Methane is difficult for a gas chromographer to detect unless its presence is in significant. It is therefore beleived that the methane was below the detection limits of the CG. The pure tungsten was observed and can be seen in the XRD spectrum of sample number 15. It was anticipated that the sample exposed to hydrogen for 16 hours would also posses just pure tungsten. But this was not observed. The XRD spectrum from the 16 hour sample showed the presence of pure tungsten, WC and some other unidentifiable compounds. These compounds were believed to be some form of hydrocarbons and tungsten. This was a logical assumption based on the fact that carbon was being evolved by the WC and that hydrogen was present at an elevated temperature. Further proof of this can be seen in the observation of the pressure in the outer chamber. Initially the pressure in the outer chamber increased with the heating of the inner chamber. This increase of pressure is due to the permeation of hydrogen through the Nb-1Zr tube. As time goes on and the formation of methane occurs the permeation through the Nb-1Zr

0diminished. The slowing of permeation through the tube corresponds to the decrease in concentration of hydrogen and the increase in the presence of methane and can explained by the difference in the molecular size of the two molecules. The change in the permeation rate during the experiment was observed and recorded.

C.2.2. The Second Group

The HfC and ZrC isothermal testing was limited to only three runs. All of which were hydrogen runs and show little more information than the isochronal tests. More time would be needed to report the significance of the extended runs on the second group.

D. Discussion:

The initial goal of this project was to develop a technique to study degradation of ceramic material by hydrogen at ultra high temperatures. This was accomplished by using a double wall vacuum chamber with induction heating of the inner chamber. The inner chamber contained the specimens which in turn were heated by conduction. This enabled the samples to be heated to the same temperature using the same induction power supply. The heating was measured directly using a pyrometer and a tungsten-rhenium thermal couple.

Two groups of samples were obtained from independent sources. The first group consisted of NbC, TaC and WC. The second group consisted of HfC and ZrC.

The first group was obtained prior to that of the second group. Therefore the data for the first group was more extensive than that of the second group. There were sixteen experiments done on group one and eleven experiments on group two. Examination of the samples was done prior to exposure to hydrogen to determine the basic structure and compositions of the materials obtained and to establish a baseline for proper comparisons. The pre and post experimental examination included XRD, SEM, EDS, metallography, and weight measurements. Gas chromography was also done on selected experiments to verify the formation of CH's. The experiments were conducted either isochronally or isothermally. The isochronal experiments ranged in temperature from 850°C to 1600°C and were all for a length of one hour. The isothermal experiments ranged in time from one hour to sixteen hours for the first group and one to eight hours for the second. Experiments done without hydrogen, which are referred to as dry runs, were also done in efforts to give a basis for only the hydrogen degradation.

Results from the SEM, EDS and metallography analyses showed little information, other than confirming the initial condition. Post exposure examination using SEM and EDS failed to help in identifying the presence of new phases due to the amounts of hydrides and oxides being below that of the detection limits of the equipment. Optical metallography also offers little insight into the degradation mechanism by hydrogen due to the high porosity of the ceramic materials. The high porosity of the ceramics caused the depth of field to be greater than that of the

microscope and limited the use to low magnifications. The metallographic structure of the as-received specimens was not altered by the exposure to either hydrogen or vacuum.

Results from XRD analysis, on the other hand, showed considerable insight to the processes that were occurring in the samples and was used extensively. Each sample was analyzed using XRD immediately after exposure. This was done in an effort to determine the existence of metastable phases. The XRD results show that within the first group, WC was the most affected by the presence of hydrogen. The WC samples transformed into pure tungsten in the presence of hydrogen by evolving carbon. The evolved carbon is believed to form a CH compound with the available hydrogen in the inner chamber. This was supported by the fact that pressure in the inner chamber decreased after an initial increase, during the course of the experiment. The initial increase in pressure is due to the permeation of hydrogen through the wall of the inner chamber. This permeation decreases as the CH's volume percent increases. Although gas chromography was performed on selected experiments in hopes of definitively identifying the forming of hydrocarbons, it failed to show the presence of methane or other CH compounds. Methane is difficult to detect unless it is in great quantity. Therefore, it was believed that the presence of CH's weas below the detection limits of the CG.

The exposure of NbC to hot hydrogen was found to result in traces of oxide in some of the experiments. The TaC also shows formation of oxides in some samples

with possible evidence of hydrides. The evidence of hydride formation is not convincing and was not substantiated from the JCPDS files. From a thermodynamic perspective, the oxides will form if any oxygen is present. Although the system was purged several times prior to the introduction of hydrogen, there always existed a partial pressure of oxygen which will contribute to the oxidation reaction.

The XRD on the second group showed oxide formation on some of the samples. There may also have been formation of small amounts of hydrides, but again this was not substantiated. Decomposition of either HfC or ZrC to pure Hf or Zr was not identified. X-ray diffraction spectra obtained from the samples were compared with one another as well as with the JCPDS cards (see Appendix). Results indicate a change in the stoichiometry of zirconium carbide after it was exposed to hot hydrogen. No free carbon, metallic elements, or hydrides were detected. With exposure to hydrogen at high temperatures, two new peaks were found in the spectra of ZrC. A comparison with the JCPDS file shows that these peaks correspond to the first two peaks of the $ZrC_{0.6}$. The other peaks were matched with the ZrC spectrum itself. The peak height increases with the temperature of exposure indicating a loss of carbon to the hydrogen and a change in the stoichiometry of the carbide on the surface of the sample.

The weight of each sample was measured prior to and immediately after each experiment was completed. The weight change offers an insight into the bulk degradation process due to reaction with hydrogen as well as thermal decomposition.

The weight change was plotted in an Arhenius fashion in an effort to determine the thermal activation aspect of the specimens. Of all five types of specimens investigated, TaC retained the largest percent of its initial weight. The WC samples tended to lose slightly more weight than TaC but less than the other samples. Degree of weight loss in WC was followed by NbC. The NbC did not lose more than two percent of its initial weight, in agreement with other studies of similar materials. The second group showed a range of weight loss for both HfC and ZrC. This range has been contributed to erroneous drying procedures that occurred in the initial experiments of the second group. On the average the ZrC tended to show greater weight loss.

In general, TaC showed the least amount of weight loss but showed oxide formation. The NbC tended to be least effected by the presence of hydrogen but lost the most weight for the first group. The WC evolved carbon to form pure tungsten and was the most effected by the hydrogen atmosphere. The ZrC tended to oxidize more readily than that of the HfC and showed the greater percent of weight loss in the second group.

E. Conclusions

1. A hot hydrogen exposure system was designed, constructed and employed successfully to study the effects of hydrogen on ceramics.
2. The degradation processes due to hydrogen exposure were investigated in five carbide systems. It was found that the reactions were very complex. The degradation processes were different amongst different carbides. Furthermore, the reaction within each ceramic changed with temperature.
3. Based on all the available data obtained (weight loss, structure, phase formation), HfC appears to be the most resistant to hydrogen. Contrarily, WC is the most suceptable to hydrogen degradation.

APPENDIX

X-RAY DIFFRACTION SPECTRA FOR THE SAMPLES INVESTIGATED

(The sample ID's given at the top of the spectra refer the sample type and the run numbers which cross reference with the number given in Table 1 in the text)

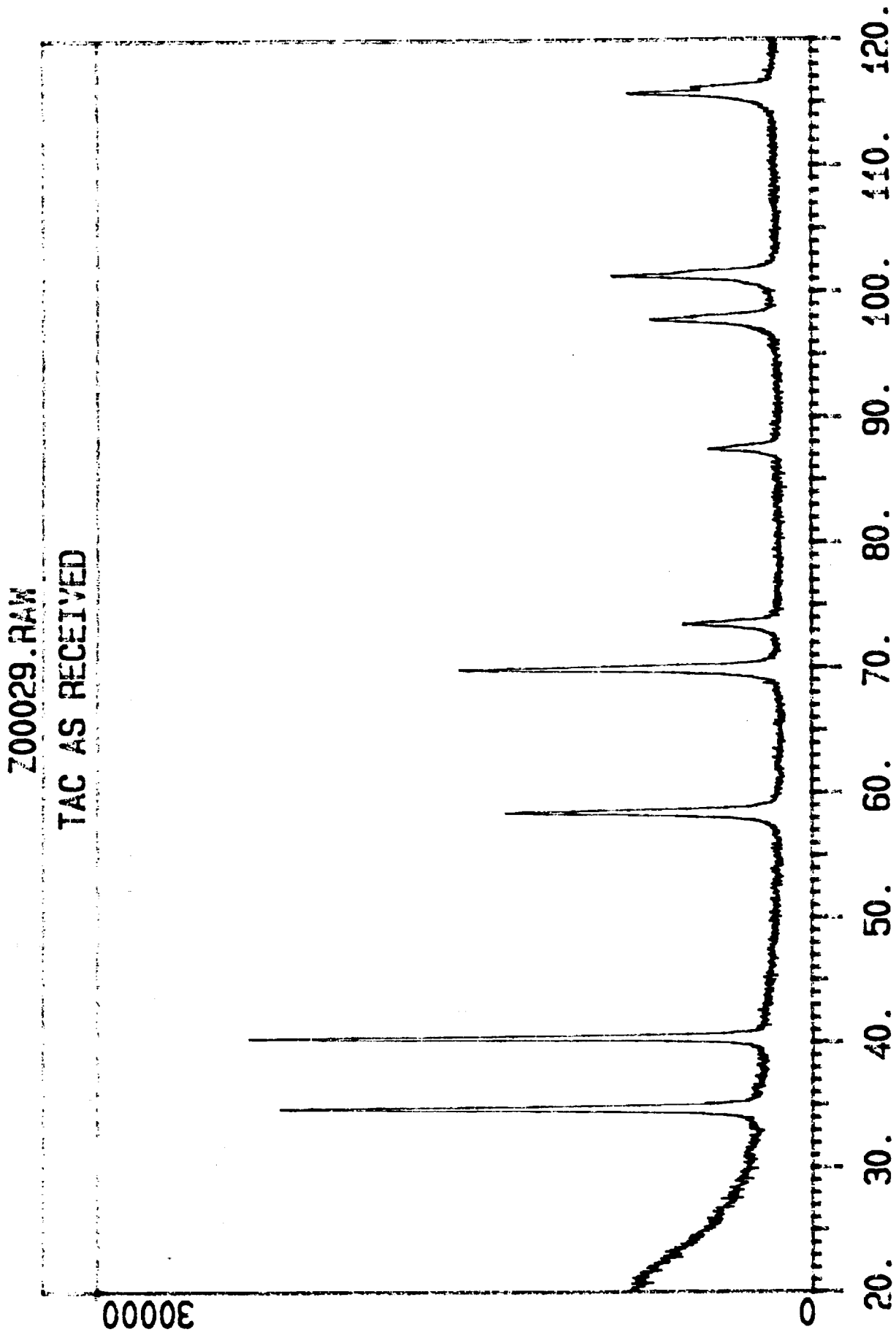
Z00029.RAW
TAC AS RECEIVED
30000
0
20.
30.
40.
50.
60.
70.
80.
90.
100.
110.
120.

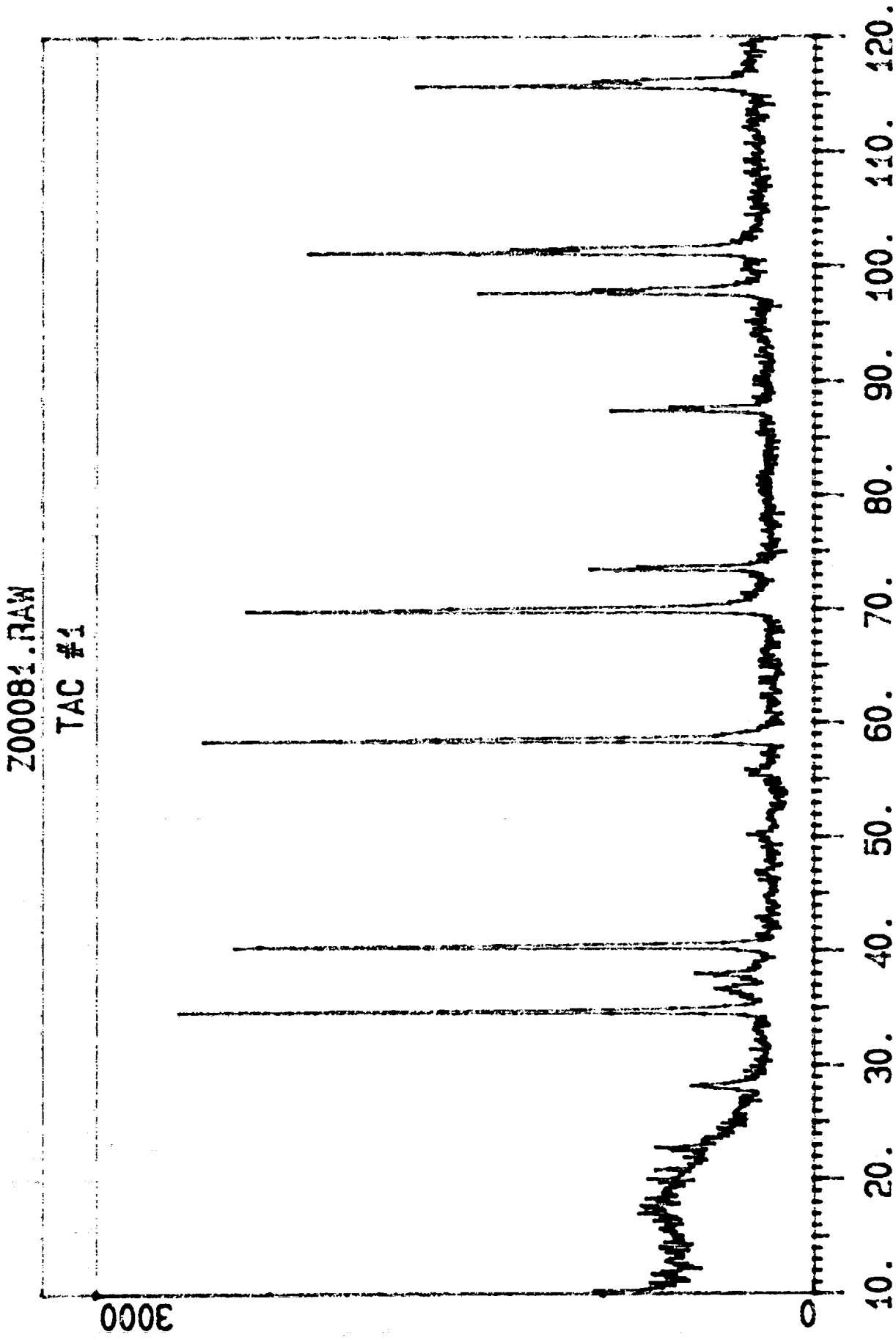
Z00081.RAW
TAC #1
3000
0
10.
20.
30.
40.
50.
60.
70.
80.
90.
100.
110.
120.

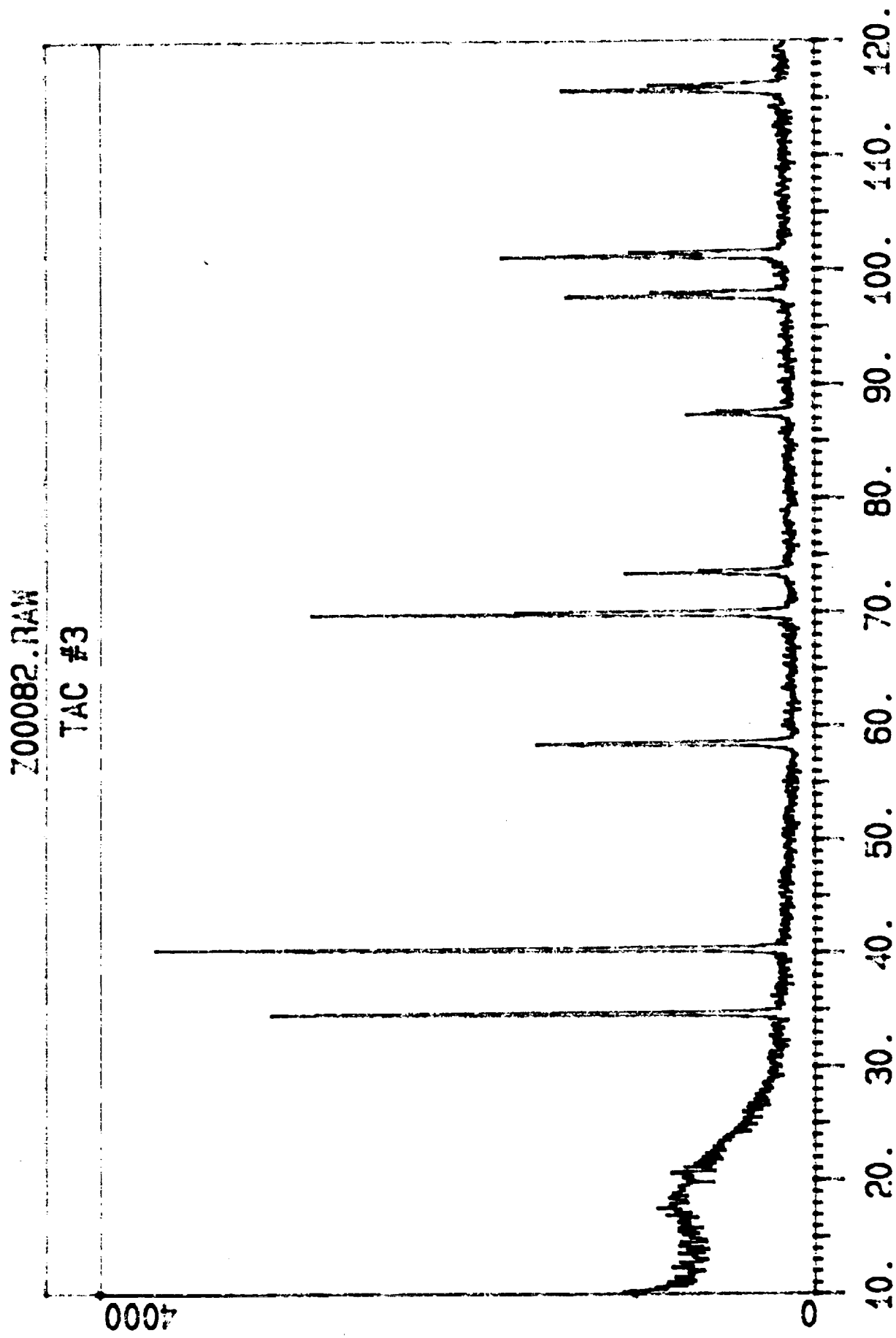
Z00082.RAW
TAC #3
4000
0
10.
20.
30.
40.
50.
60.
70.
80.
90.
100.
110.
120.

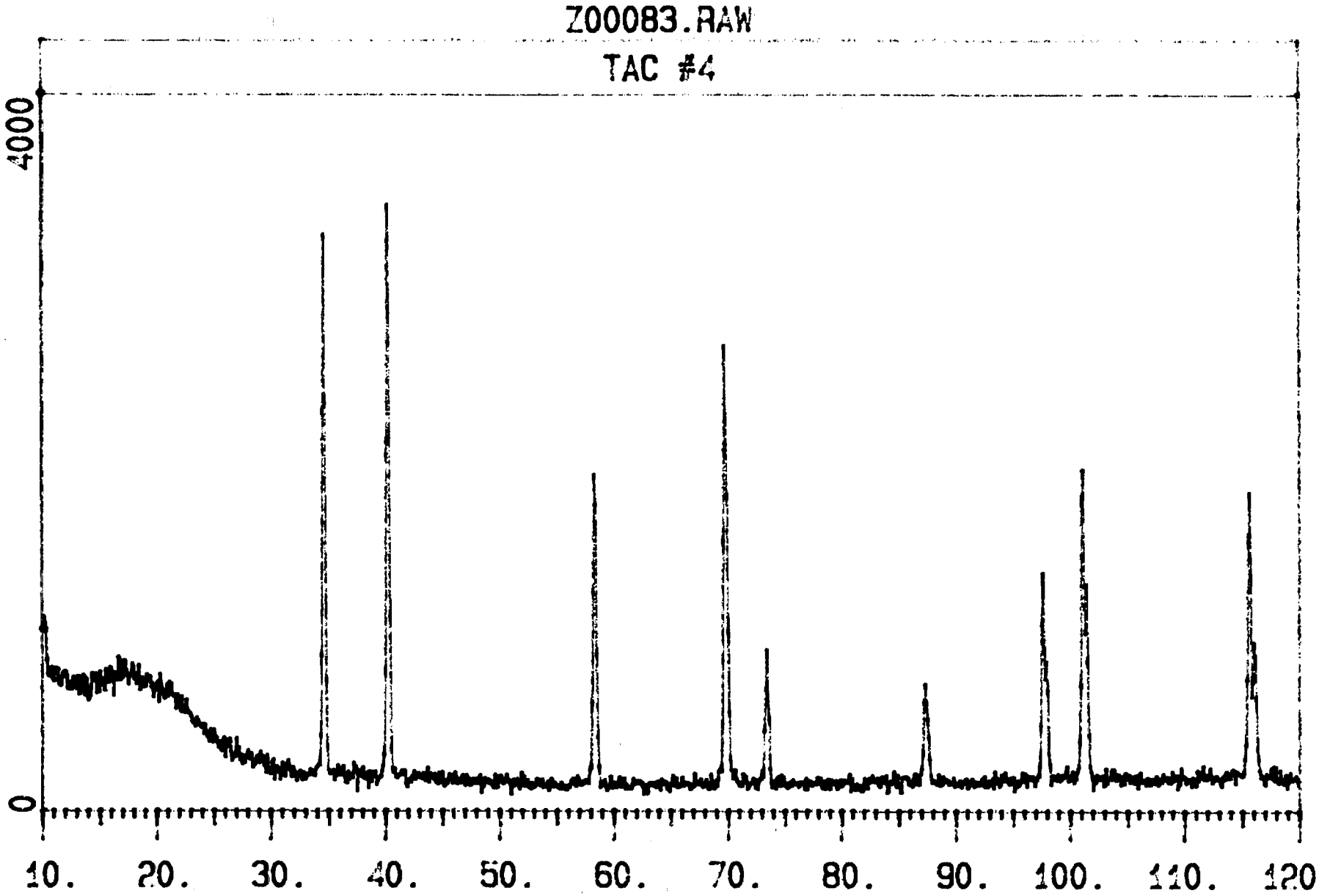
Z00083.RAW
TAC #4
4000
0
10.
20.
30.
40.
50.
60.
70.
80.
90.
100.
110.
120.

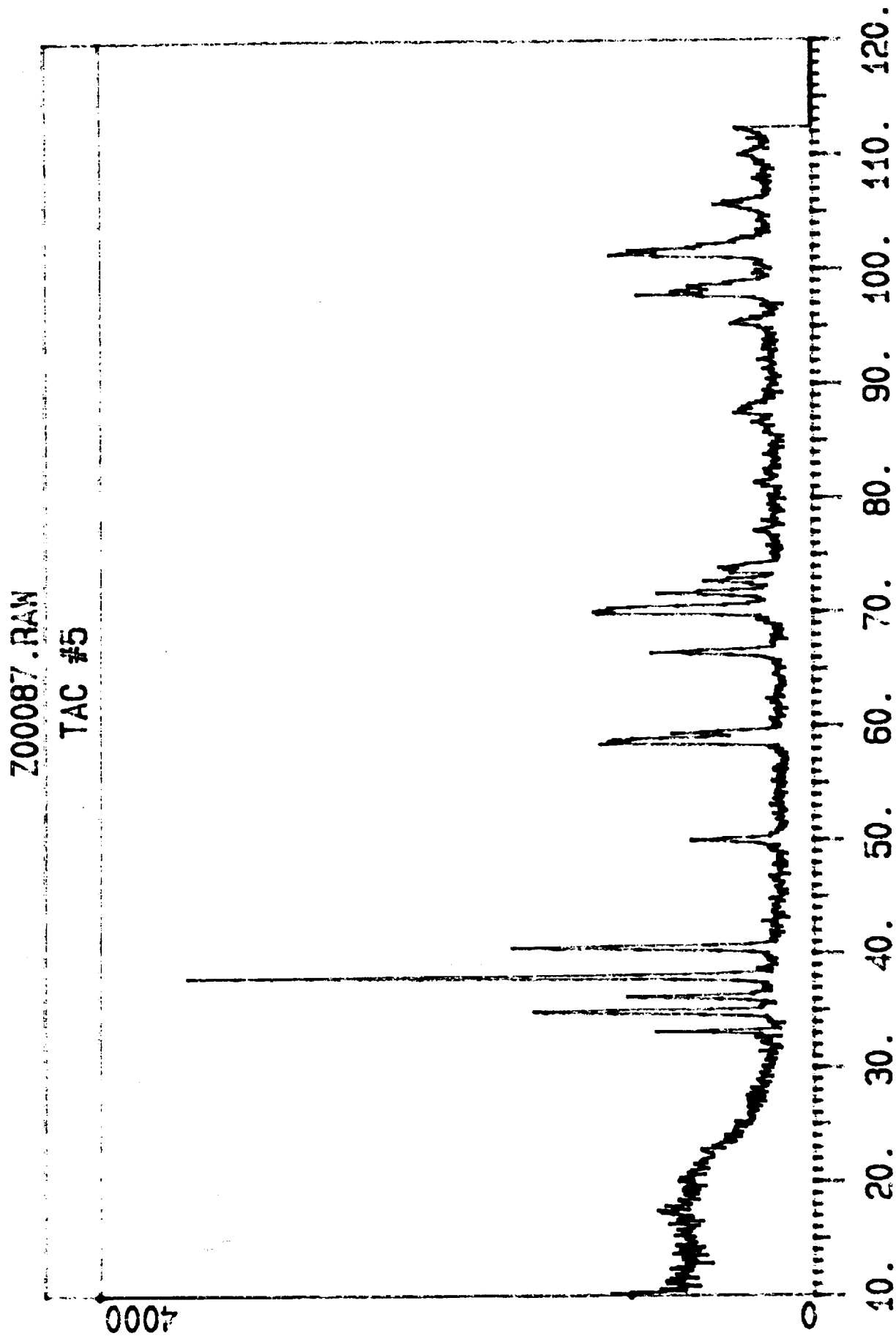
Z00087.RAW
TAC #5
4000
0
10.
20.
30.
40.
50.
60.
70.
80.
90.
100.
110.
120.

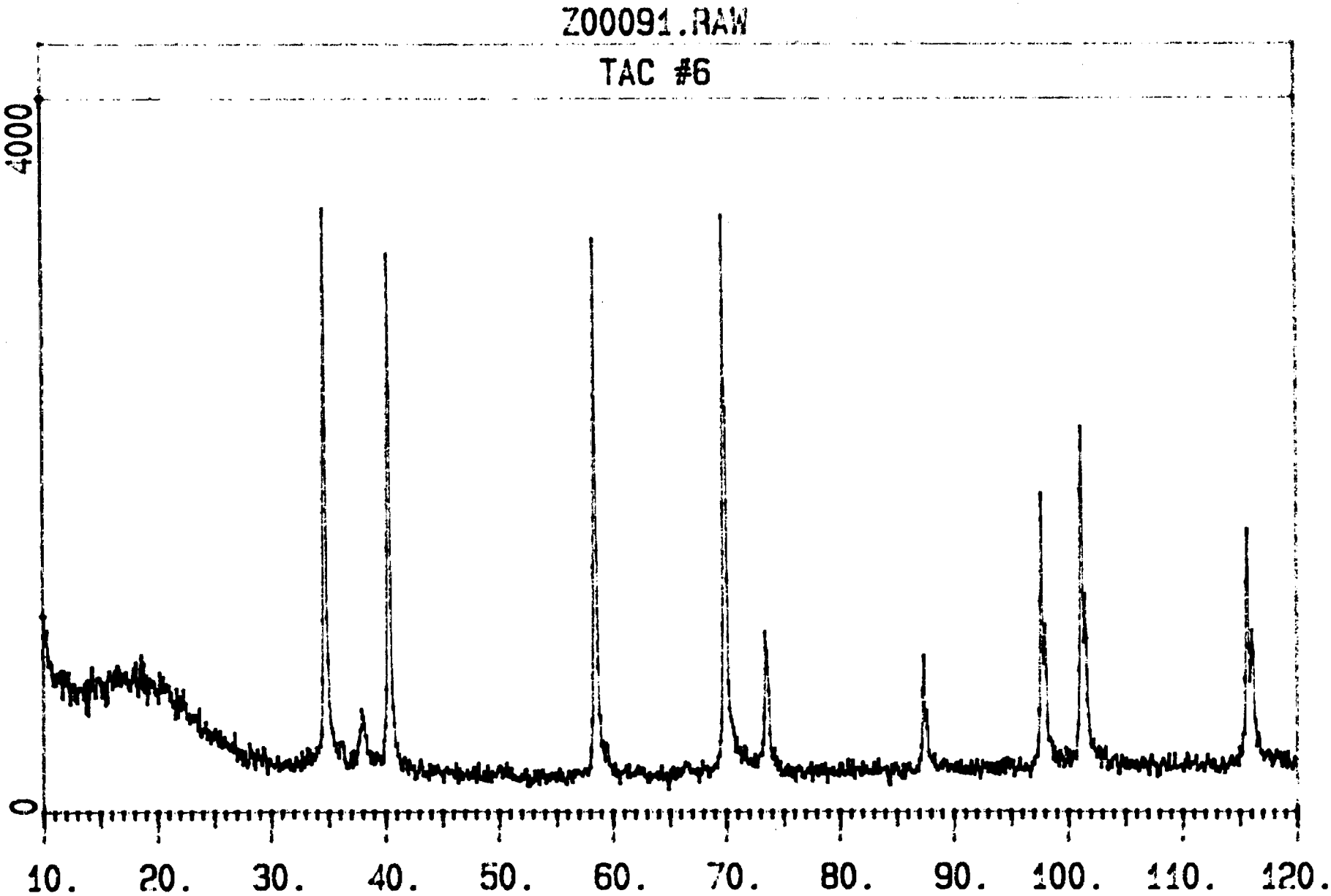
Z00091.RAW
TAC #6
4000
0
10.
20.
30.
40.
50.
60.
70.
80.
90.
100.
110.
120.

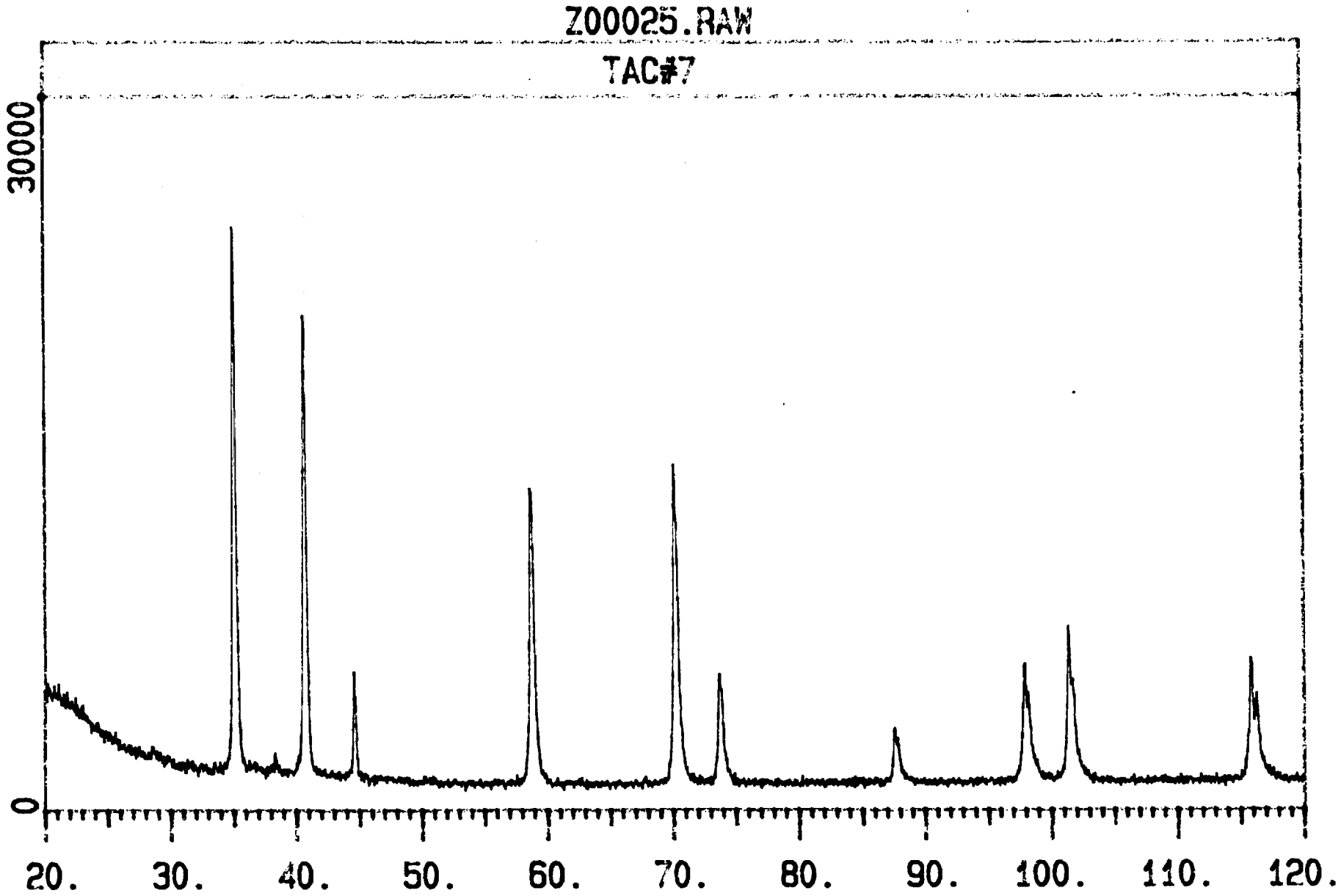
Z00025.RAW
TAC#7
30000
0
20.
30.
40.
50.
60.
70.
80.
90.
100.
110.
120.

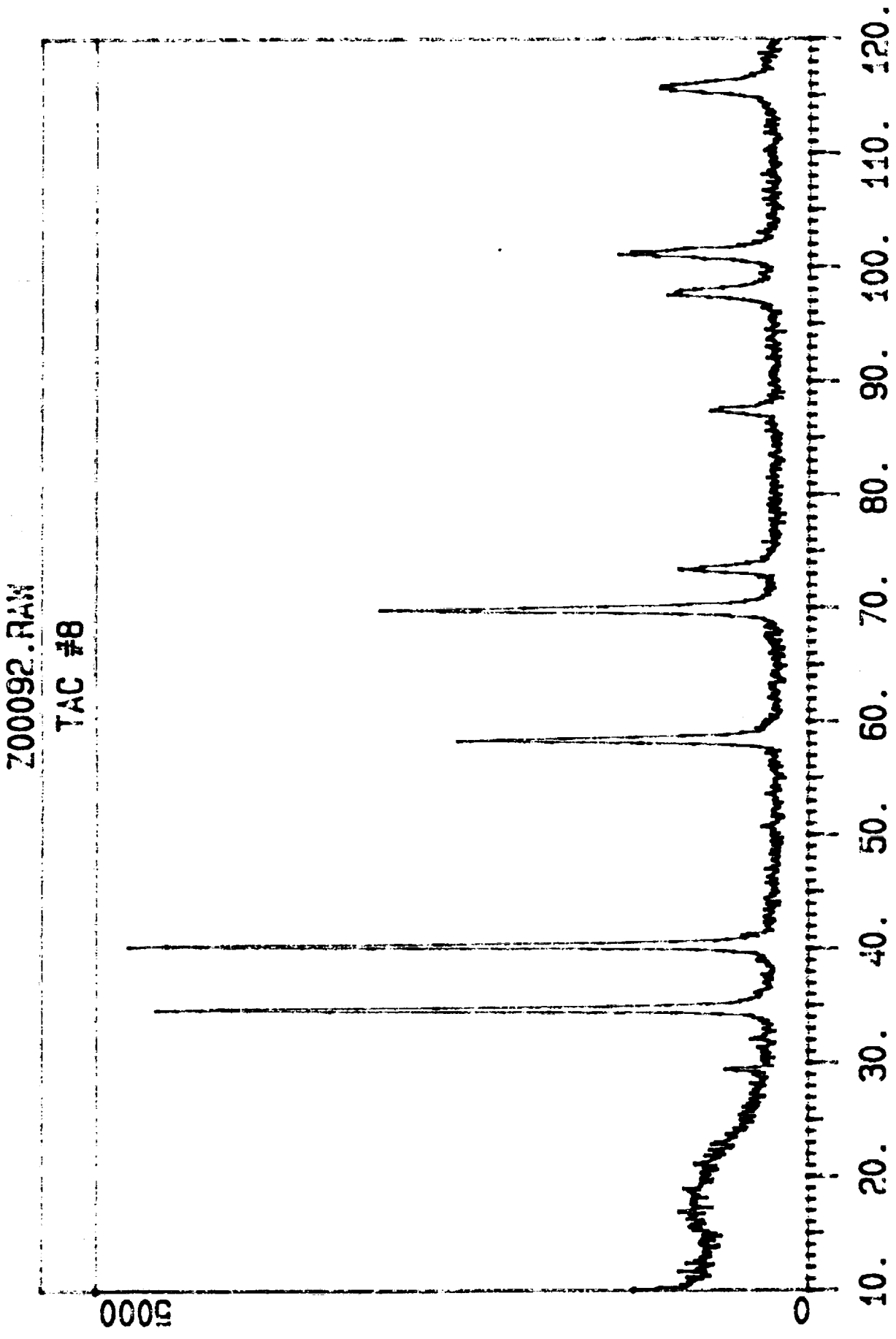
Z00092.RAW
TAC #8
5000
0
10.
20.
30.
40.
50.
60.
70.
80.
90.
100.
110.
120.

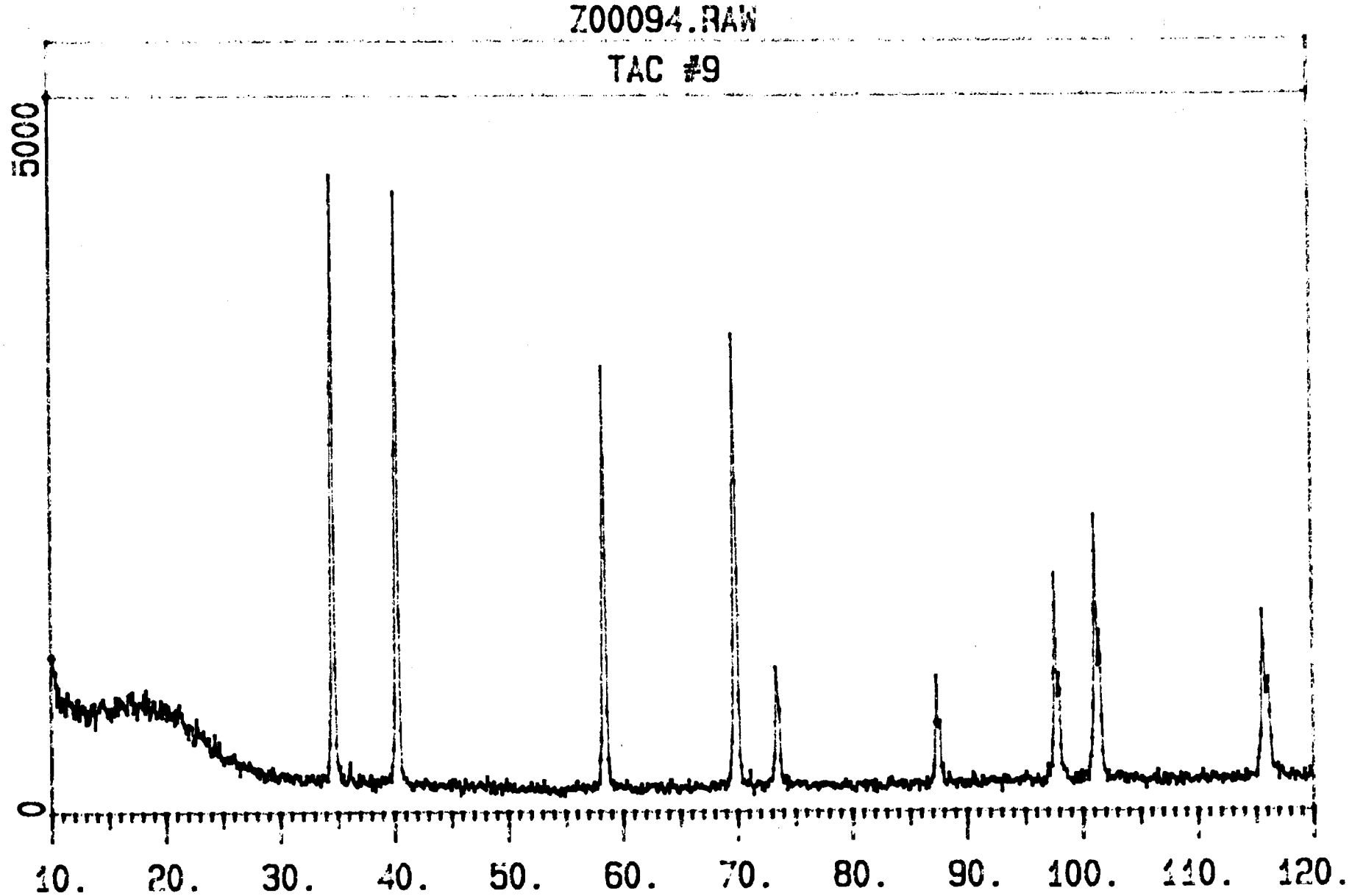
Z00094.RAW
TAC #9
5000
0
10.
20.
30.
40.
50.
60.
70.
80.
90.
100.
110.
120.

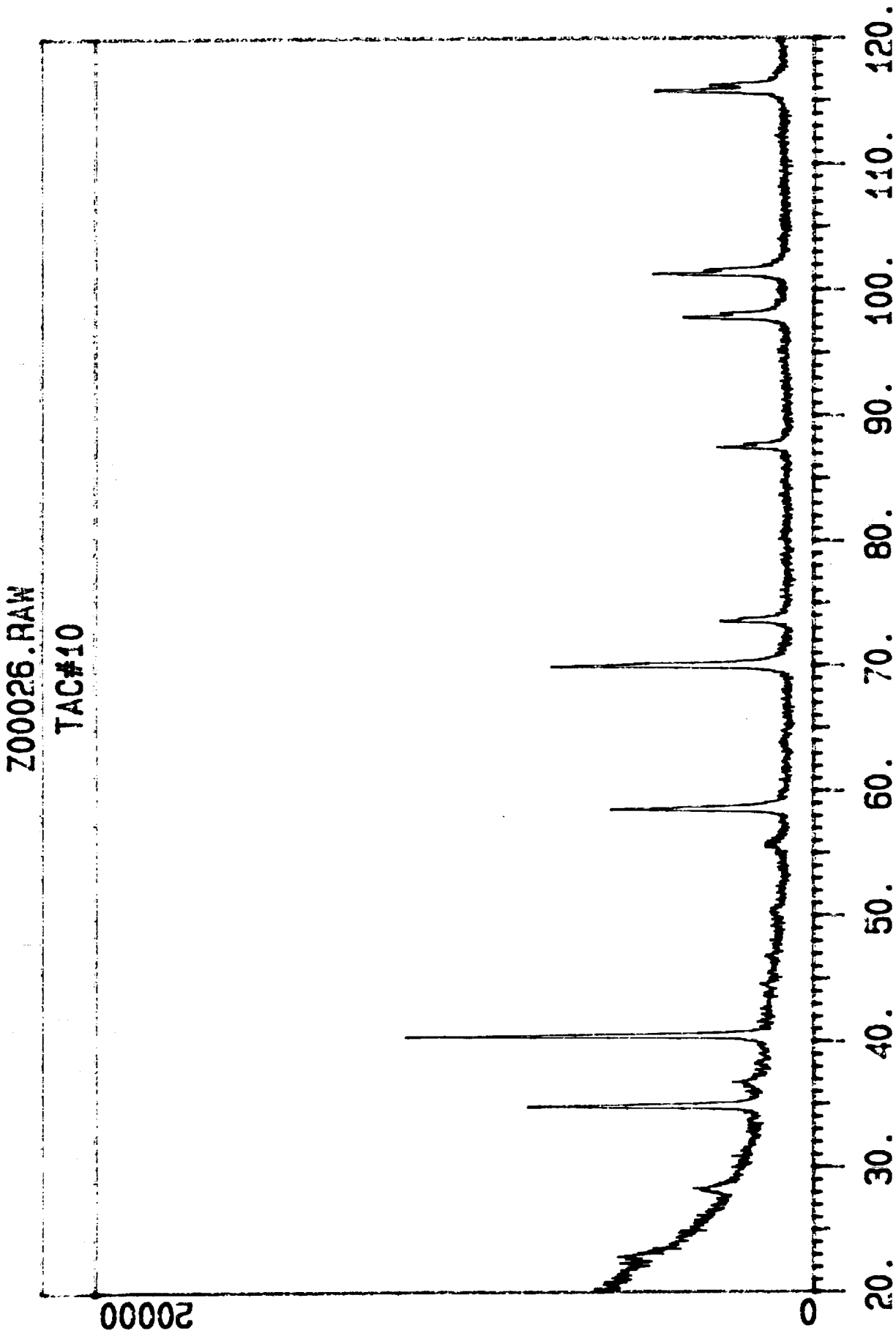
Z00026.RAW
TAC#10
20000
0
20.
30.
40.
50.
60.
70.
80.
90.
100.
110.
120.

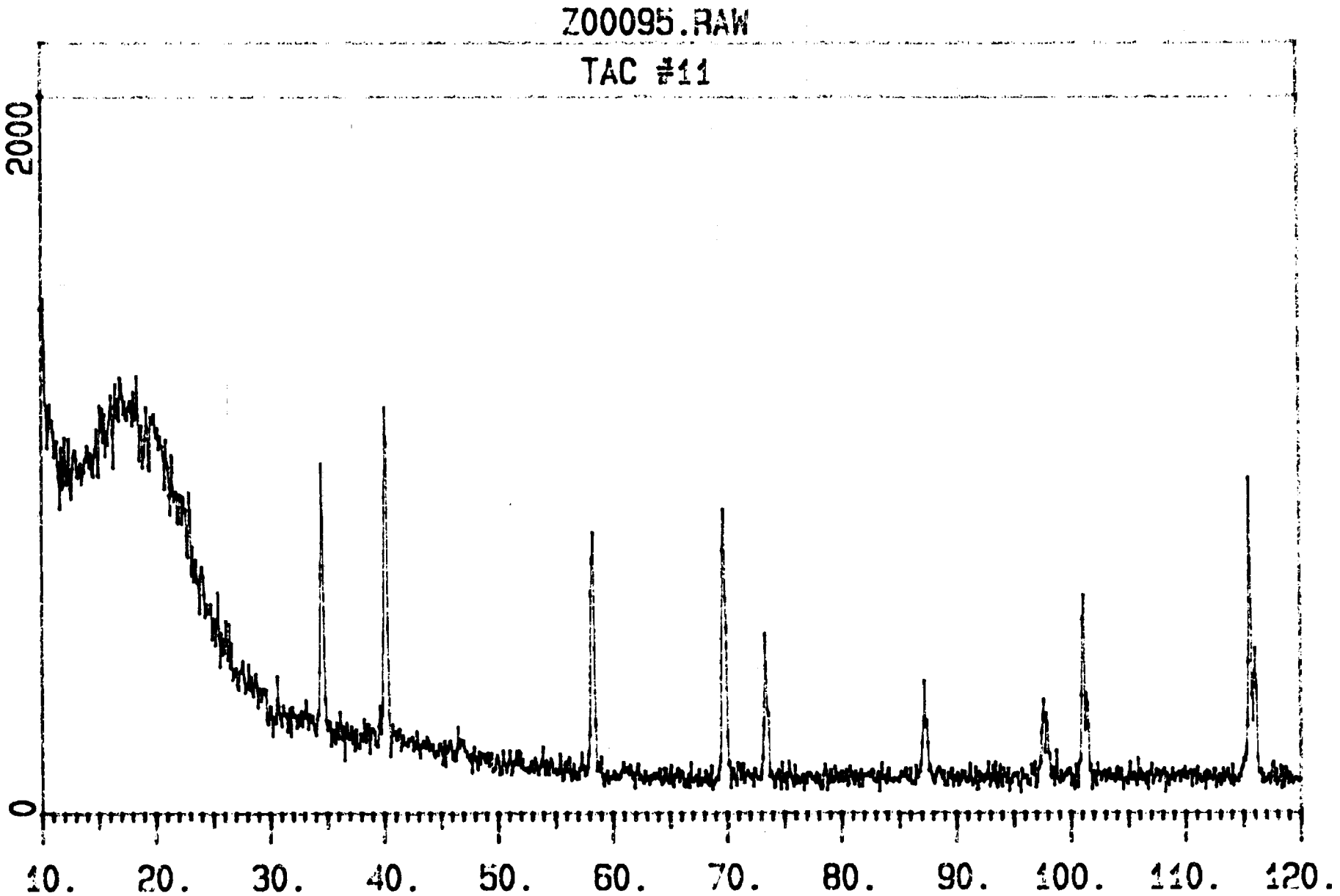
Z00095.RAW
TAC #11
2000
0
10.
20.
30.
40.
50.
60.
70.
80.
90.
100.
110.
120.

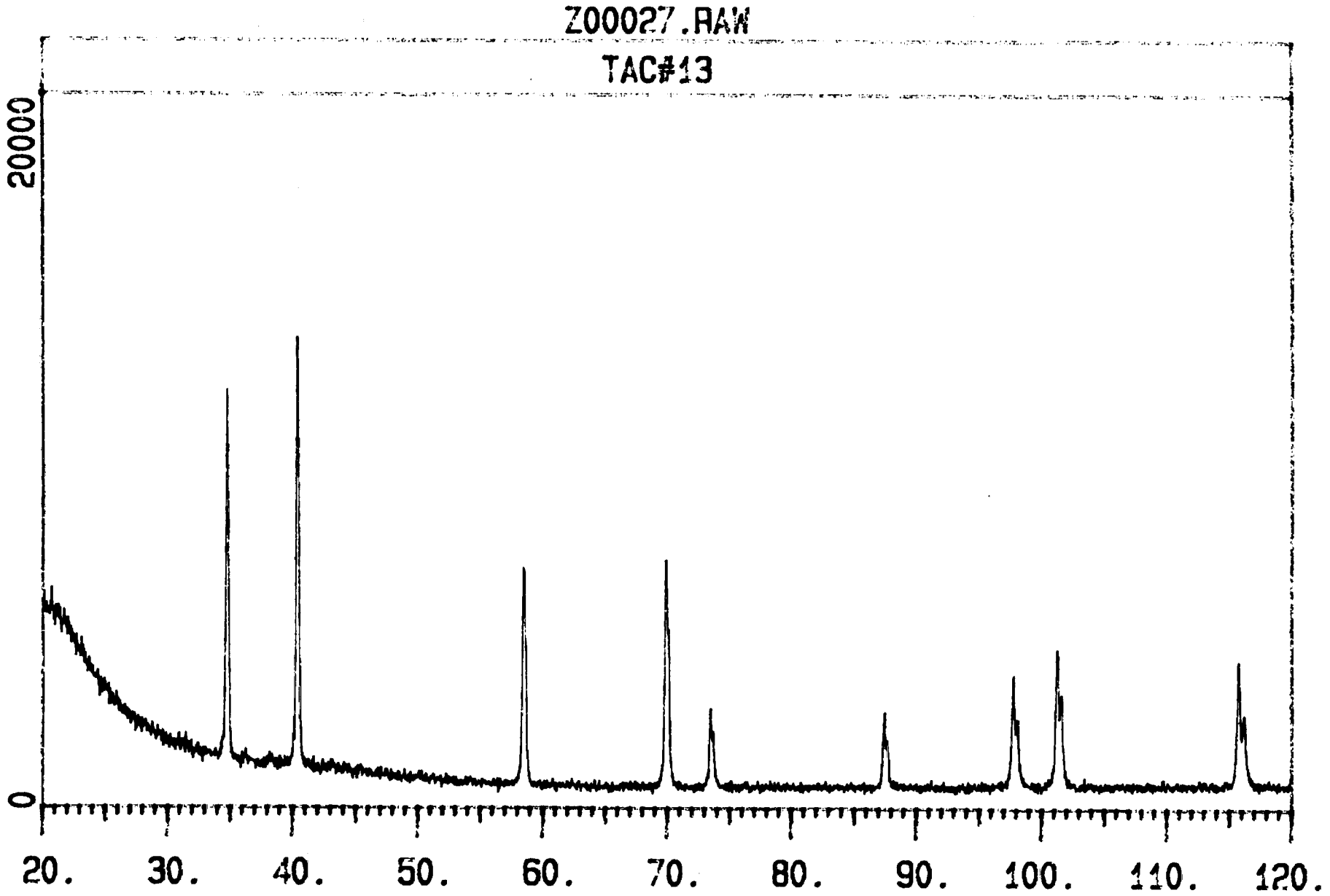
Z00027.RAW
TAC#13
20000
0
20.
30.
40.
50.
60.
70.
80.
90.
100.
110.
120.

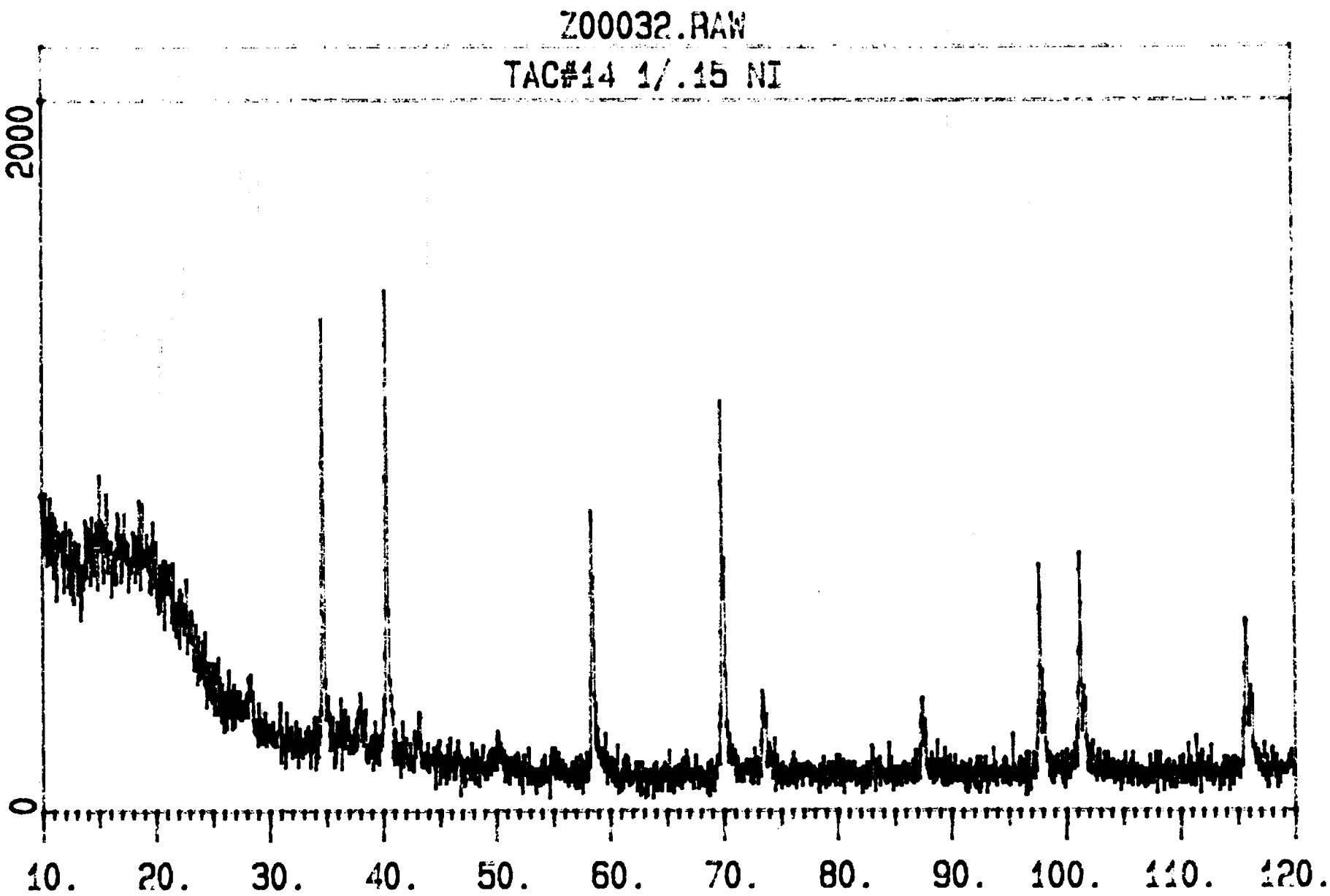
Z00032.RAW
TAC#14 1/.15 NI
2000
0
10.
20.
30.
40.
50.
60.
70.
80.
90.
100.
110.
120.

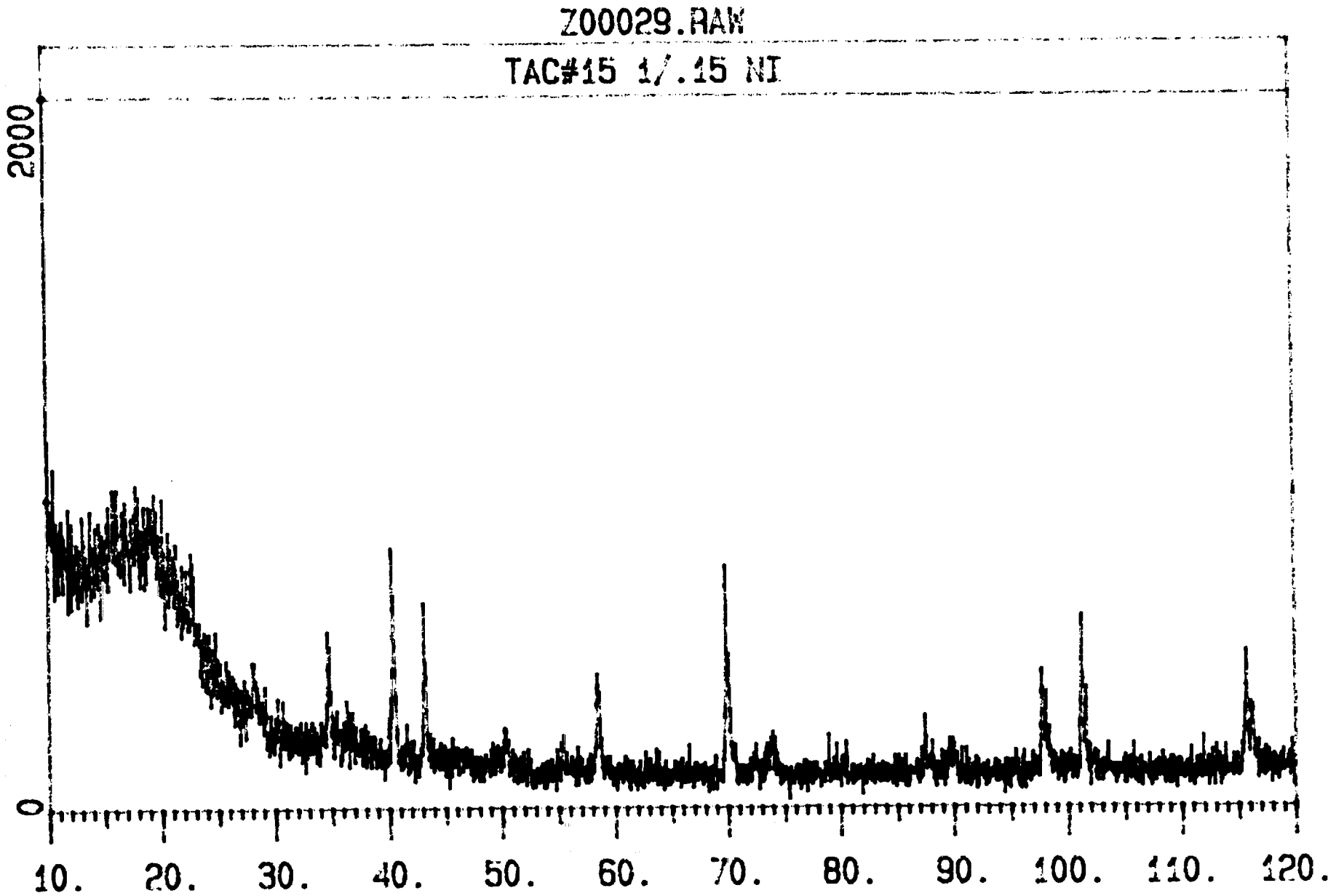
Z00029.RAW
TAC#15 1/.15 NI
2000
0
10.
20.
30.
40.
50.
60.
70.
80.
90.
100.
110.
120.

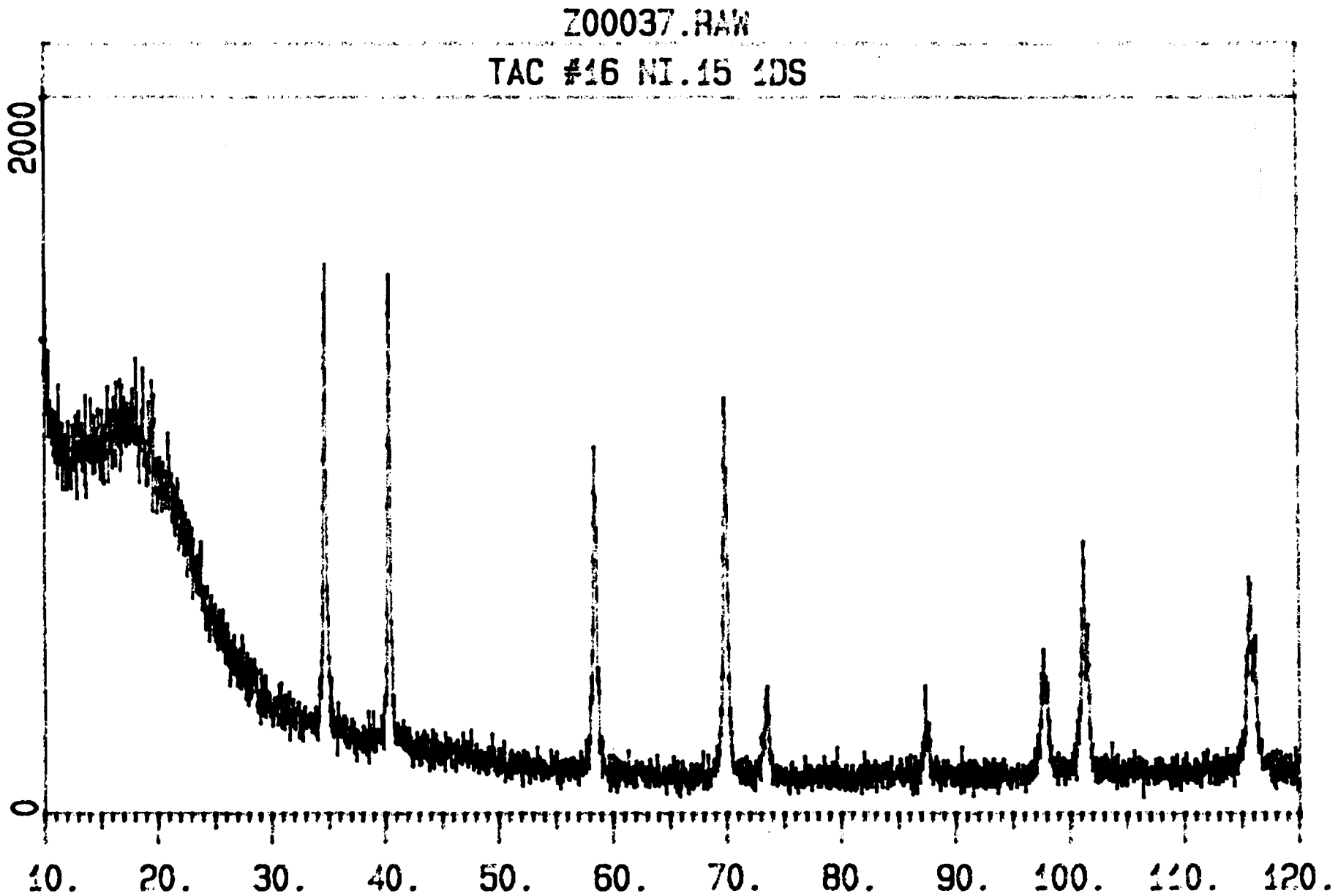
Z00037.RAW
TAC #16 NI.15 1DS
2000
0
10.
20.
30.
40.
50.
60.
70.
80.
90.
100.
110.
120.

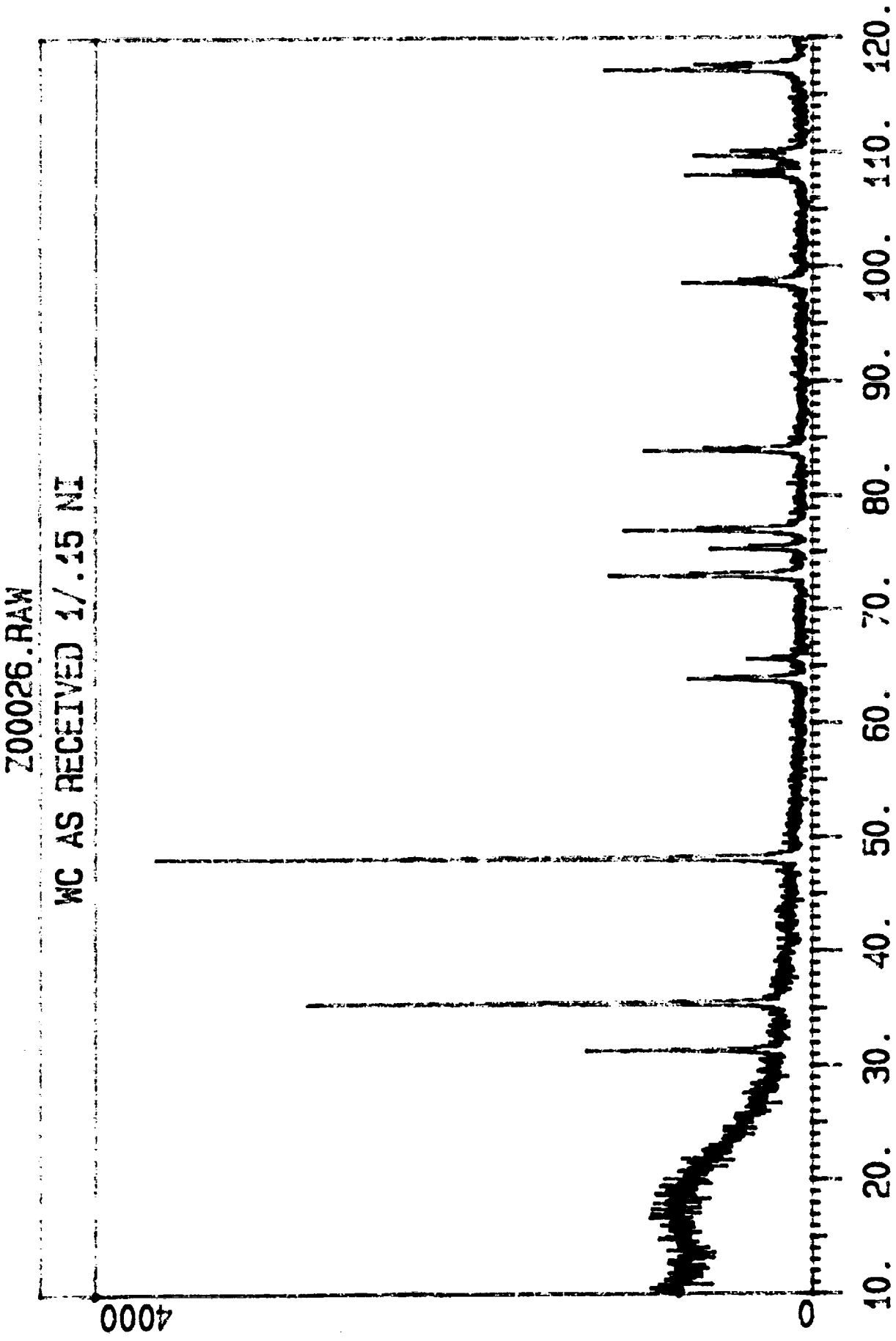
Z00026.RAW
WC AS RECEIVED 1/.15 NI
4000
0
10.
20.
30.
40.
50.
60.
70.
80.
90.
100.
110.
120.

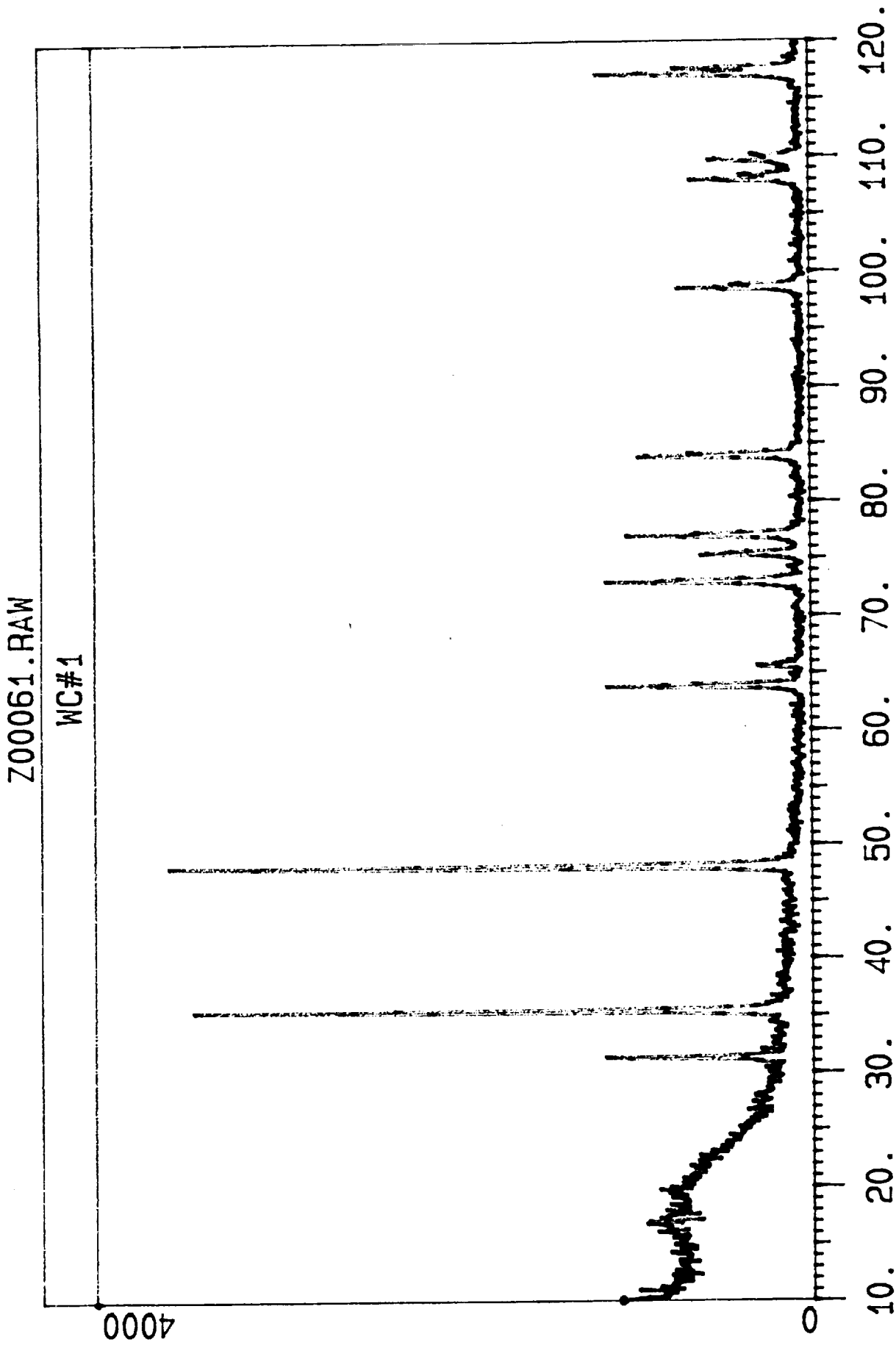
Z00061.RAW
WC#1
4000
0
10.
20.
30.
40.
50.
60.
70.
80.
90.
100.
110.
120.

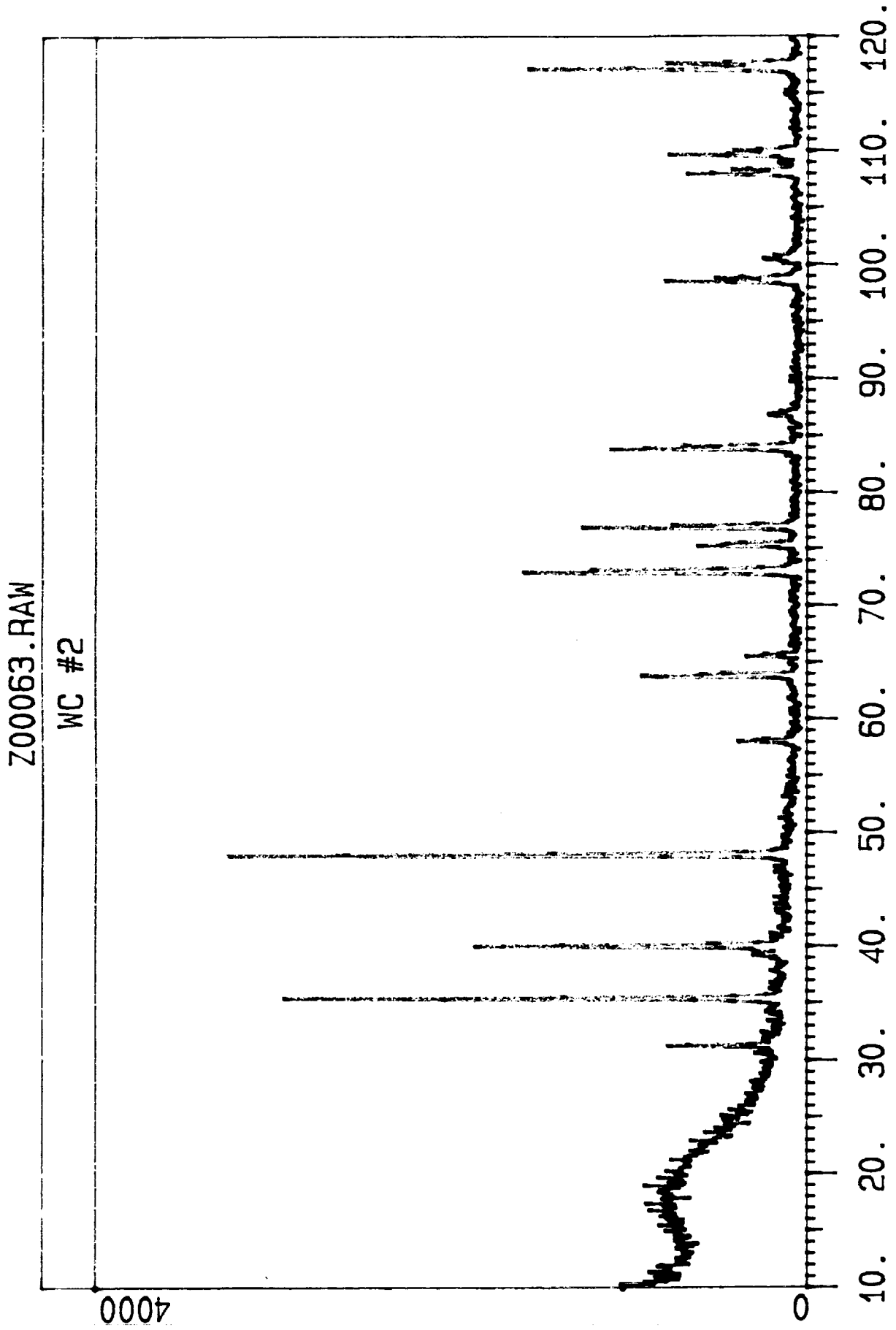
Z00063.RAW
WC #2
4000
0
10.
20.
30.
40.
50.
60.
70.
80.
90.
100.
110.
120.

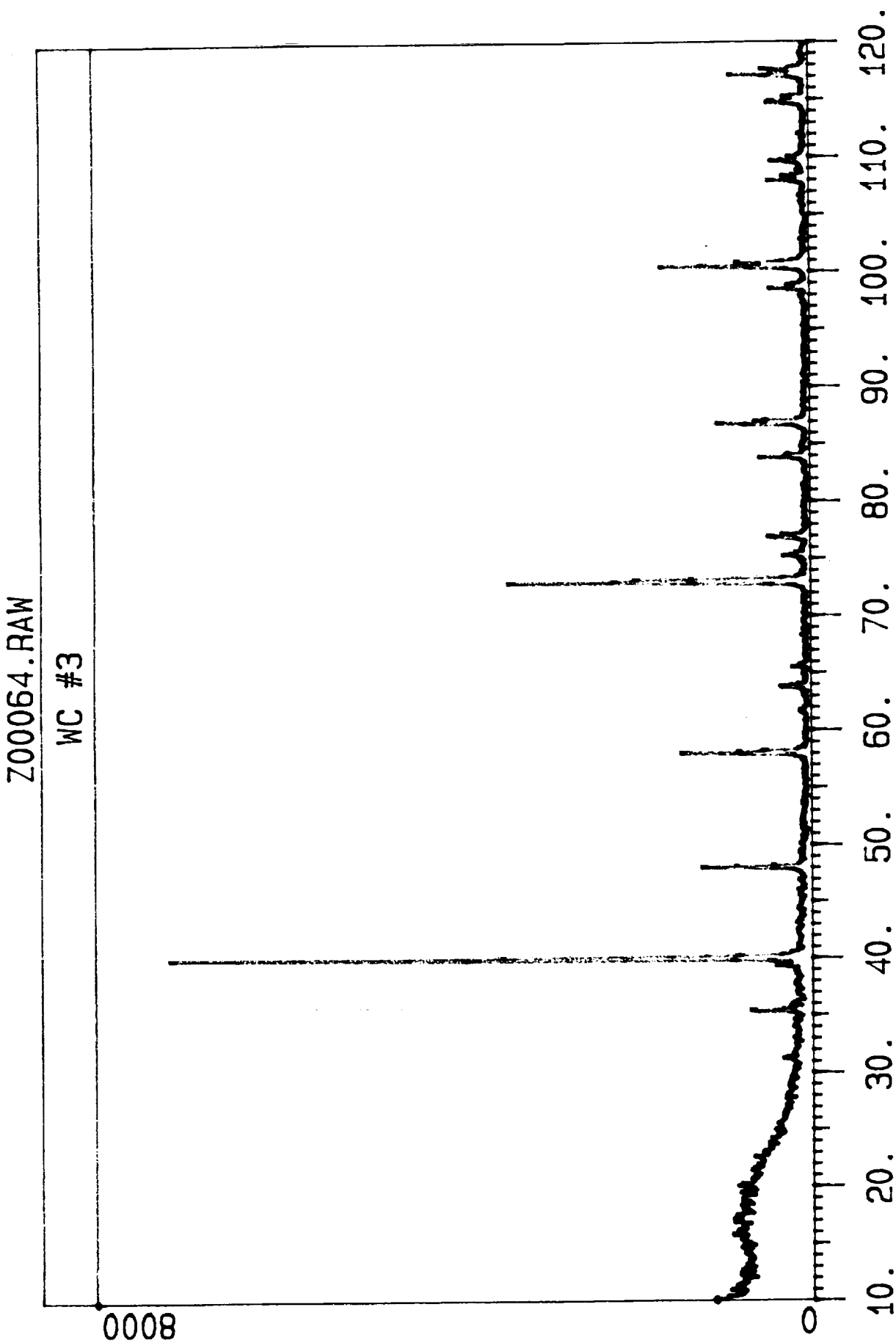
Z00064.RAW
WC #3
8000
0
10.
20.
30.
40.
50.
60.
70.
80.
90.
100.
110.
120.

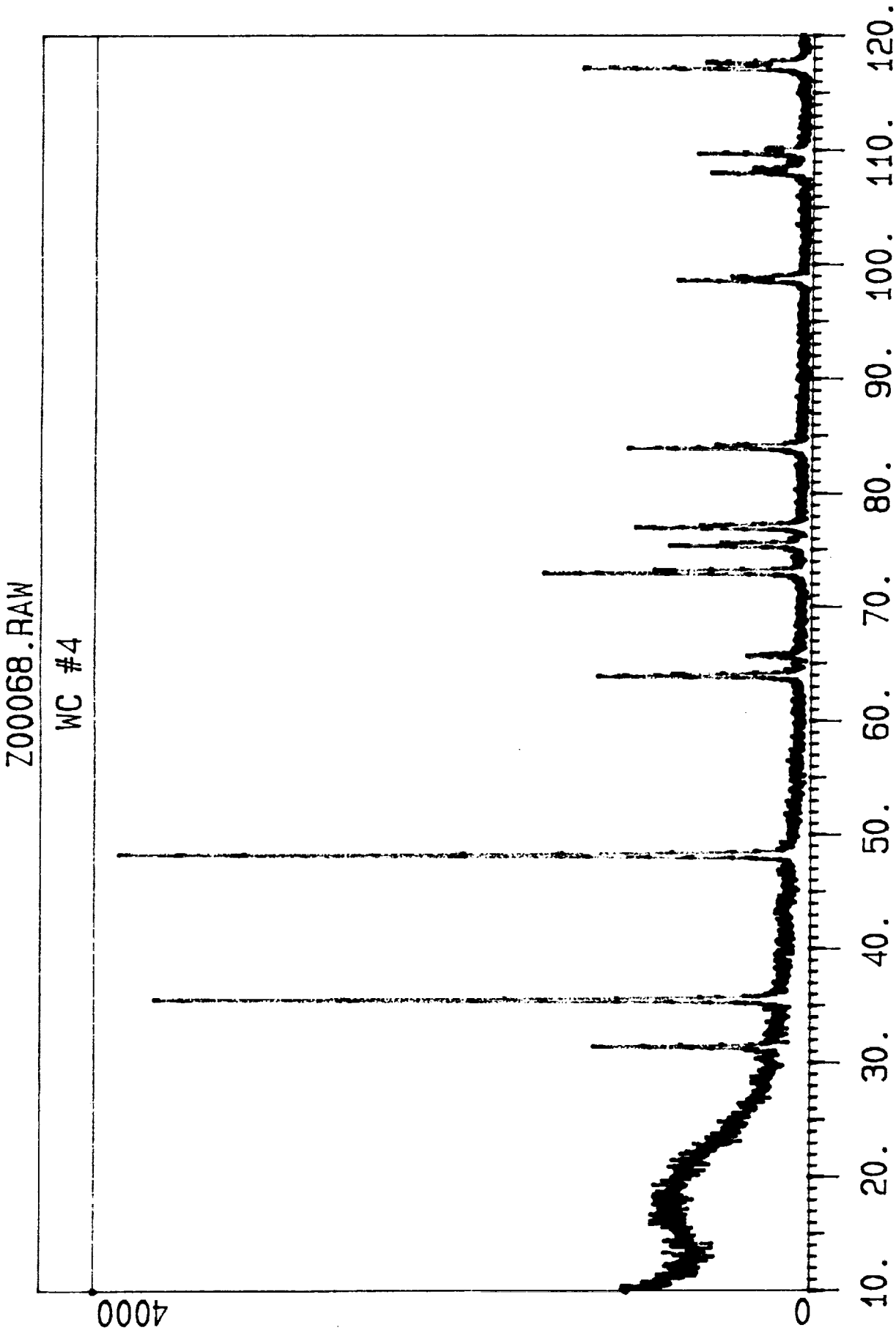
Z00068.RAW
WC #4
4000
0
10.
20.
30.
40.
50.
60.
70.
80.
90.
100.
110.
120.

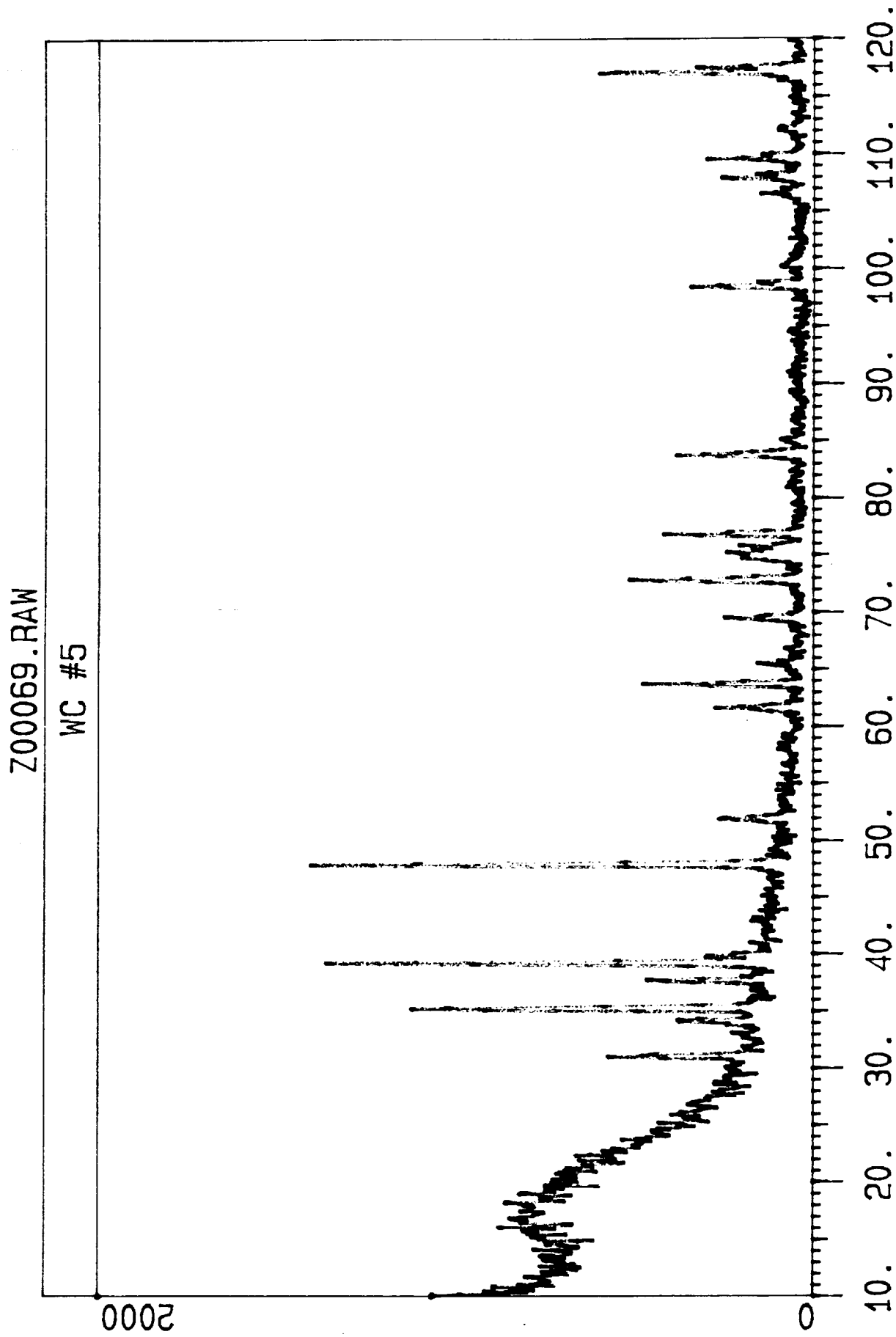
Z00069.RAW
WC #5
2000
0
10.
20.
30.
40.
50.
60.
70.
80.
90.
100.
110.
120.

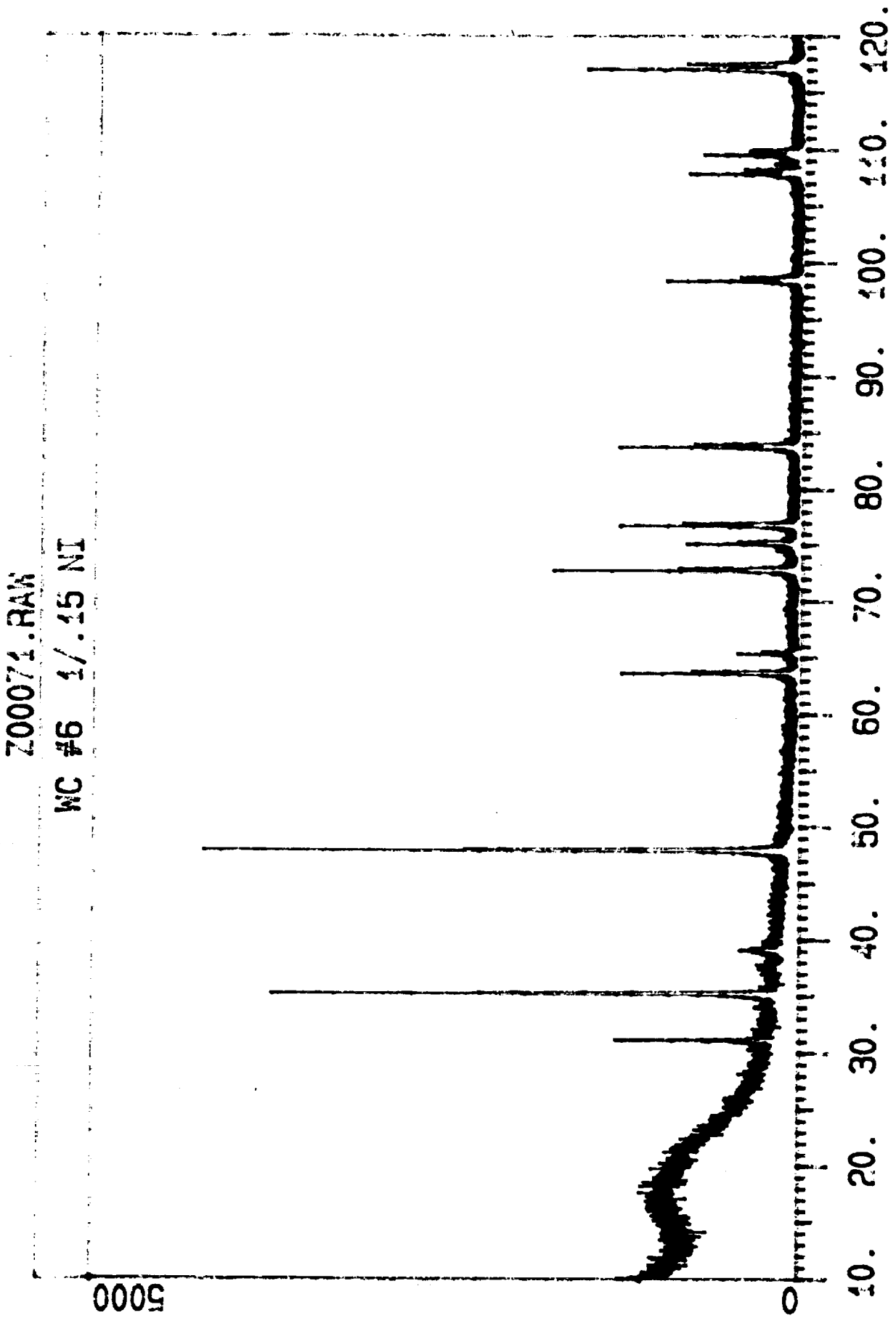
Z00071.RAW
WC #6 1/.15 NI
5000
0
10.
20.
30.
40.
50.
60.
70.
80.
90.
100.
110.
120.

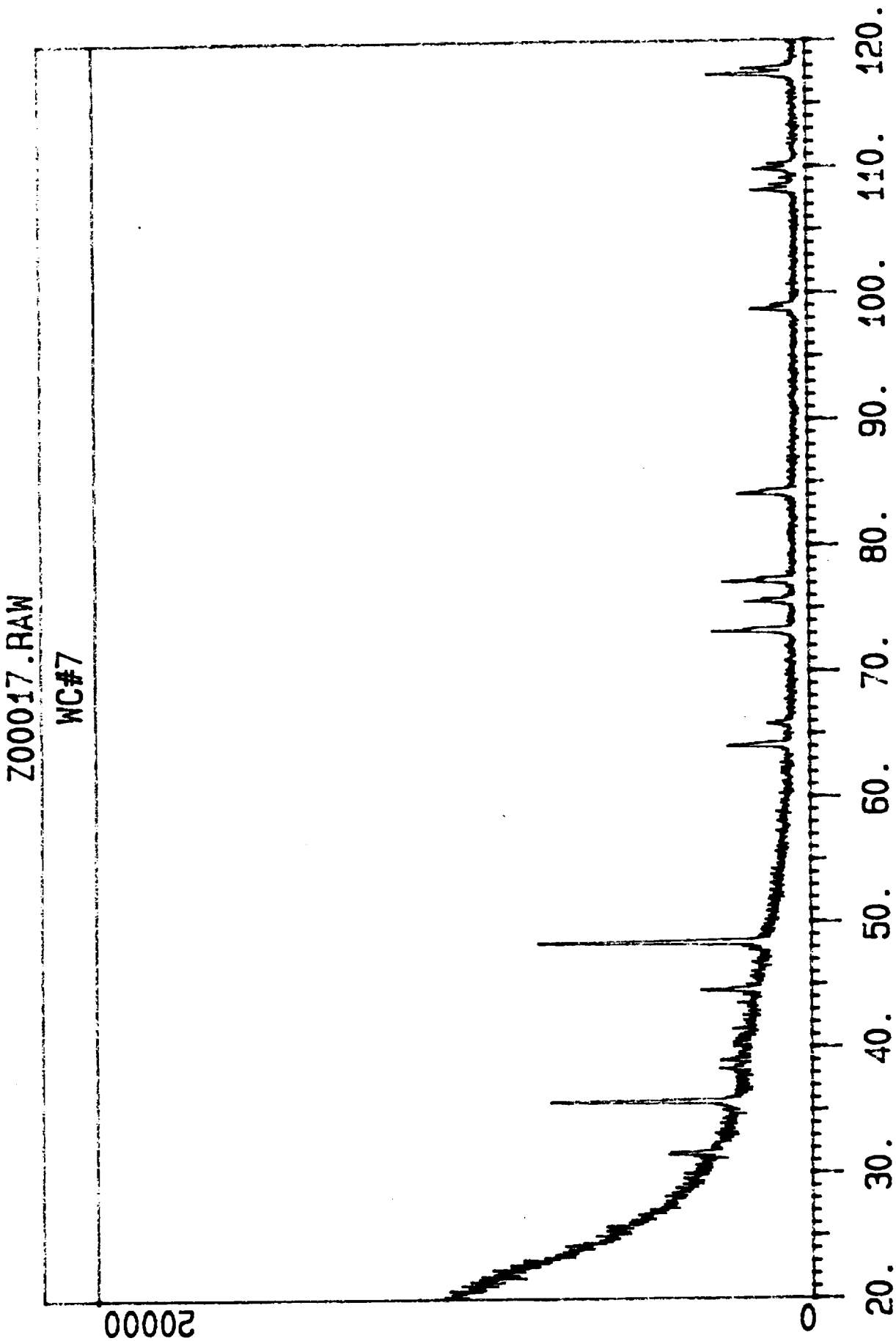
Z00017.RAW
WC#7
20000
0
20.
30.
40.
50.
60.
70.
80.
90.
100.
110.
120.

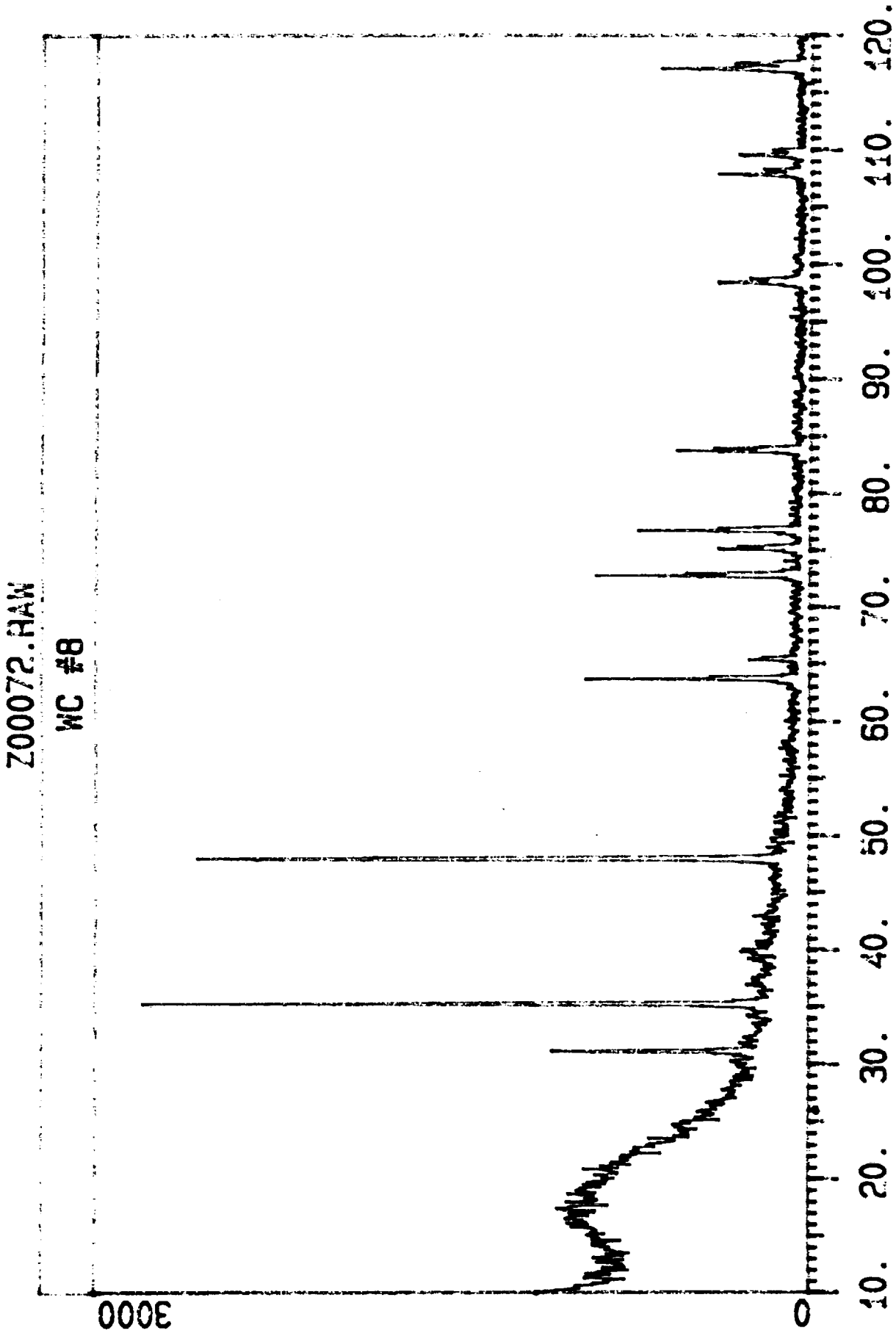
Z00072.RAW
WC #8
3000
0
10.
20.
30.
40.
50.
60.
70.
80.
90.
100.
110.
120.

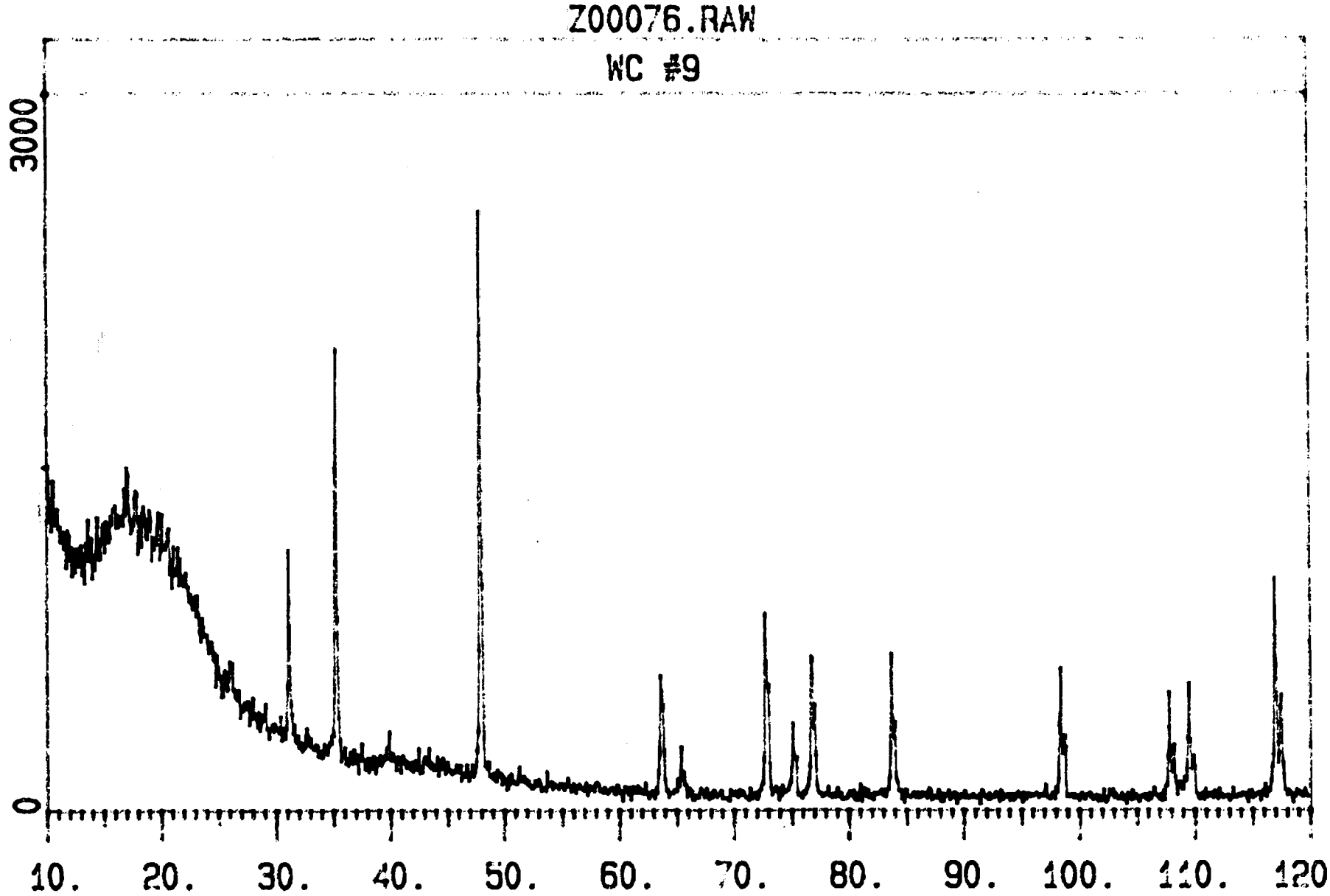
Z00076.RAW
WC #9
3000
0
10.
20.
30.
40.
50.
60.
70.
80.
90.
100.
110.
120.

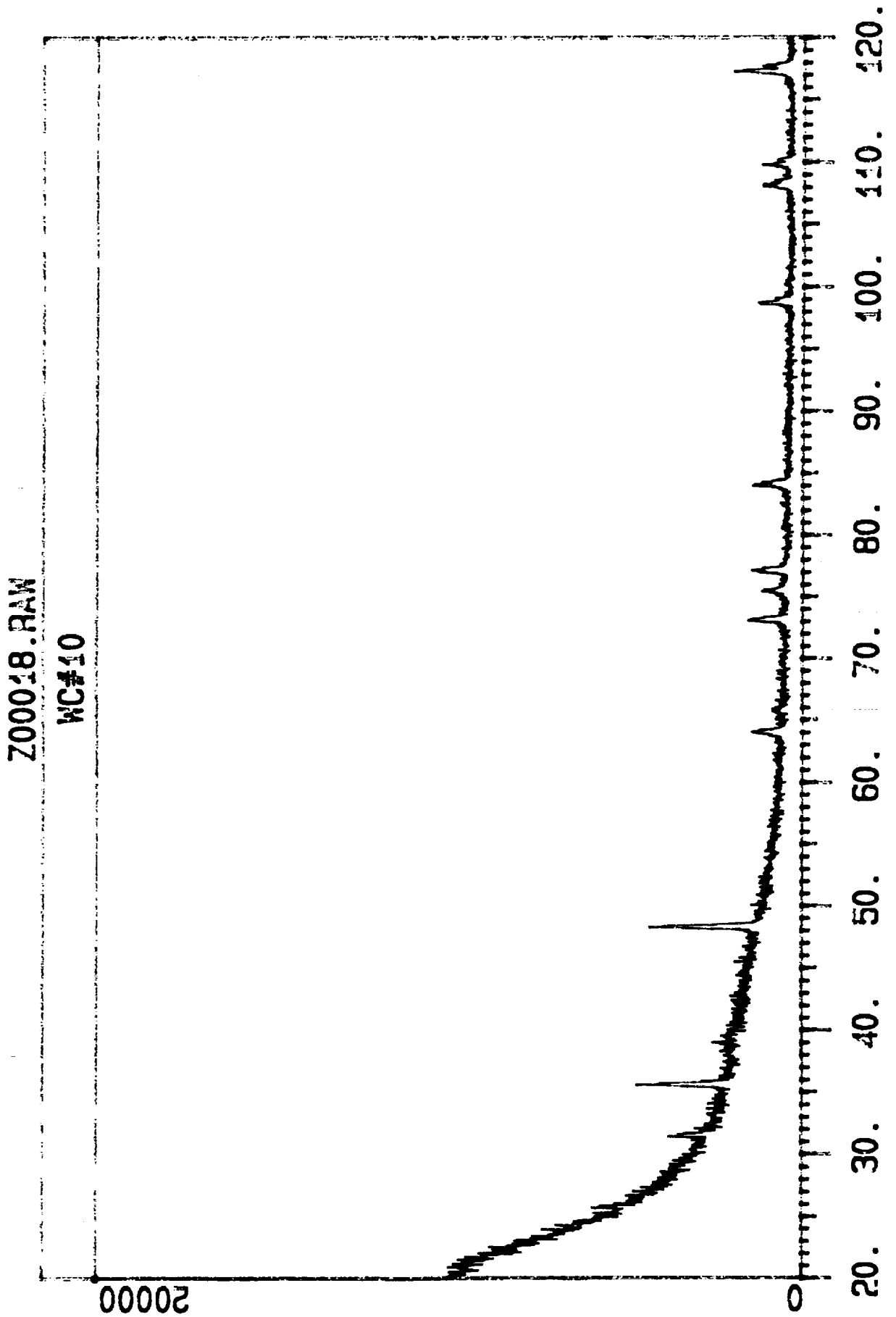
Z00018.RAW
WC#10
20000
0
20.
30.
40.
50.
60.
70.
80.
90.
100.
110.
120.

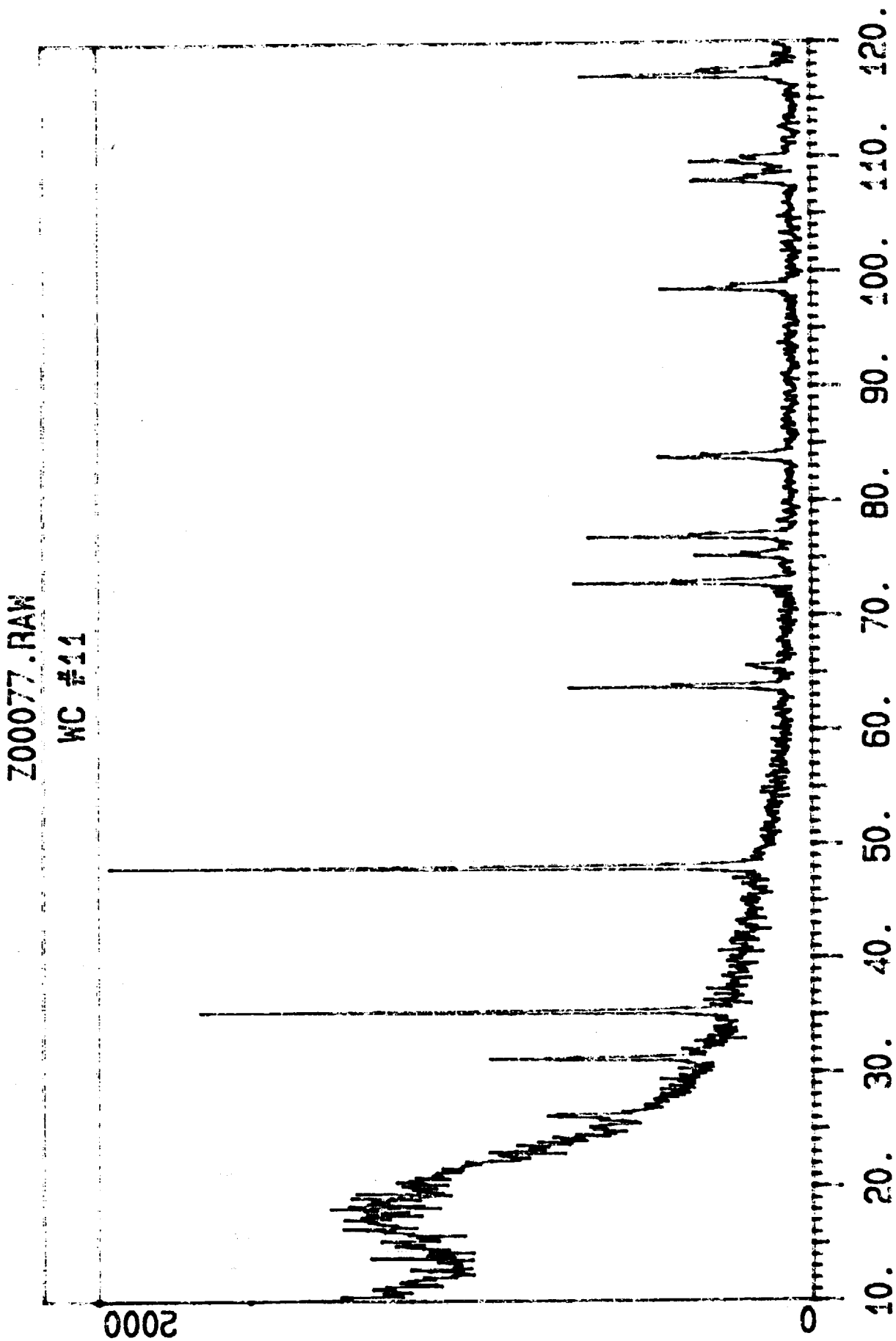
Z00077.RAW
WC #11
2000
0
10.
20.
30.
40.
50.
60.
70.
80.
90.
100.
110.
120.

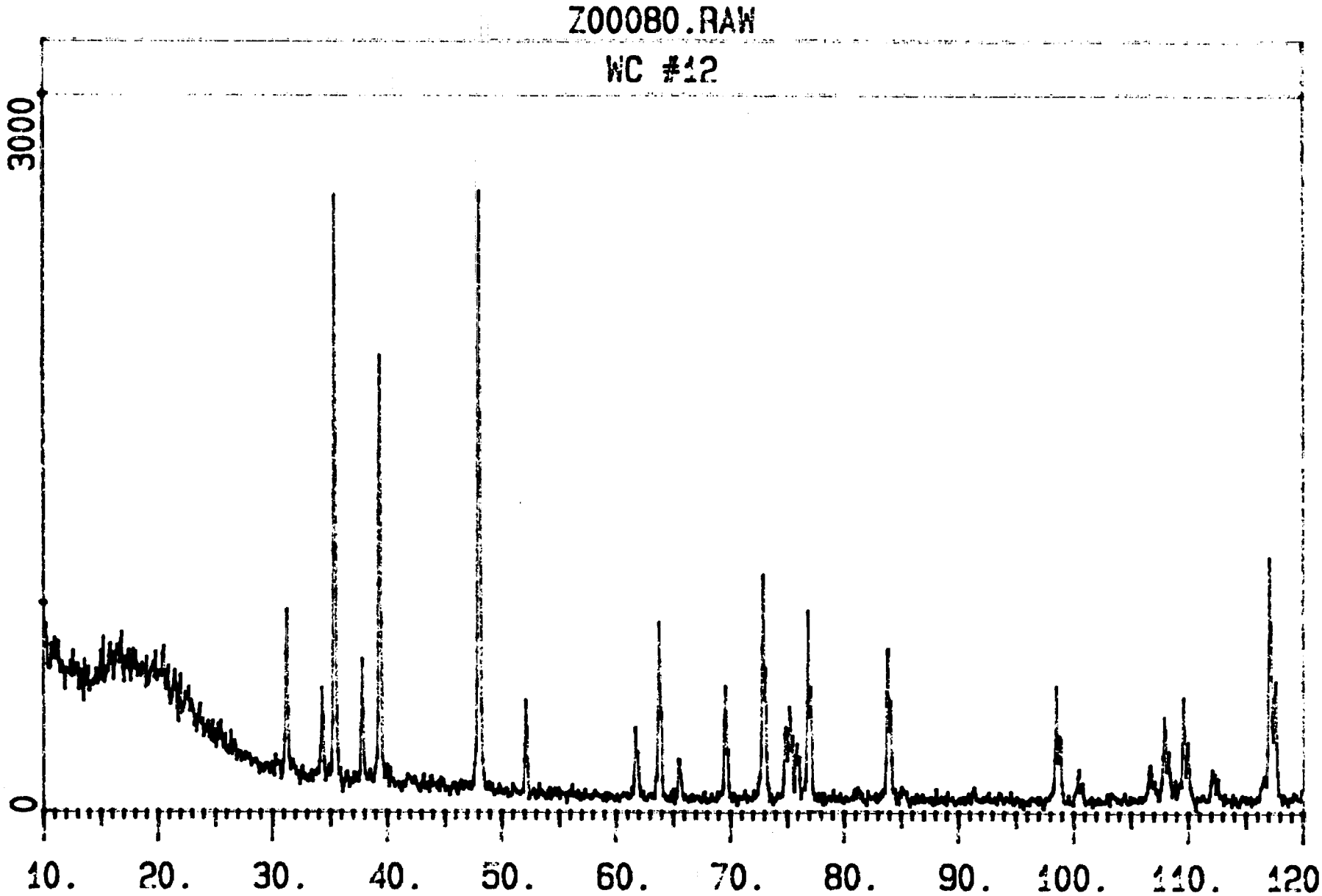
Z00080.RAW
WC #12
3000
0
10.
20.
30.
40.
50.
60.
70.
80.
90.
100.
110.
120.

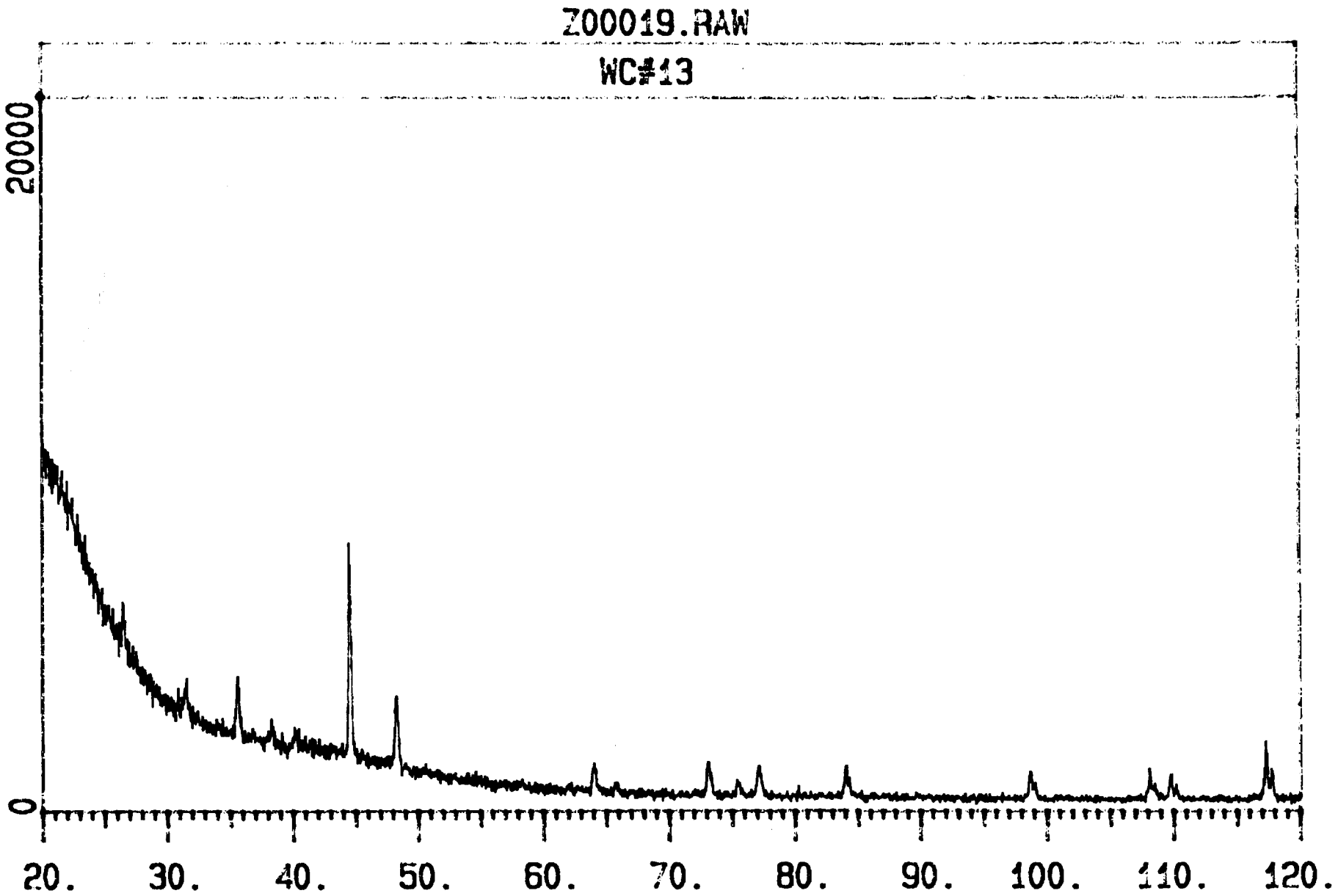
Z00019.RAW
WC#13
20000
0
20.
30.
40.
50.
60.
70.
80.
90.
100.
110.
120.

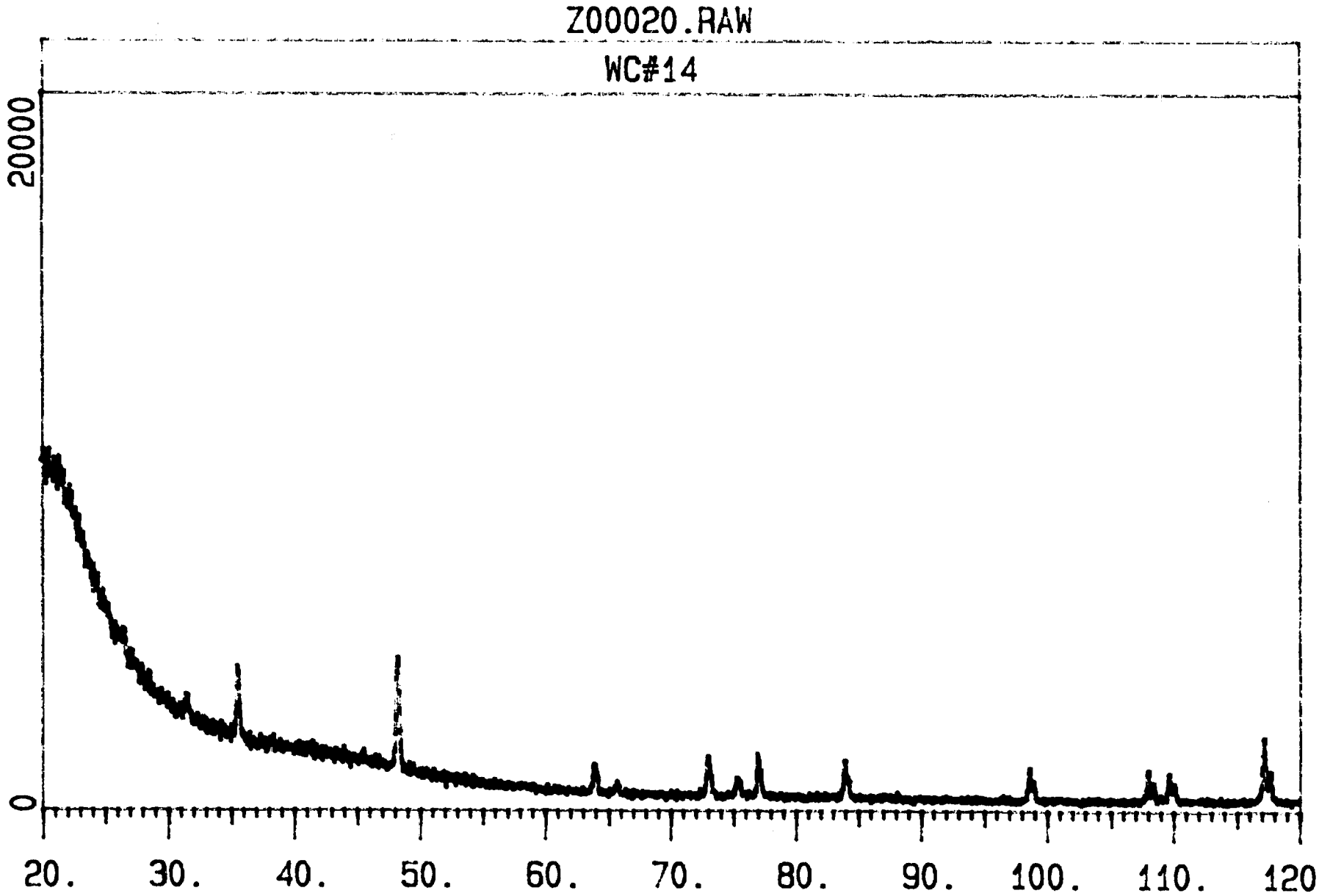
Z00020.RAW
WC#14
20000
0
20.
30.
40.
50.
60.
70.
80.
90.
100.
110.
120.

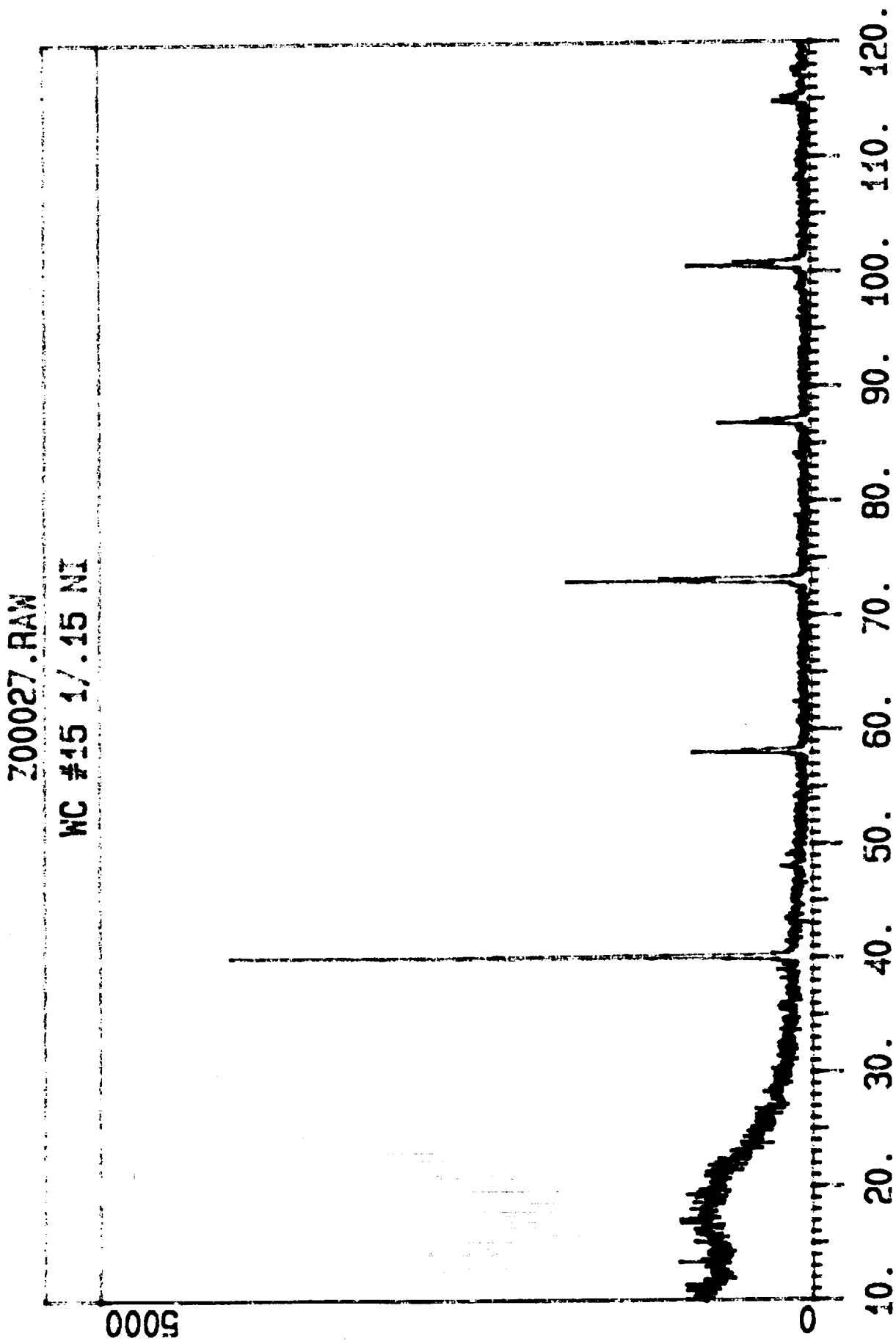
Z00027.RAW
WC #15 1/.15 NI
5000
0
10.
20.
30.
40.
50.
60.
70.
80.
90.
100.
110.
120.

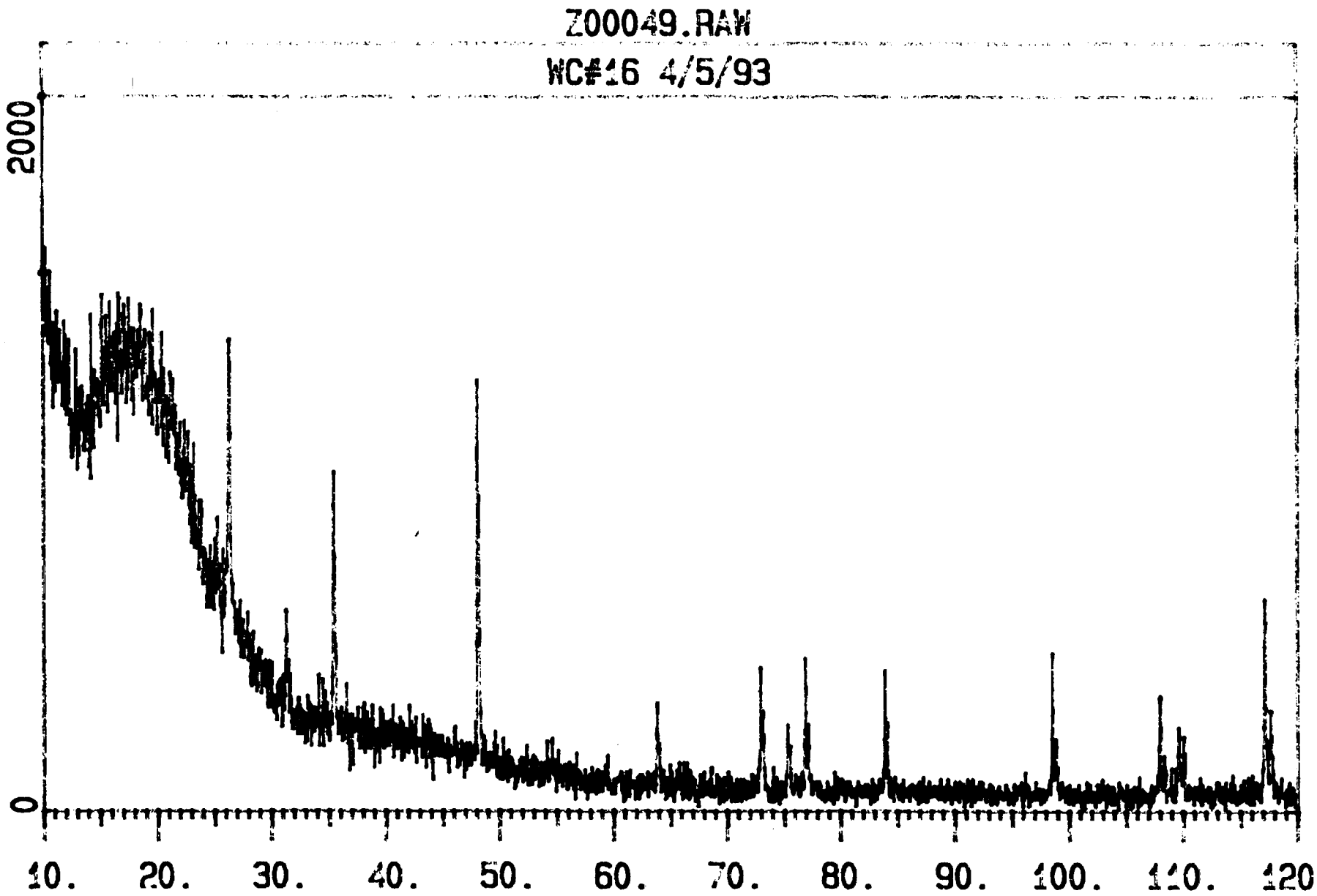
Z00049.RAW
WC#16 4/5/93
2000
0
10.
20.
30.
40.
50.
60.
70.
80.
90.
100.
110.
120.

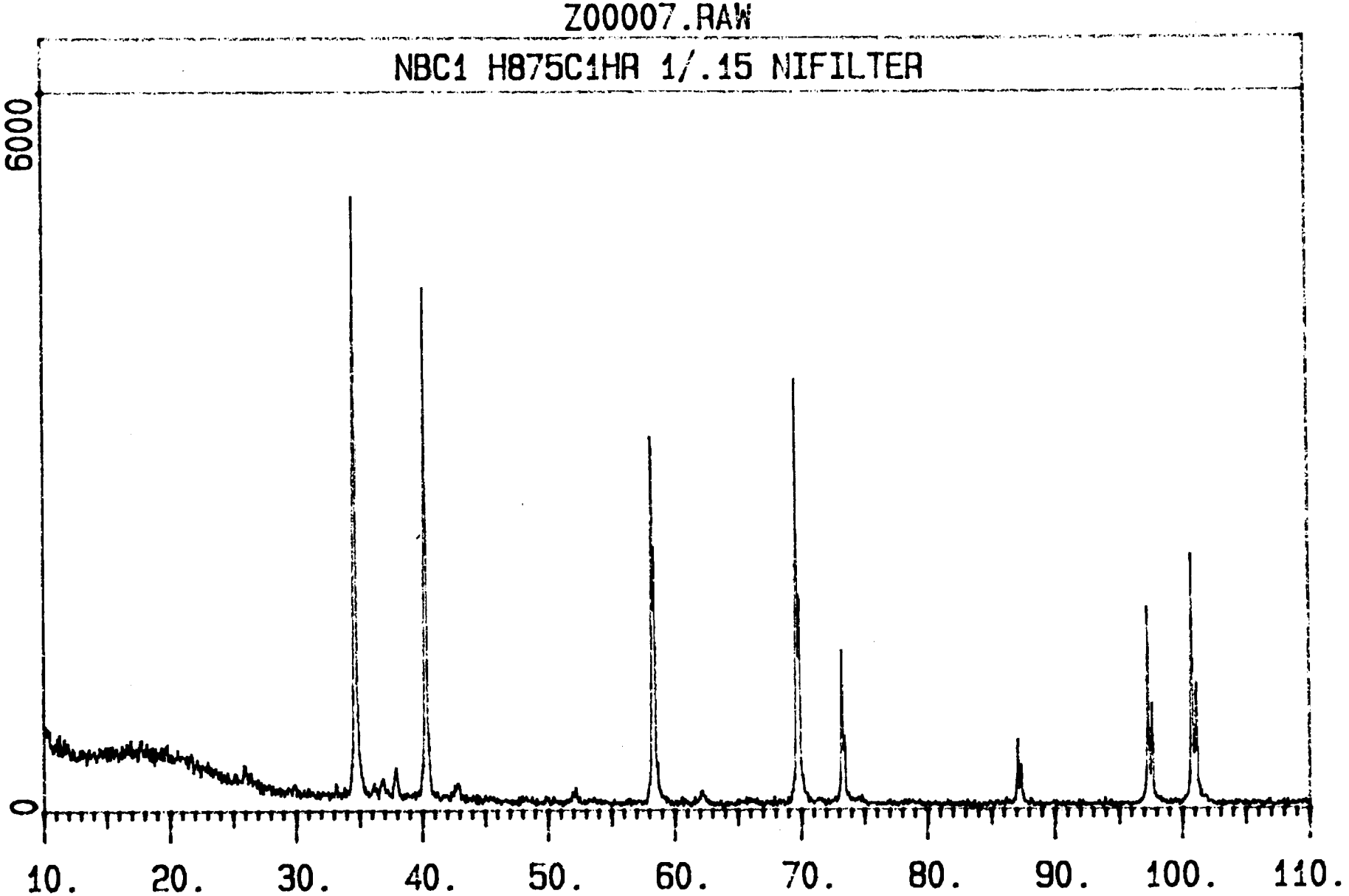
Z00007.RAW
NBC1 H875C1HR 1/.15 NIFILTER
6000
0
10.
20.
30.
40.
50.
60.
70.
80.
90.
100.
110.

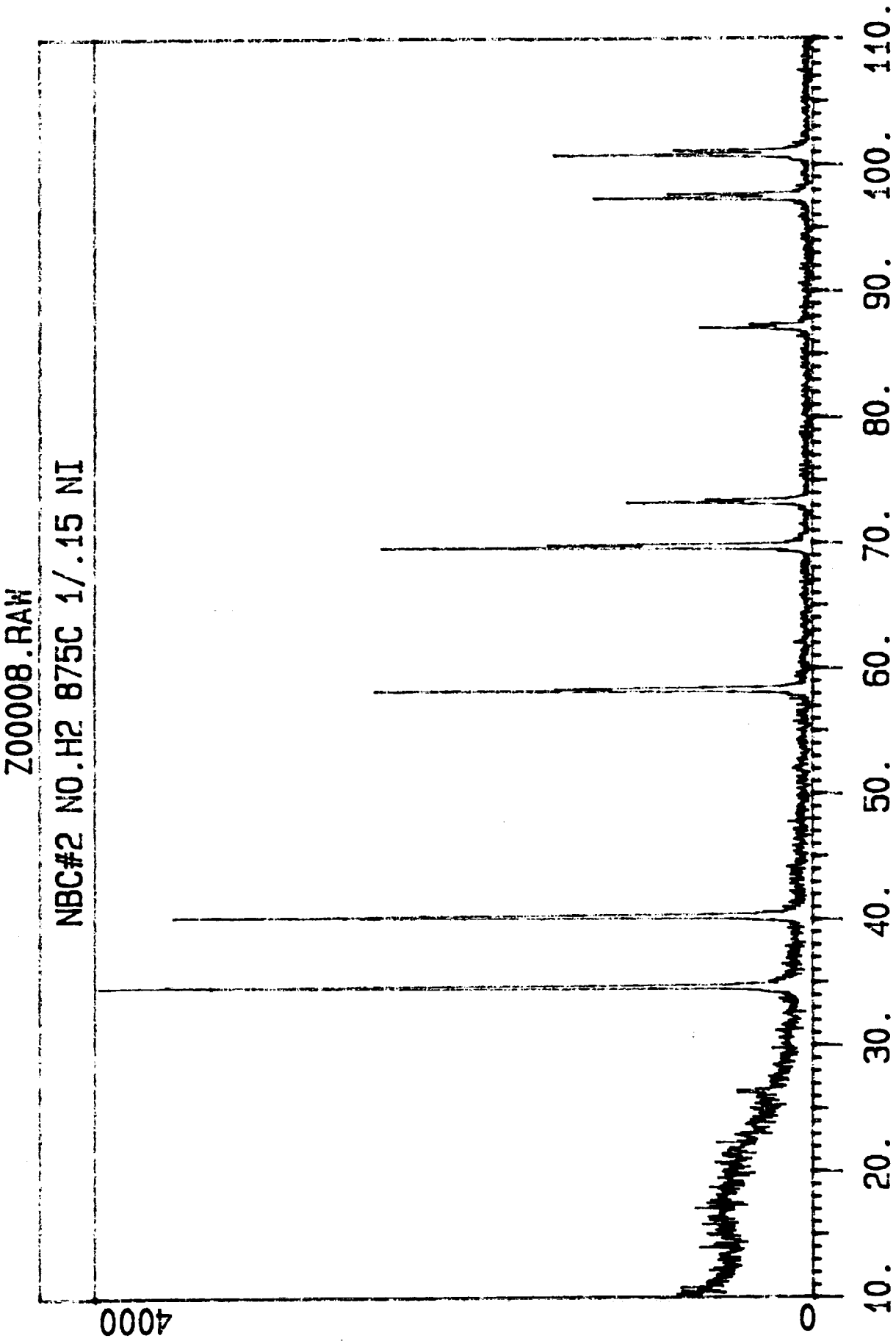
Z00008.RAW
NBC#2 NO.H2 875C 1/.15 NI
4000
0
10.
20.
30.
40.
50.
60.
70.
80.
90.
100.
110.

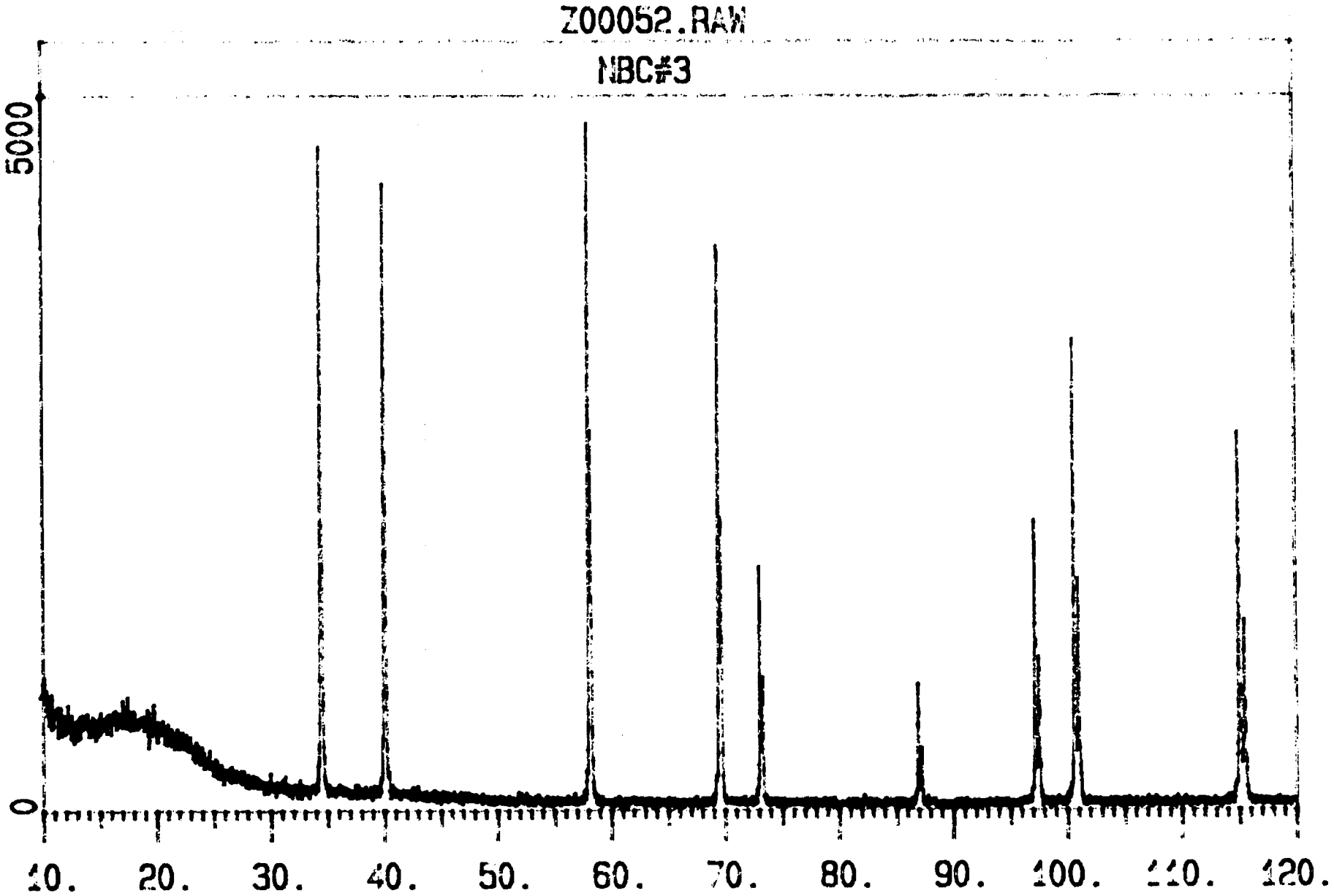
Z00052.RAW
NBC#3
5000
0
10.
20.
30.
40.
50.
60.
70.
80.
90.
100.
110.
120.

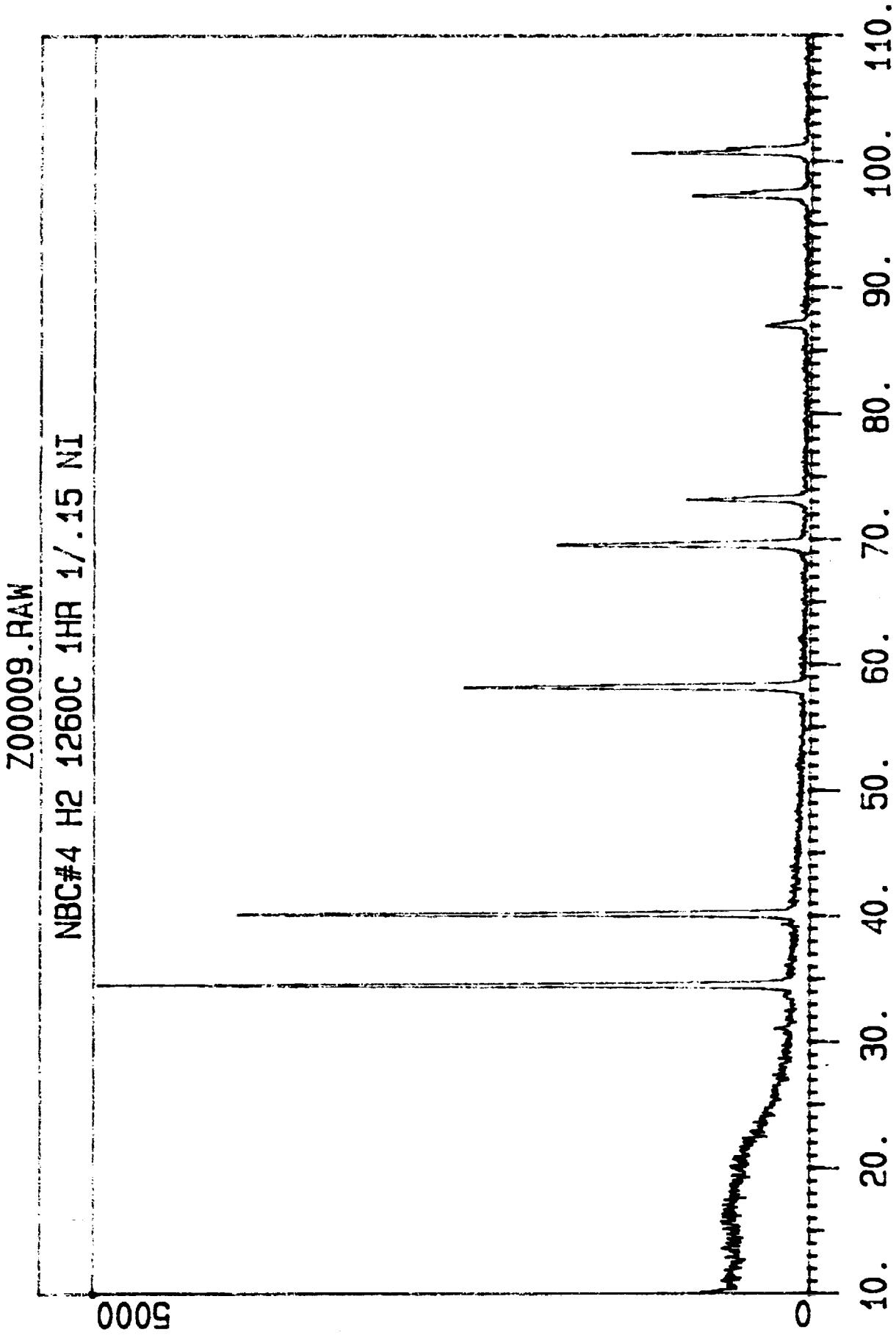
Z00009.RAW
NBC#4 H2 1260C 1HR 1/.15 NI
5000
0
10.
20.
30.
40.
50.
60.
70.
80.
90.
100.
110.

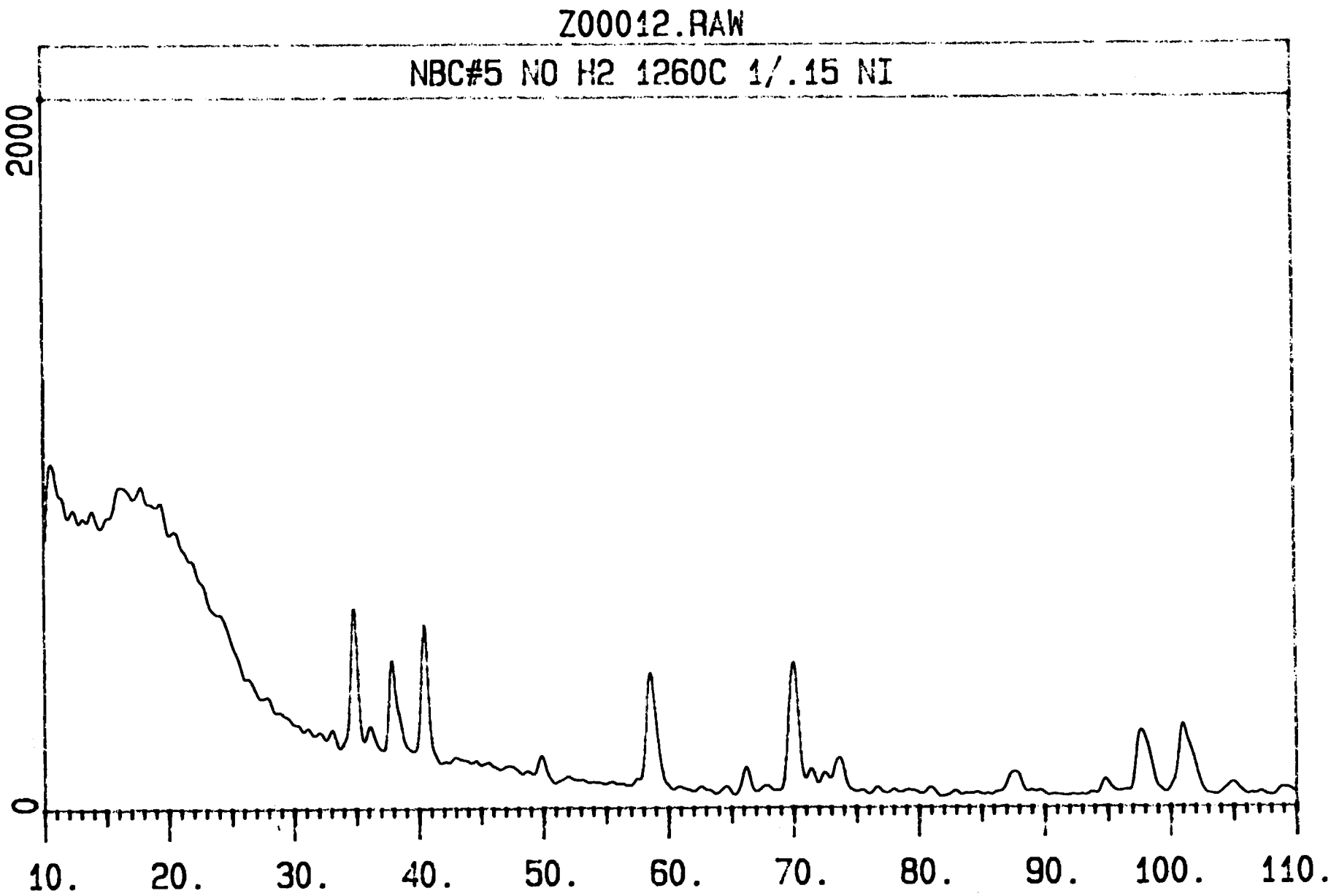
Z00012.RAW
NBC#5 NO H2 1260C 1/.15 NI
2000
0
10.
20.
30.
40.
50.
60.
70.
80.
90.
100.
110.

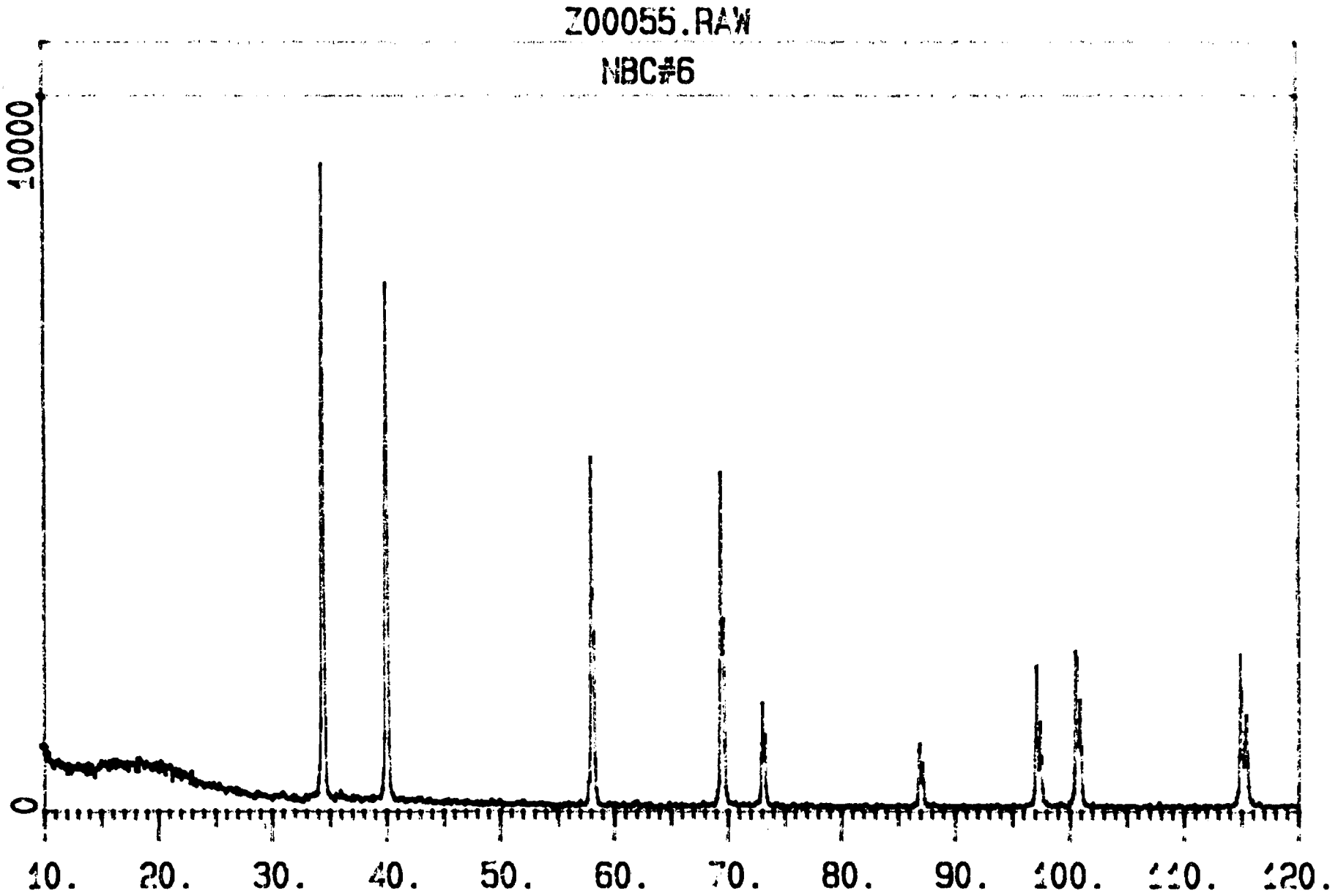
Z00055.RAW
NBC#6
10000
0
10.
20.
30.
40.
50.
60.
70.
80.
90.
100.
110.
120.

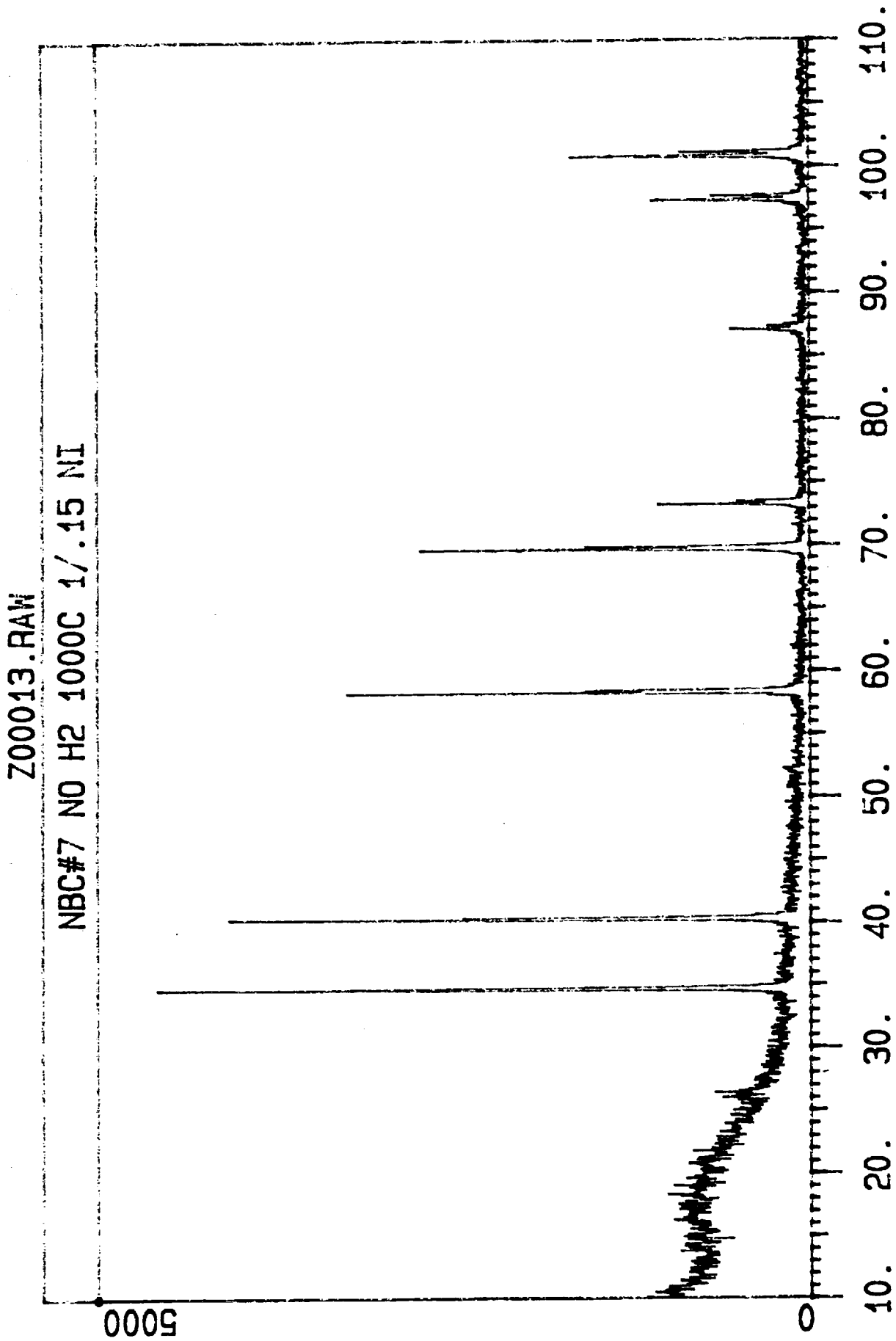
Z00013.RAW
NBC#7 NO H2 1000C 1/.15 NI
5000
0
10.
20.
30.
40.
50.
60.
70.
80.
90.
100.
110.

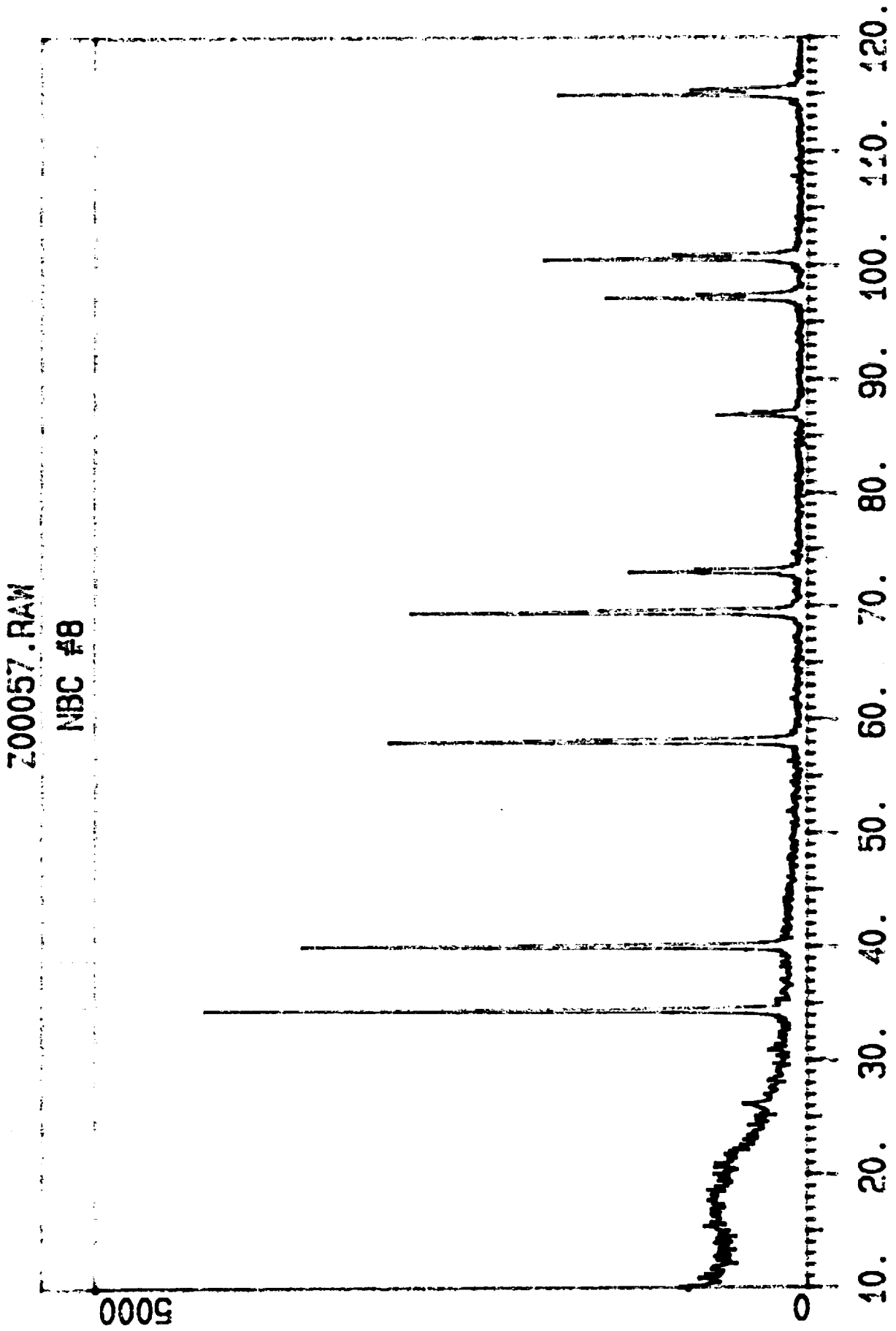
Z000057.RAW
NBC #8
5000
0
10.
20.
30.
40.
50.
60.
70.
80.
90.
100.
110.
120.

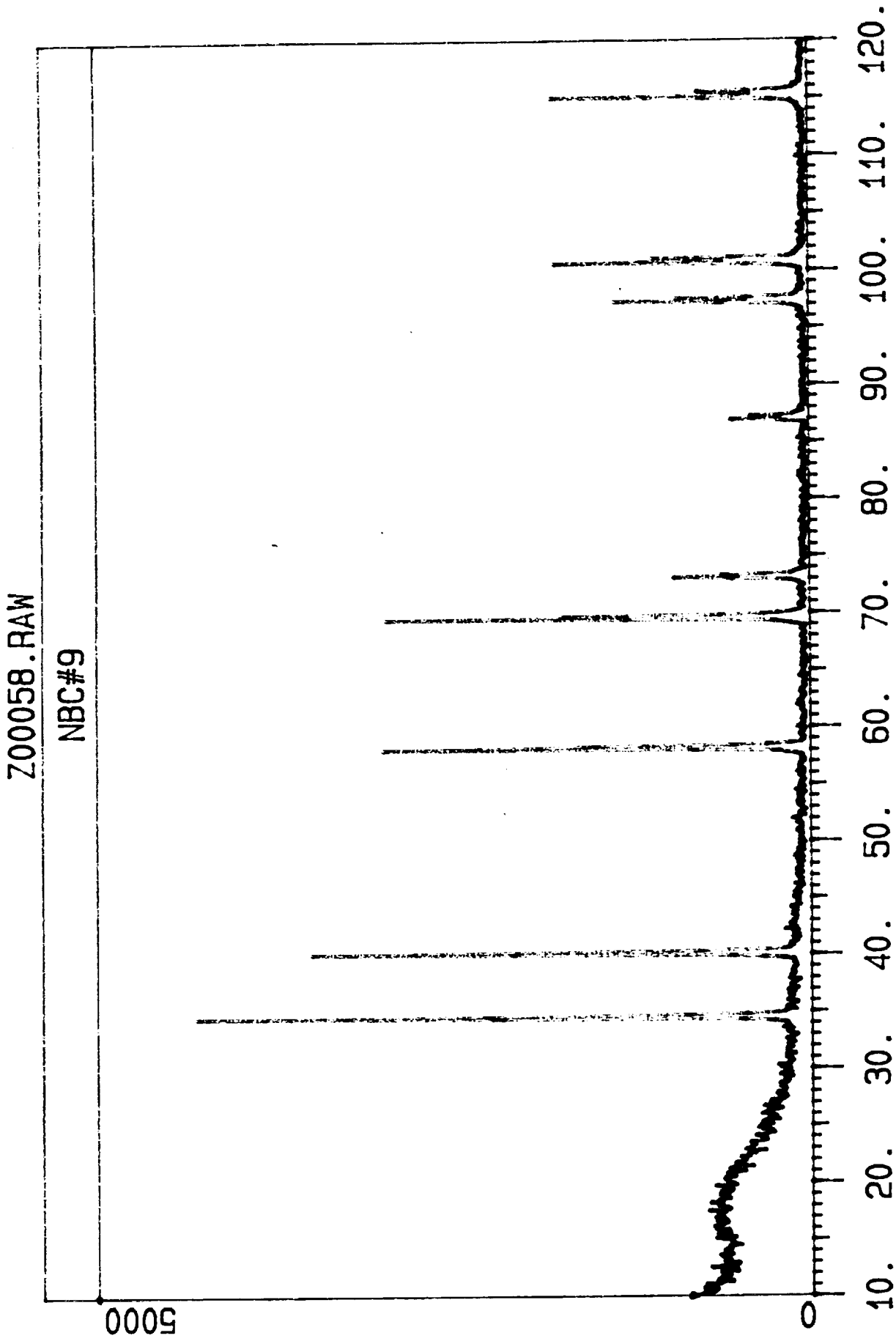
Z00058.RAW
NBC#9
5000
0
10.
20.
30.
40.
50.
60.
70.
80.
90.
100.
110.
120.

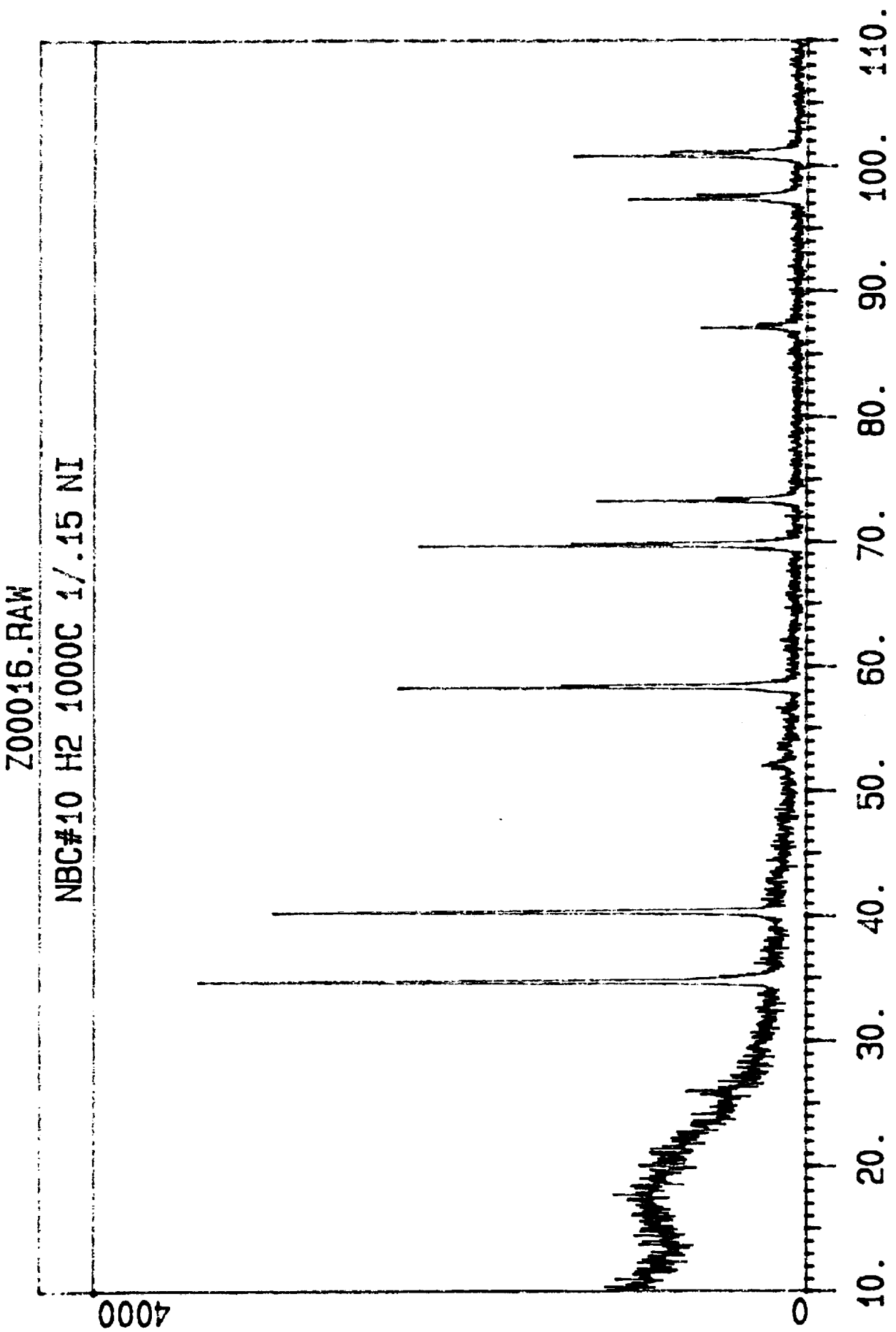
Z00016.RAW
NBC#10 H2 1000C 1/.15 NI
4000
0
10.
20.
30.
40.
50.
60.
70.
80.
90.
100.
110.

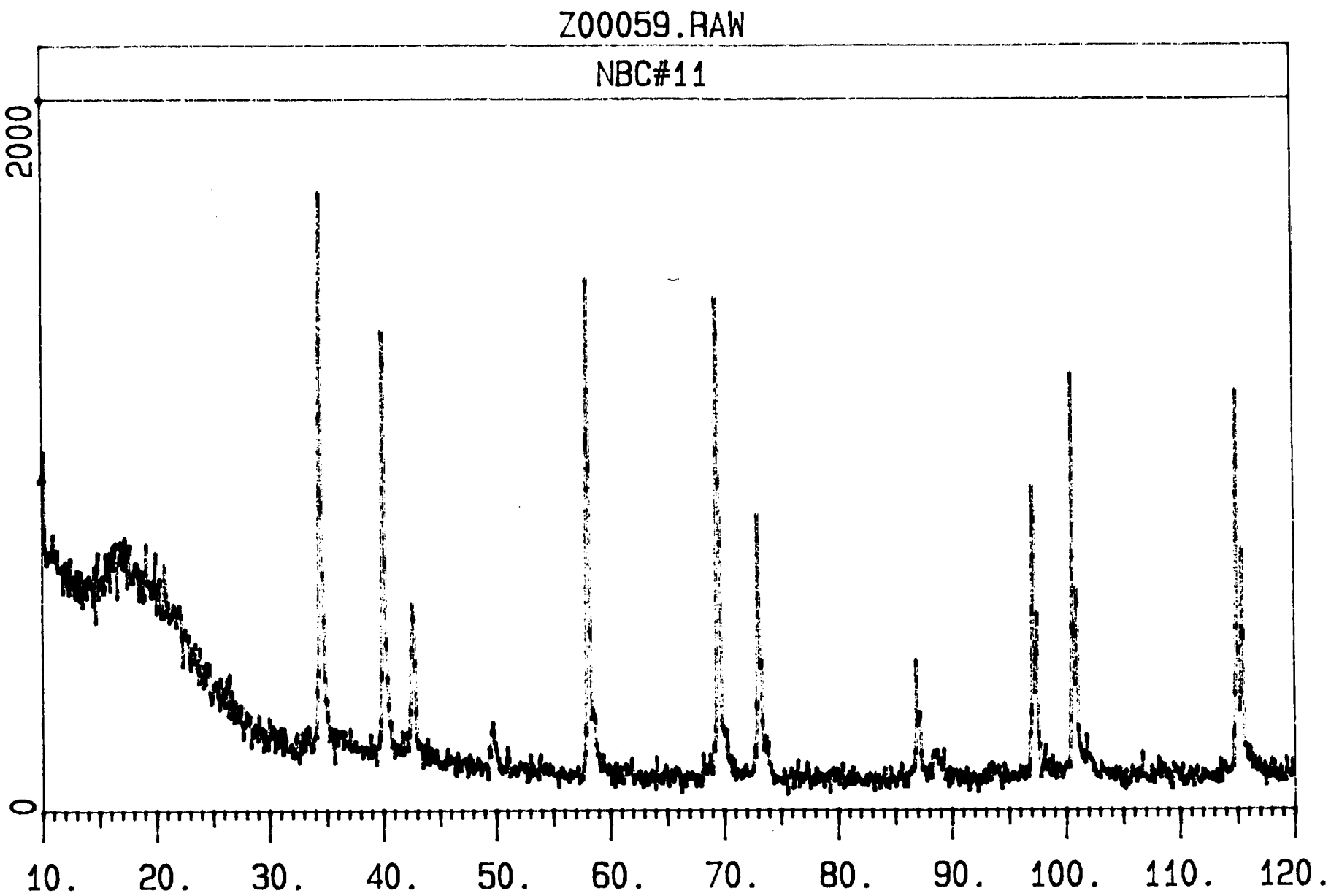
Z00059.RAW
NBC#11
2000
0
10.
20.
30.
40.
50.
60.
70.
80.
90.
100.
110.
120.

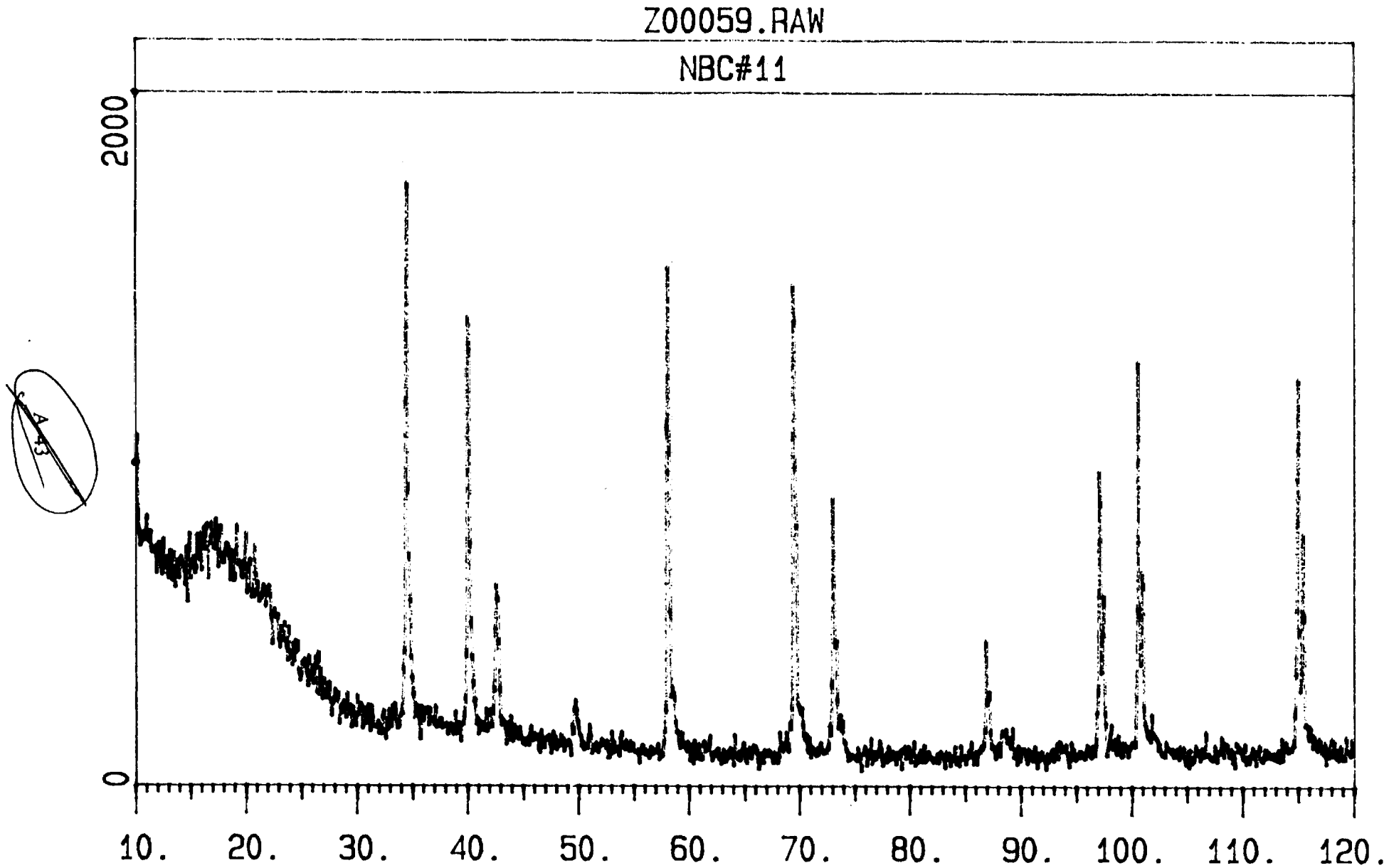
Z00059.RAW
NBC#11
2000
0
10.
20.
30.
40.
50.
60.
70.
80.
90.
100.
110.
120.

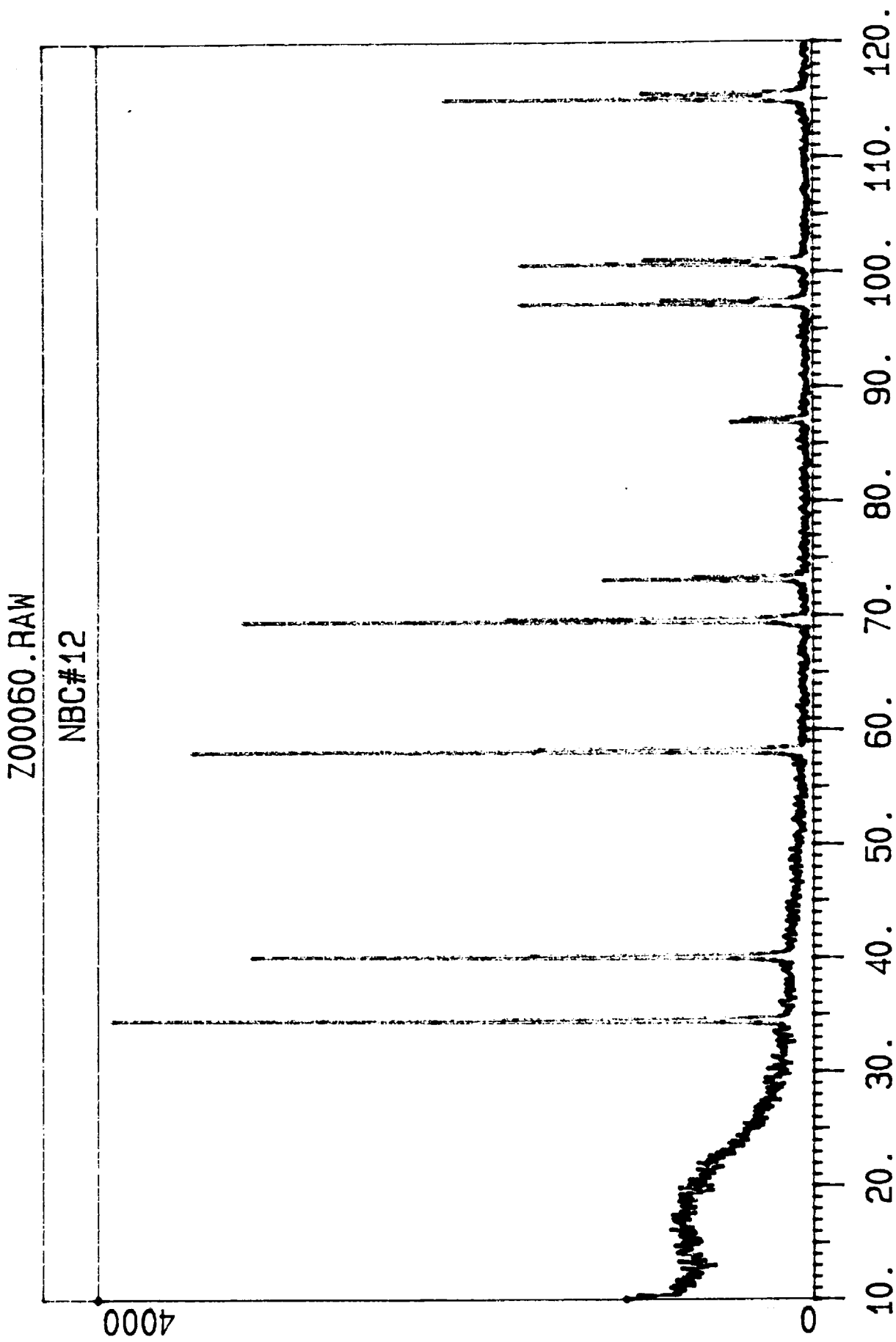
Z00060.RAW
NBC#12
4000
0
10.
20.
30.
40.
50.
60.
70.
80.
90.
100.
110.
120.

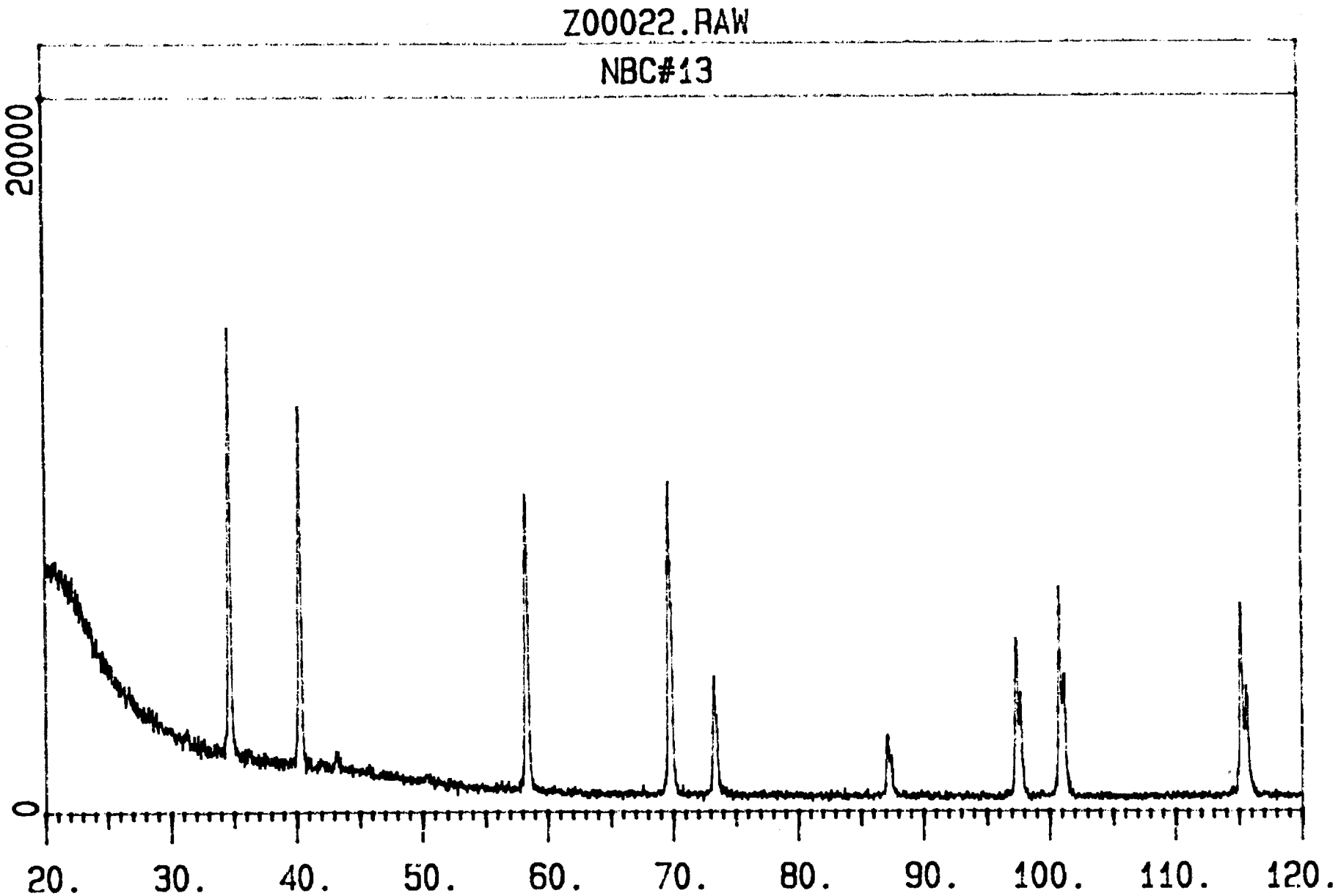
Z00022.RAW
NBC#13
20000
0
20.
30.
40.
50.
60.
70.
80.
90.
100.
110.
120.

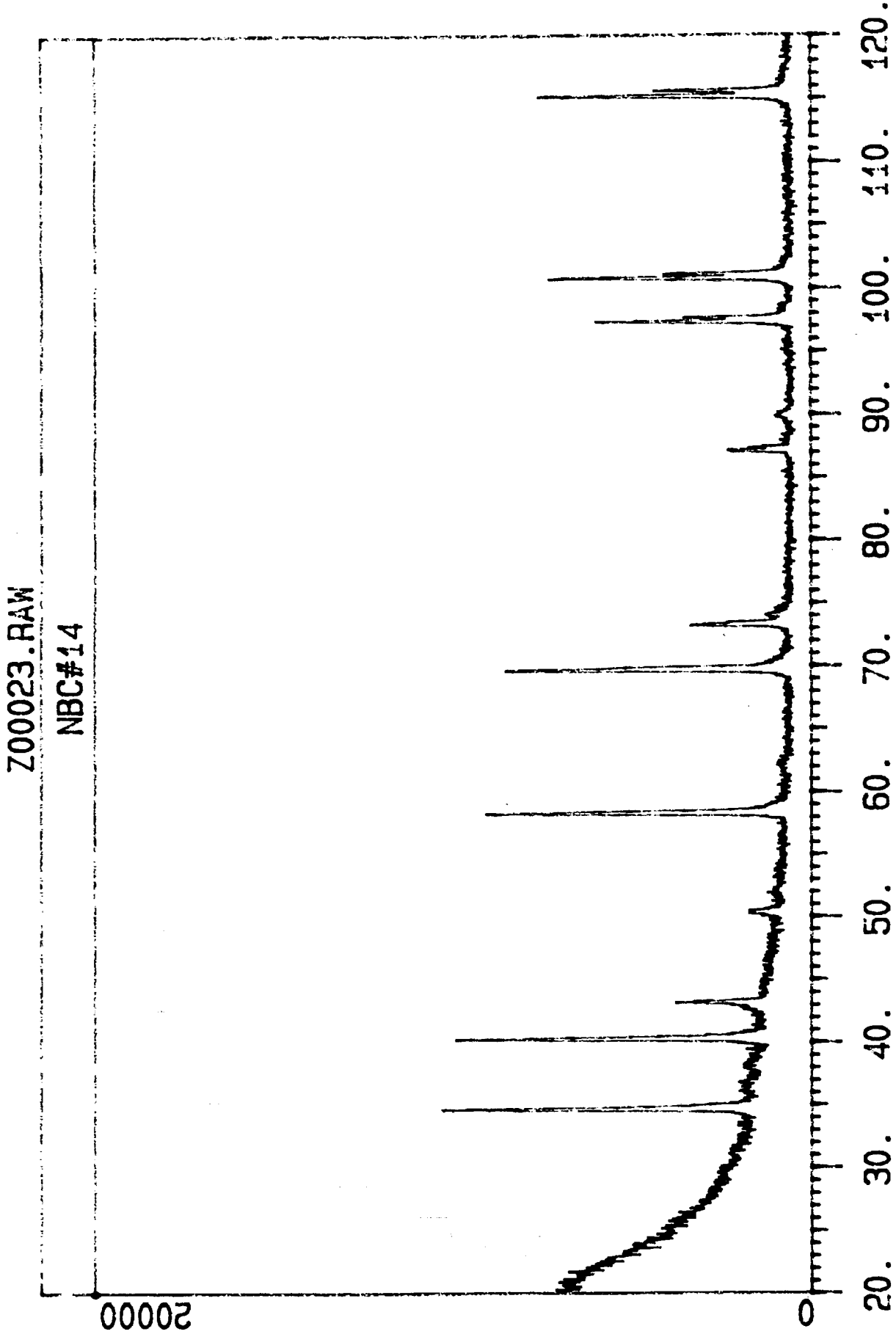
Z00023.RAW
NBC#14
20000
0
20.
30.
40.
50.
60.
70.
80.
90.
100.
110.
120.

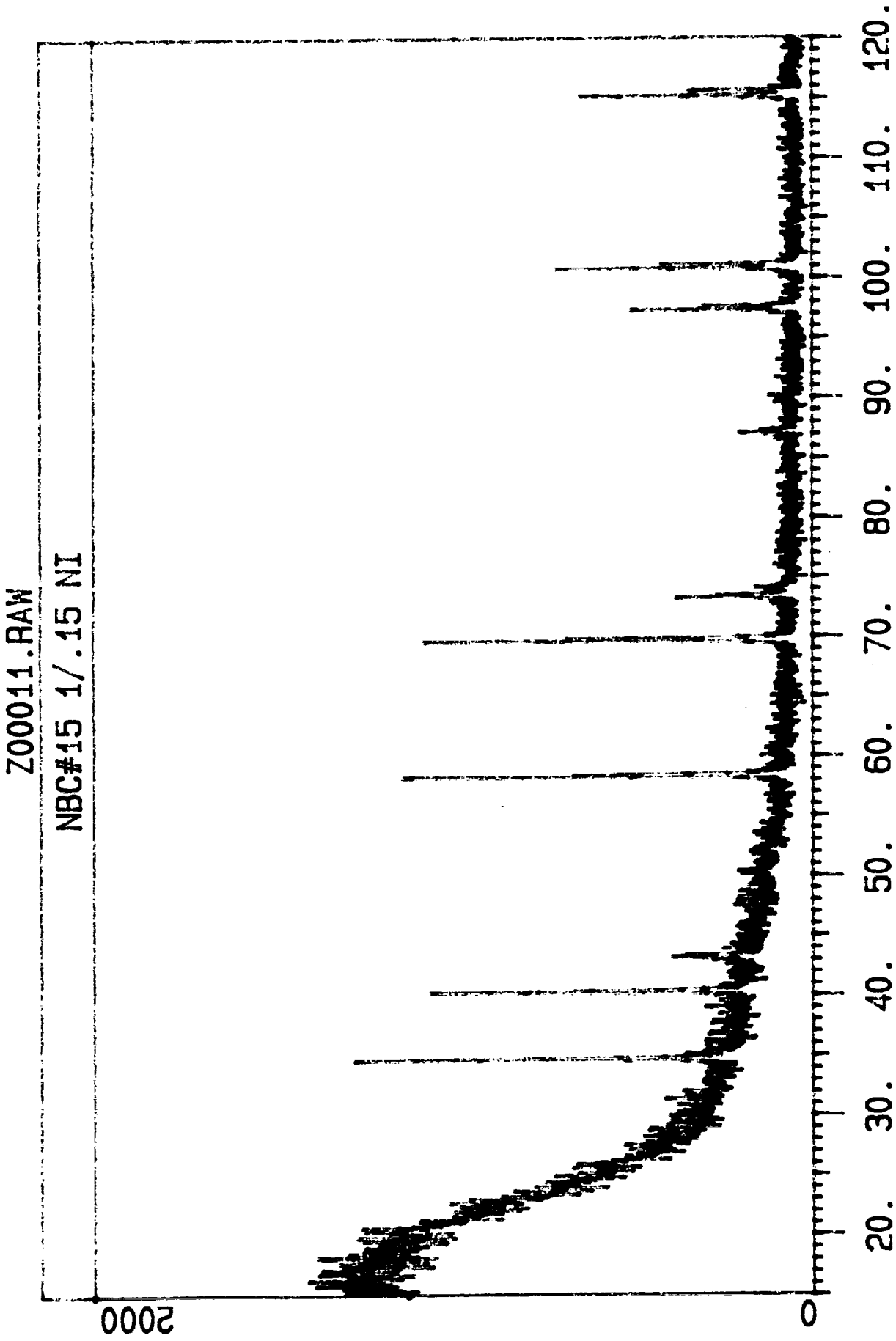
Z00011.RAW
NBC#15 1/.15 NI
2000
0
20.
30.
40.
50.
60.
70.
80.
90.
100.
110.
120.

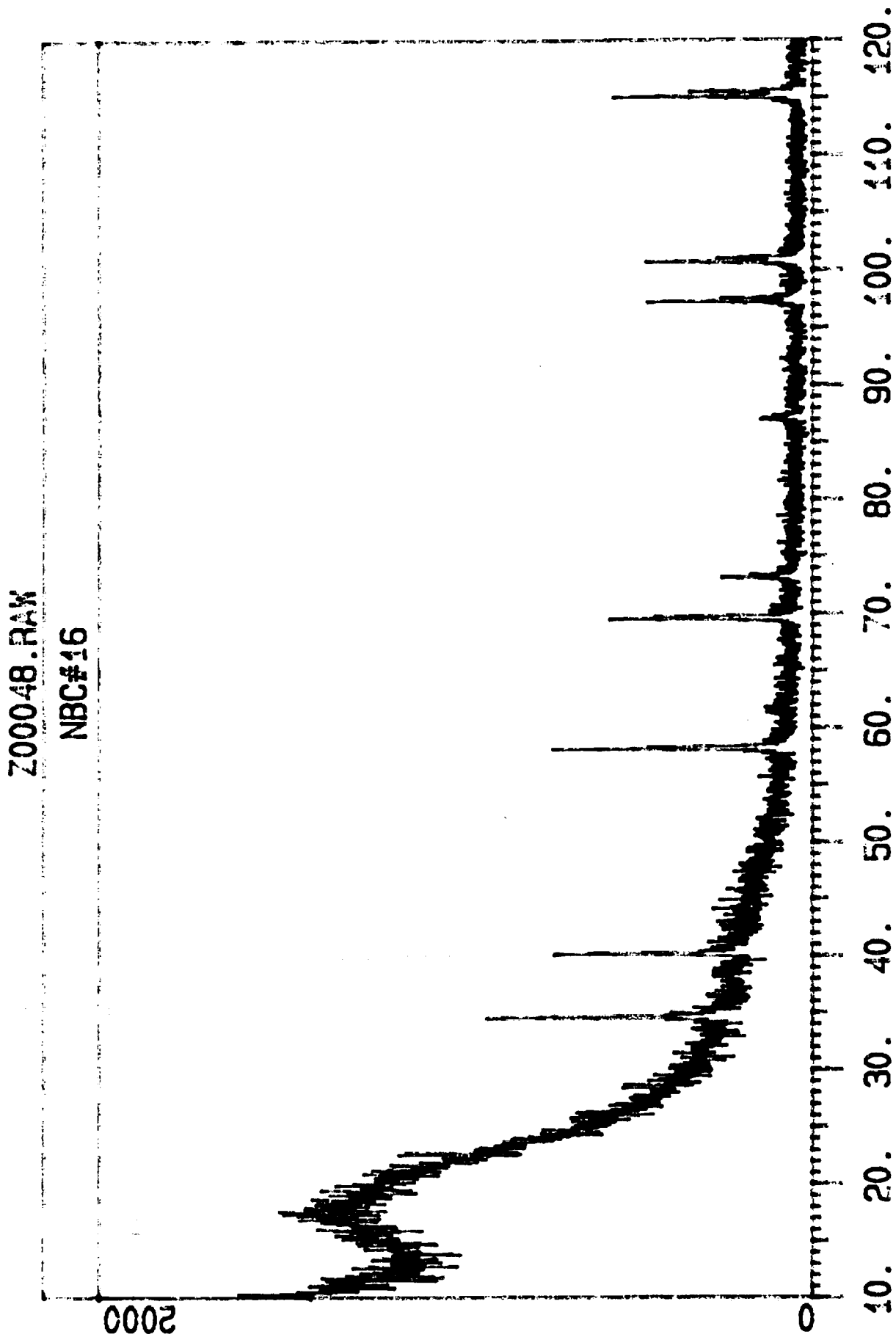
Z00048.RAW
NBC#16
2000
0
10.
20.
30.
40.
50.
60.
70.
80.
90.
100.
110.
120.

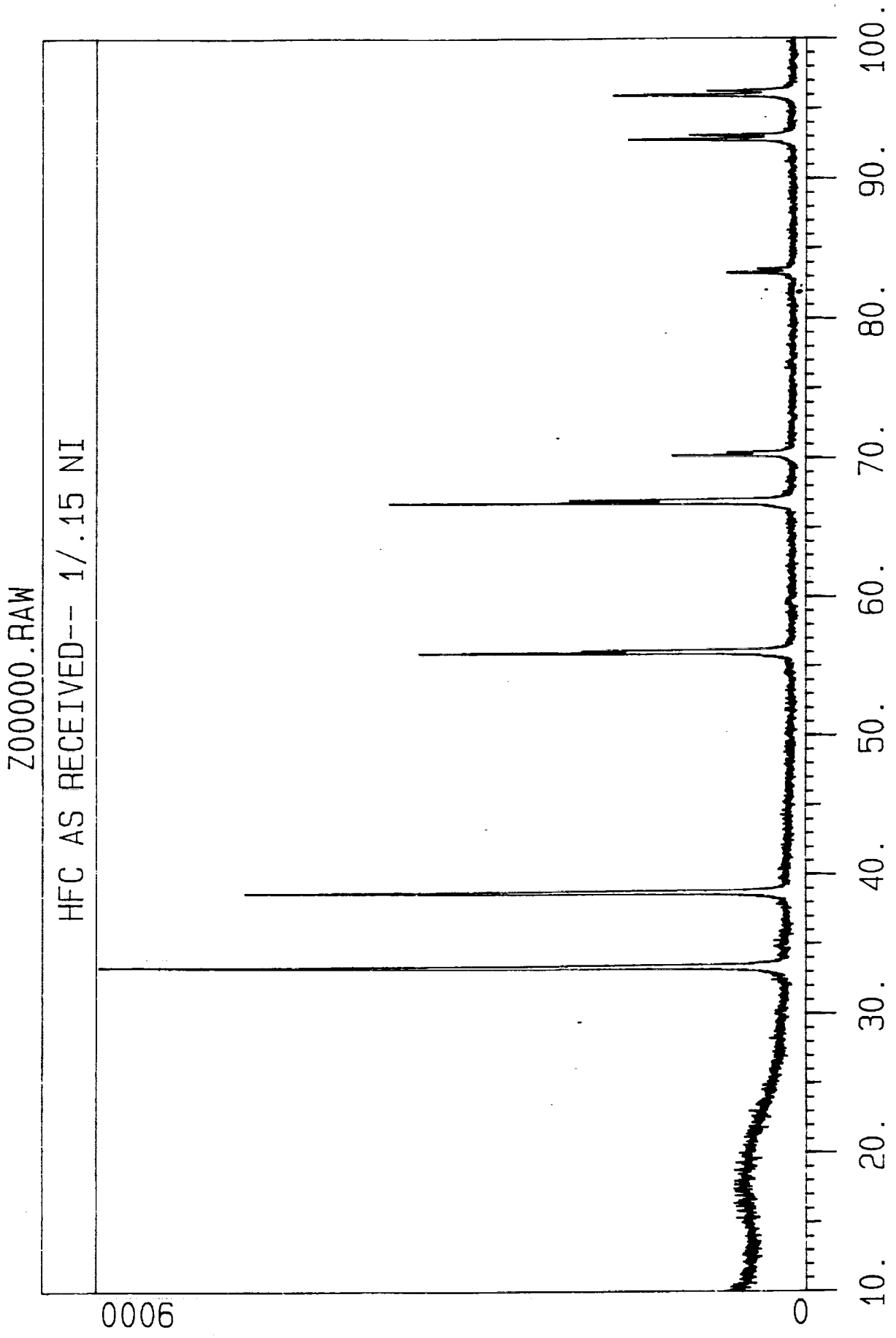
Z00000.RAW
HFC AS RECEIVED-- 1/.15 NI
0006
0
10.
20.
30.
40.
50.
60.
70.
80.
90.
100.

C-2

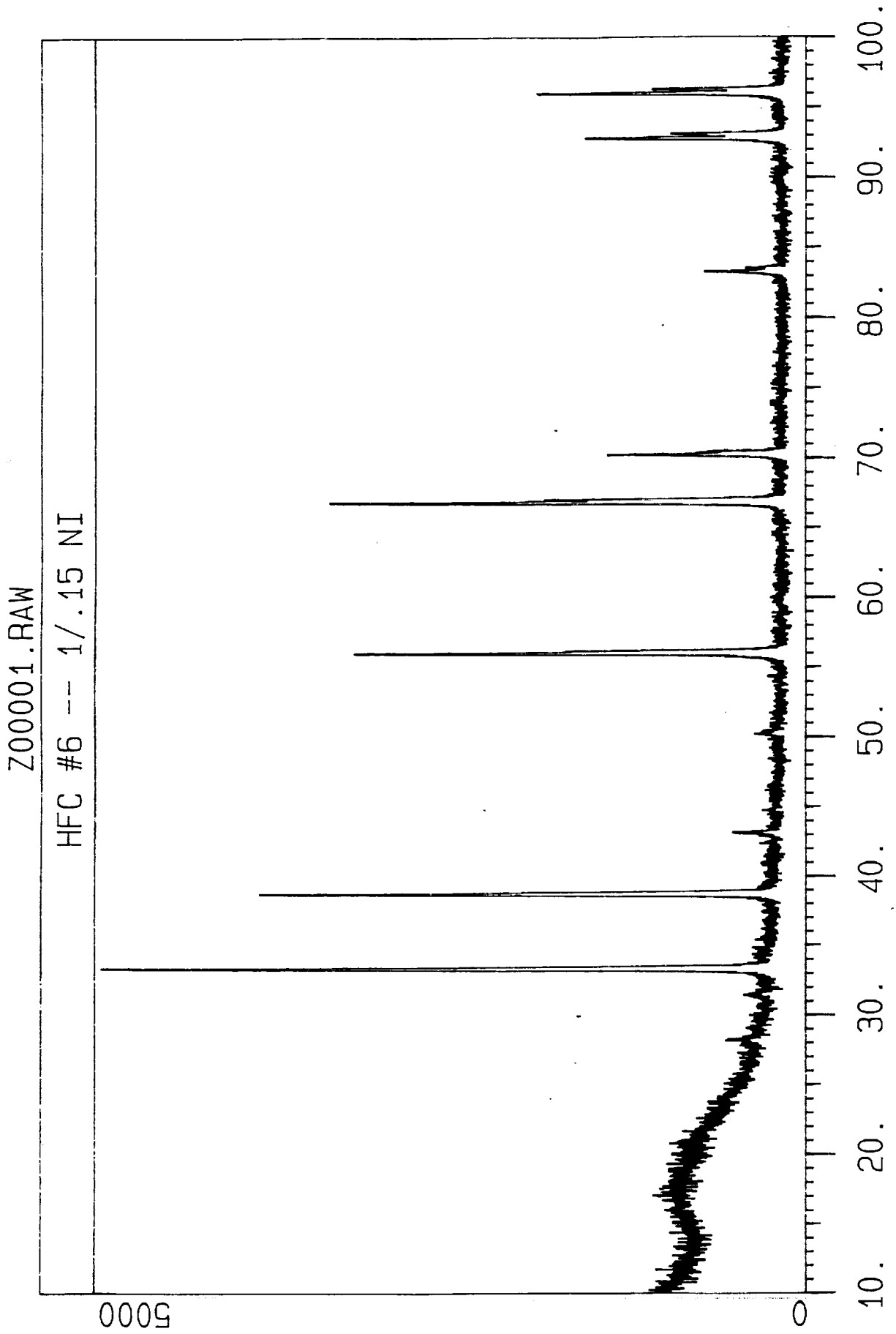
Z00001.RAW
HFC #6 -- 1/.15 NI
5000
0
10.
20.
30.
40.
50.
60.
70.
80.
90.
100.

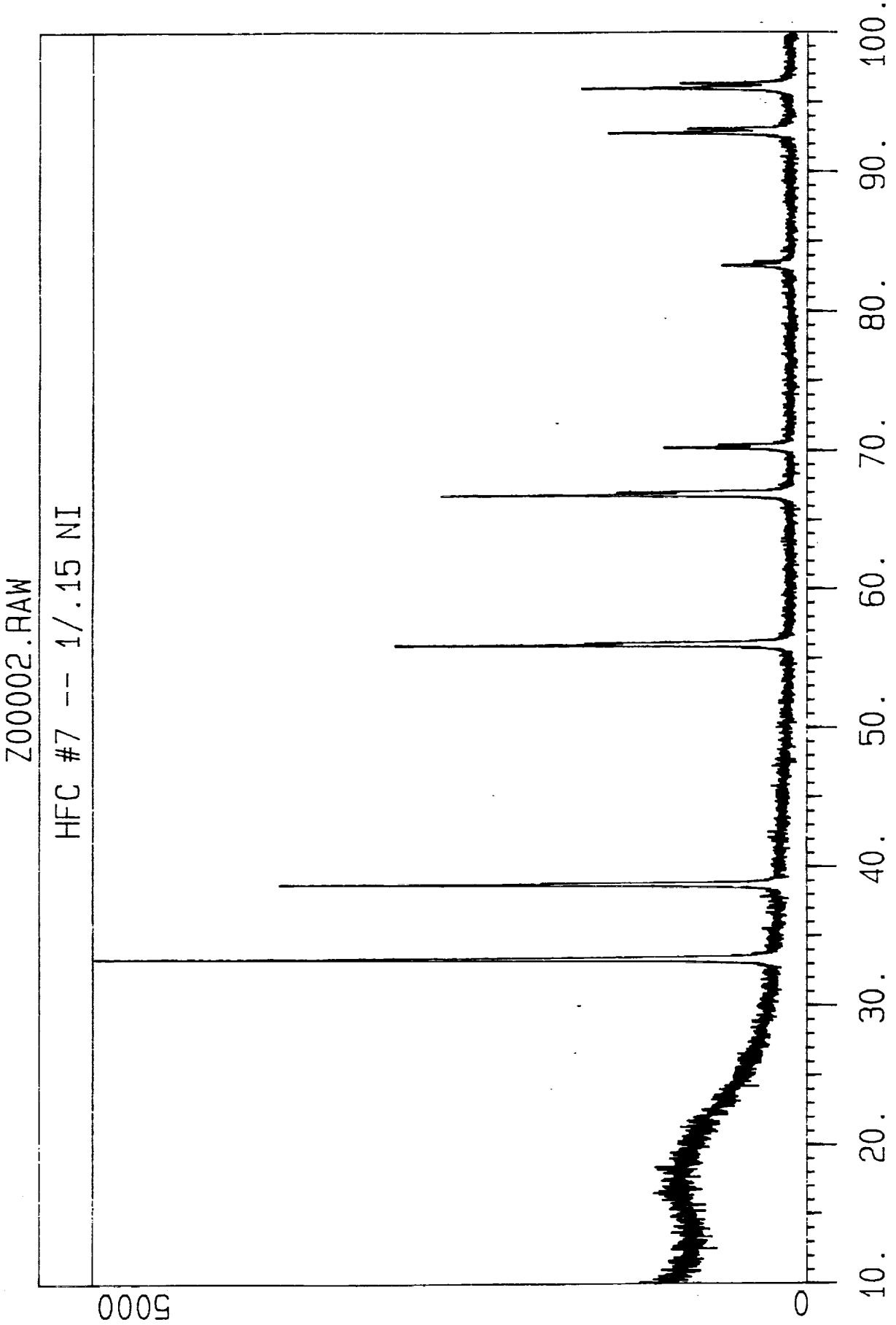
Z00002.RAW
HFC #7 -- 1/.15 NI
5000
0
10.
20.
30.
40.
50.
60.
70.
80.
90.
100.

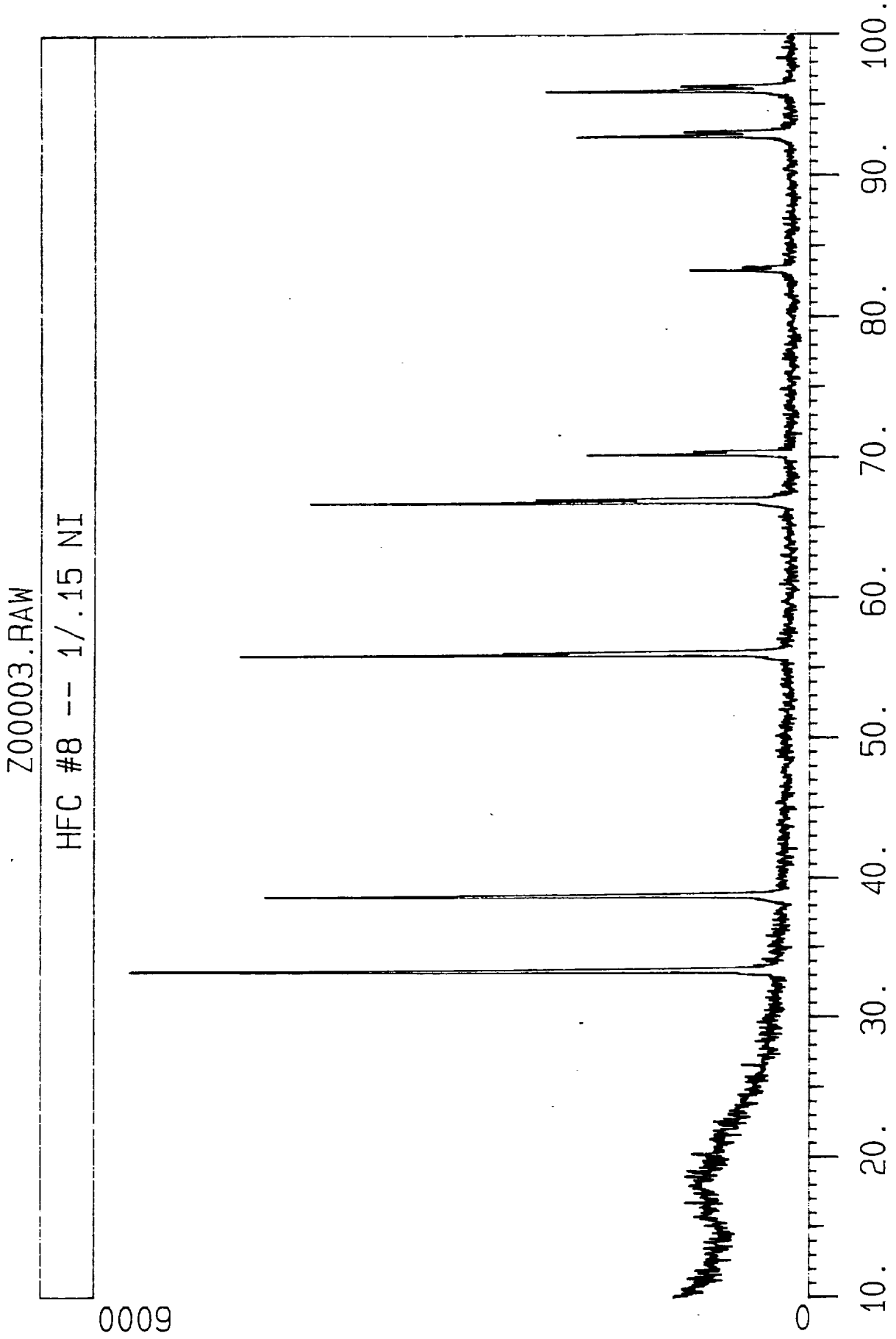
Z00003.RAW
HFC #8 -- 1/.15 NI
6000
0
10.
20.
30.
40.
50.
60.
70.
80.
90.
100.

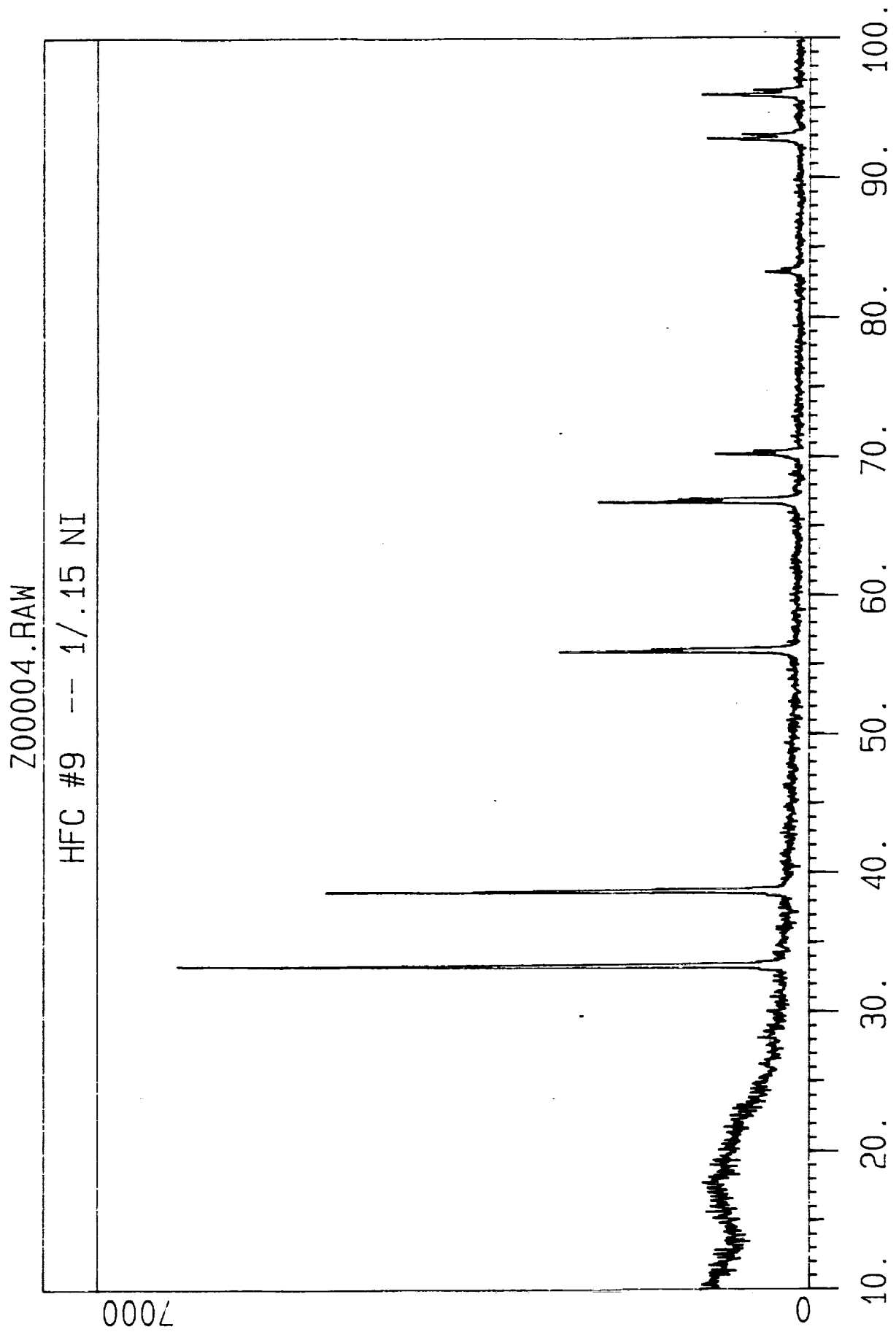
Z00004.RAW
HFC #9 -- 1/.15 NI
7000
0
10.
20.
30.
40.
50.
60.
70.
80.
90.
100.

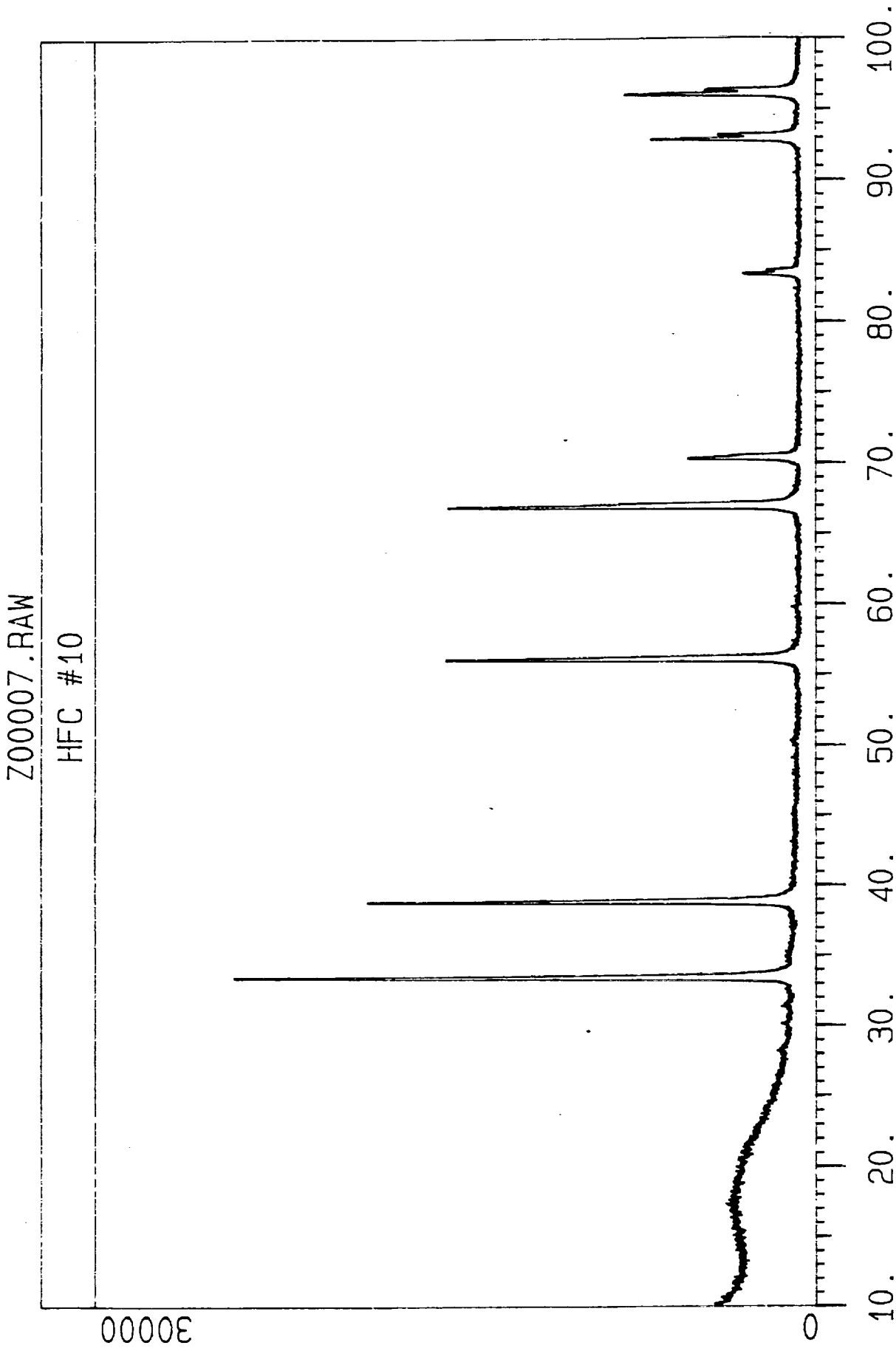
Z00007.RAW
HFC #10
30000
0
10.
20.
30.
40.
50.
60.
70.
80.
90.
100.

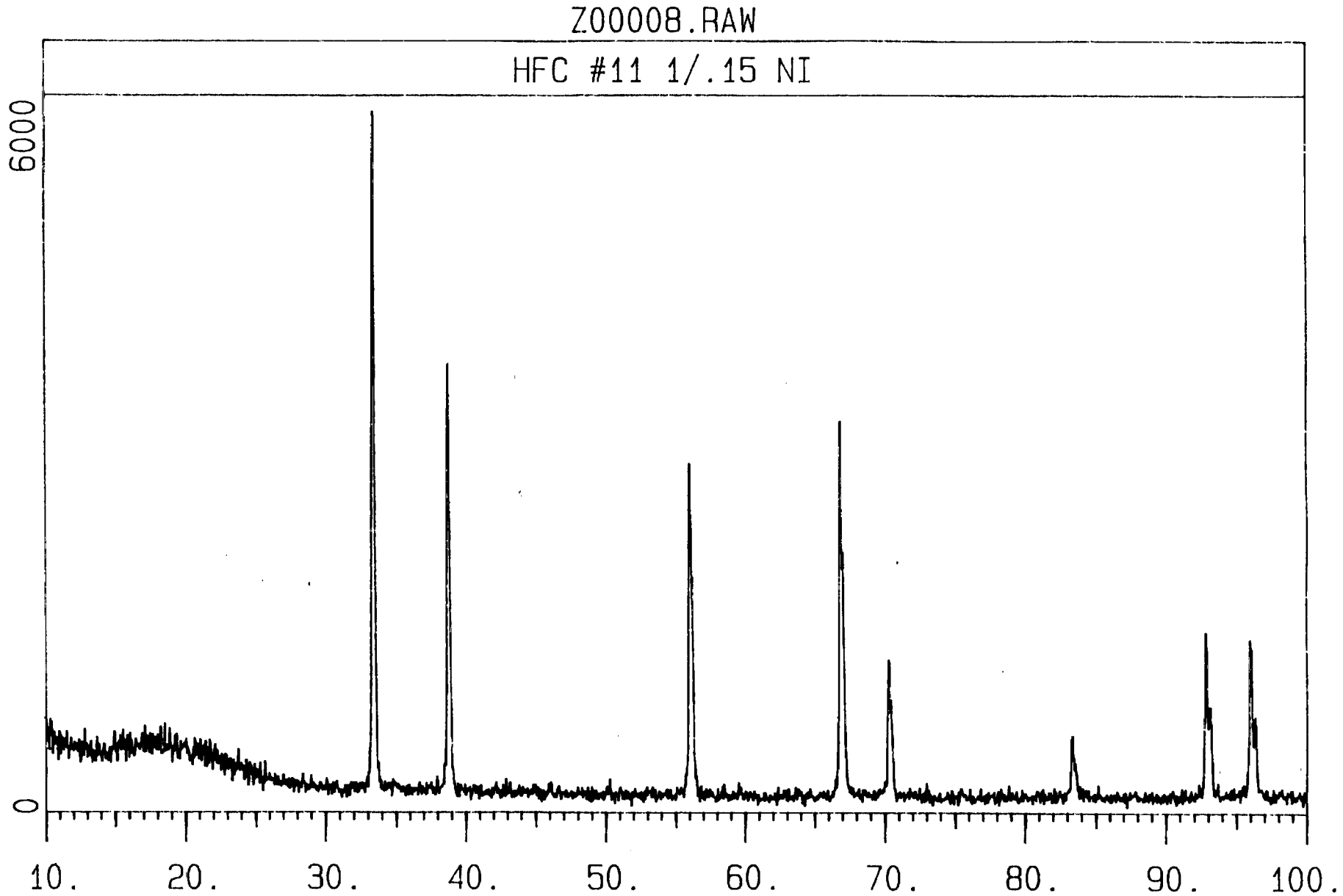
Z00008.RAW
HFC #11 1/.15 NI
6000
0
10.
20.
30.
40.
50.
60.
70.
80.
90.
100.

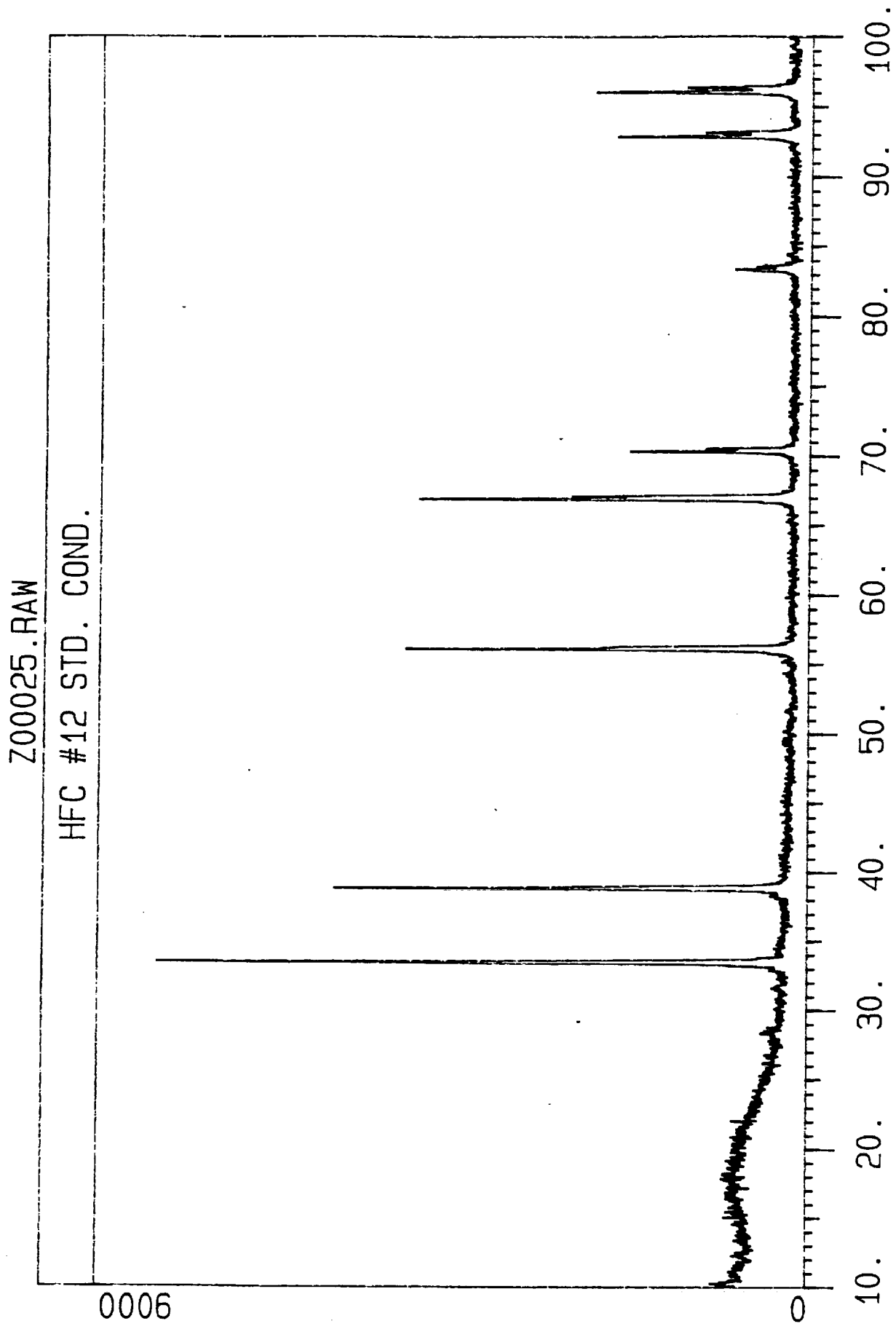
Z00025.RAW
HFC #12 STD. COND.
0006
0
10.
20.
30.
40.
50.
60.
70.
80.
90.
100.

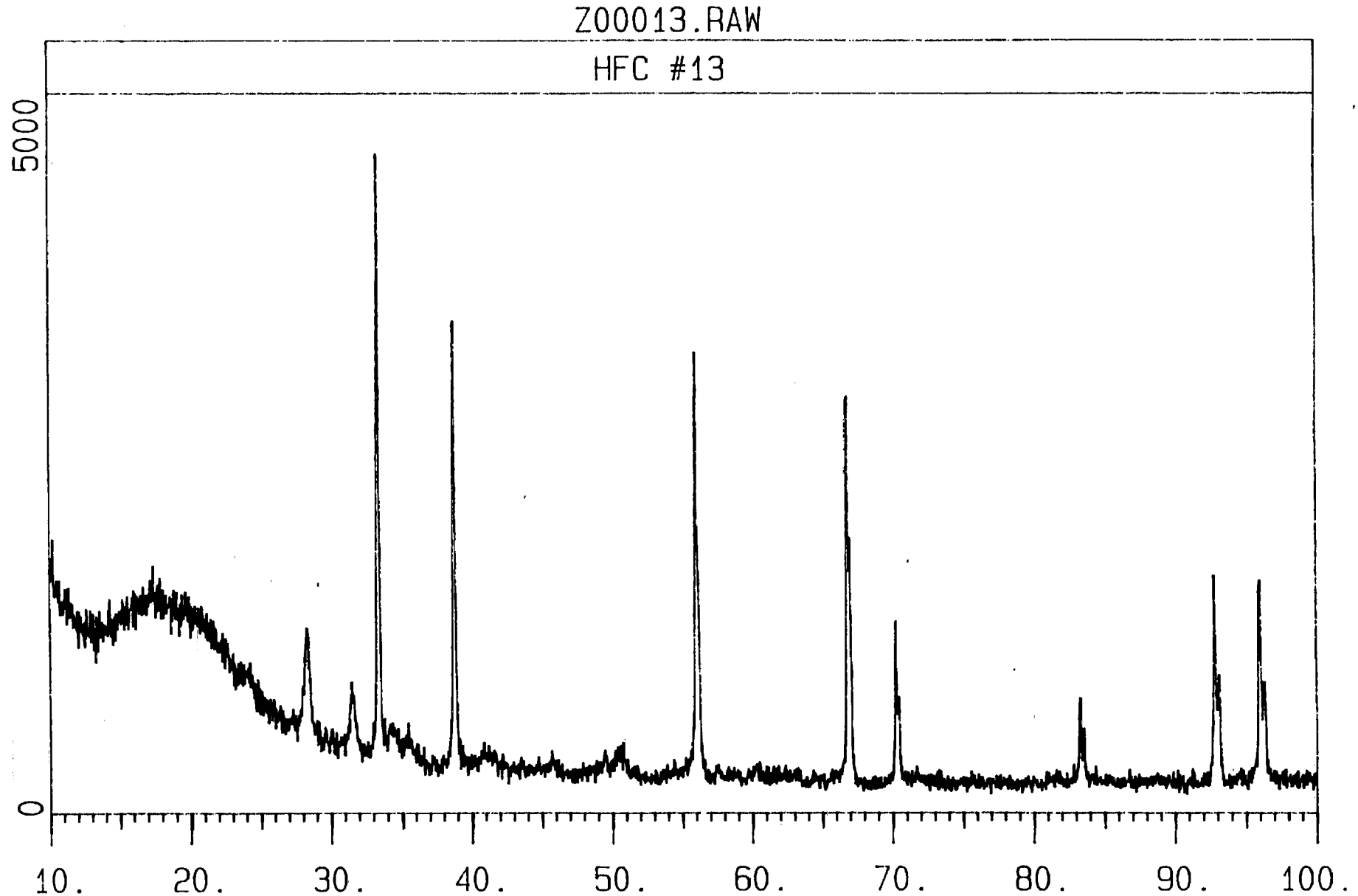
Z00013.RAW
HFC #13
5000
0
10.
20.
30.
40.
50.
60.
70.
80.
90.
100.

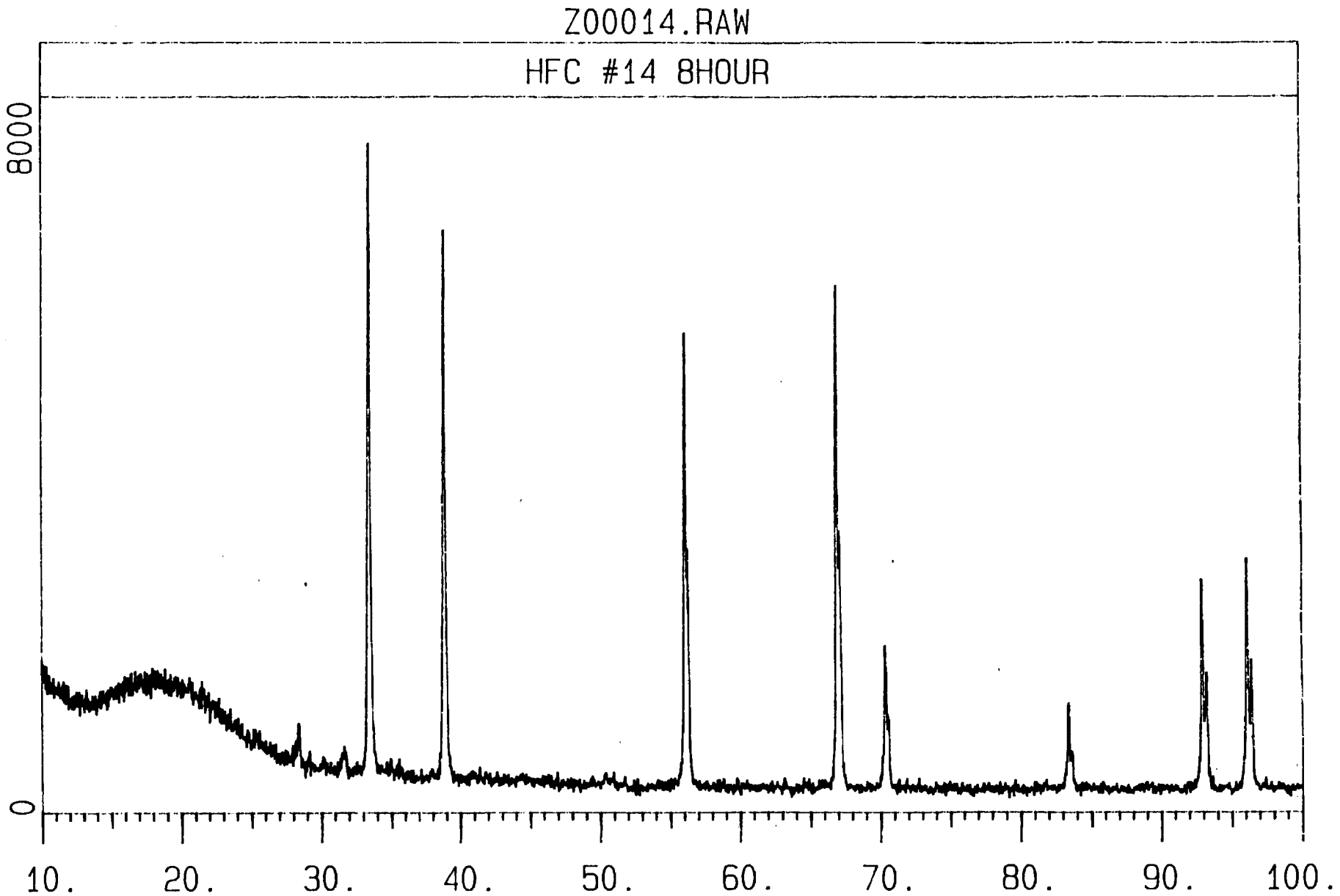
Z00014.RAW
HFC #14 8HOUR
8000
0
10.
20.
30.
40.
50.
60.
70.
80.
90.
100.

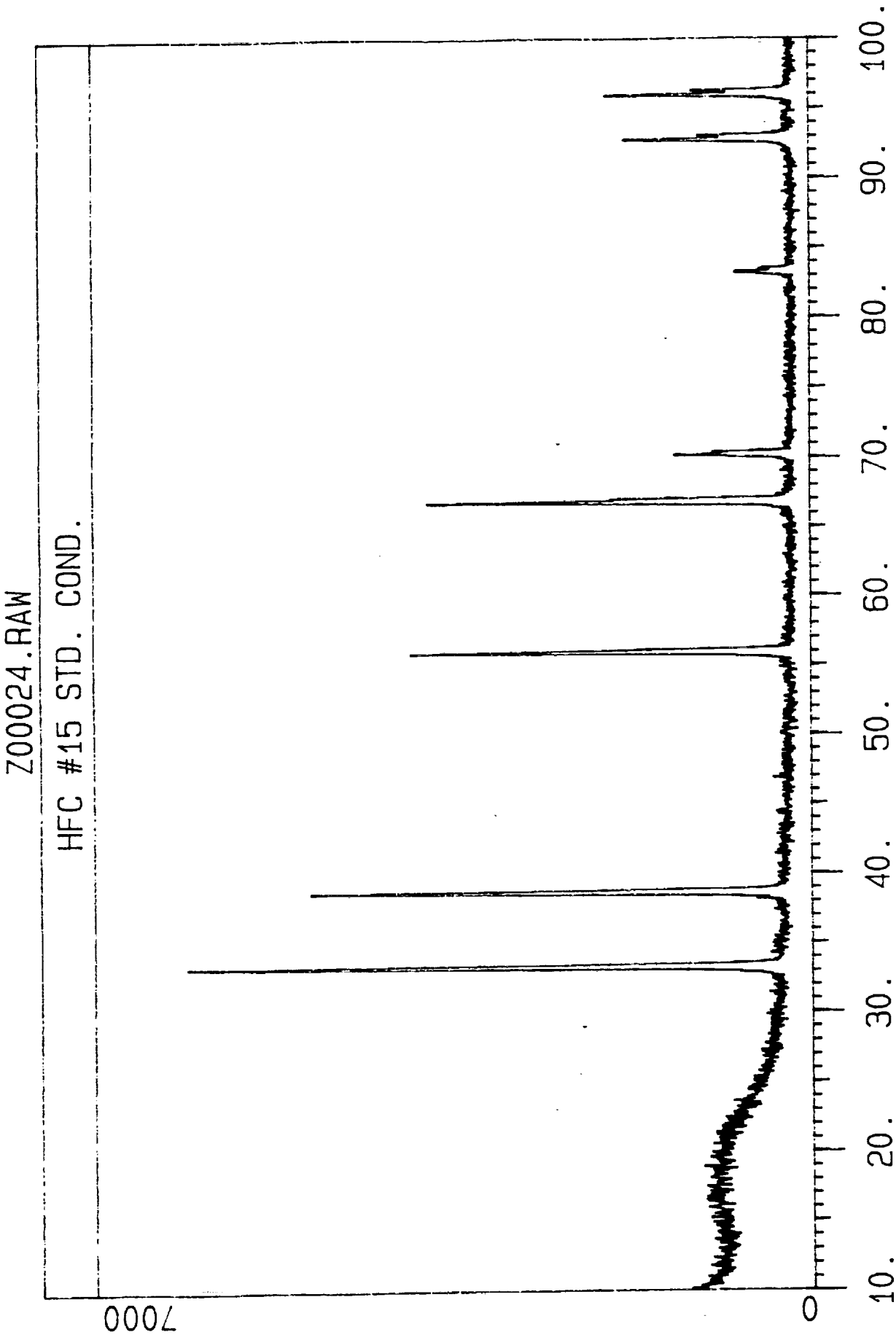
Z00024.RAW
HFC #15 STD. COND.
7000
0
10.
20.
30.
40.
50.
60.
70.
80.
90.
100.

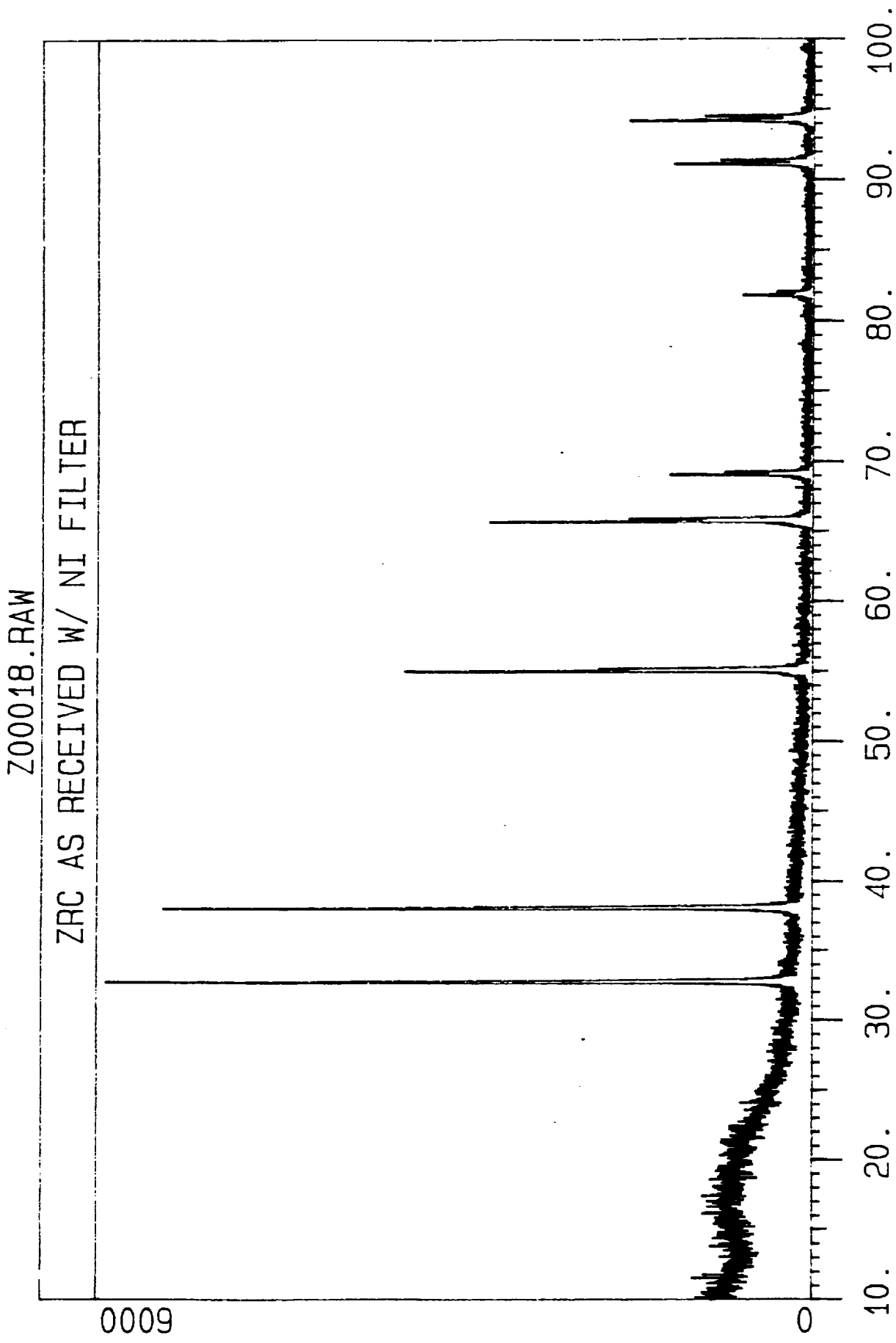
Z00018.RAW
ZRC AS RECEIVED W/ NI FILTER
6000
0
10.
20.
30.
40.
50.
60.
70.
80.
90.
100.

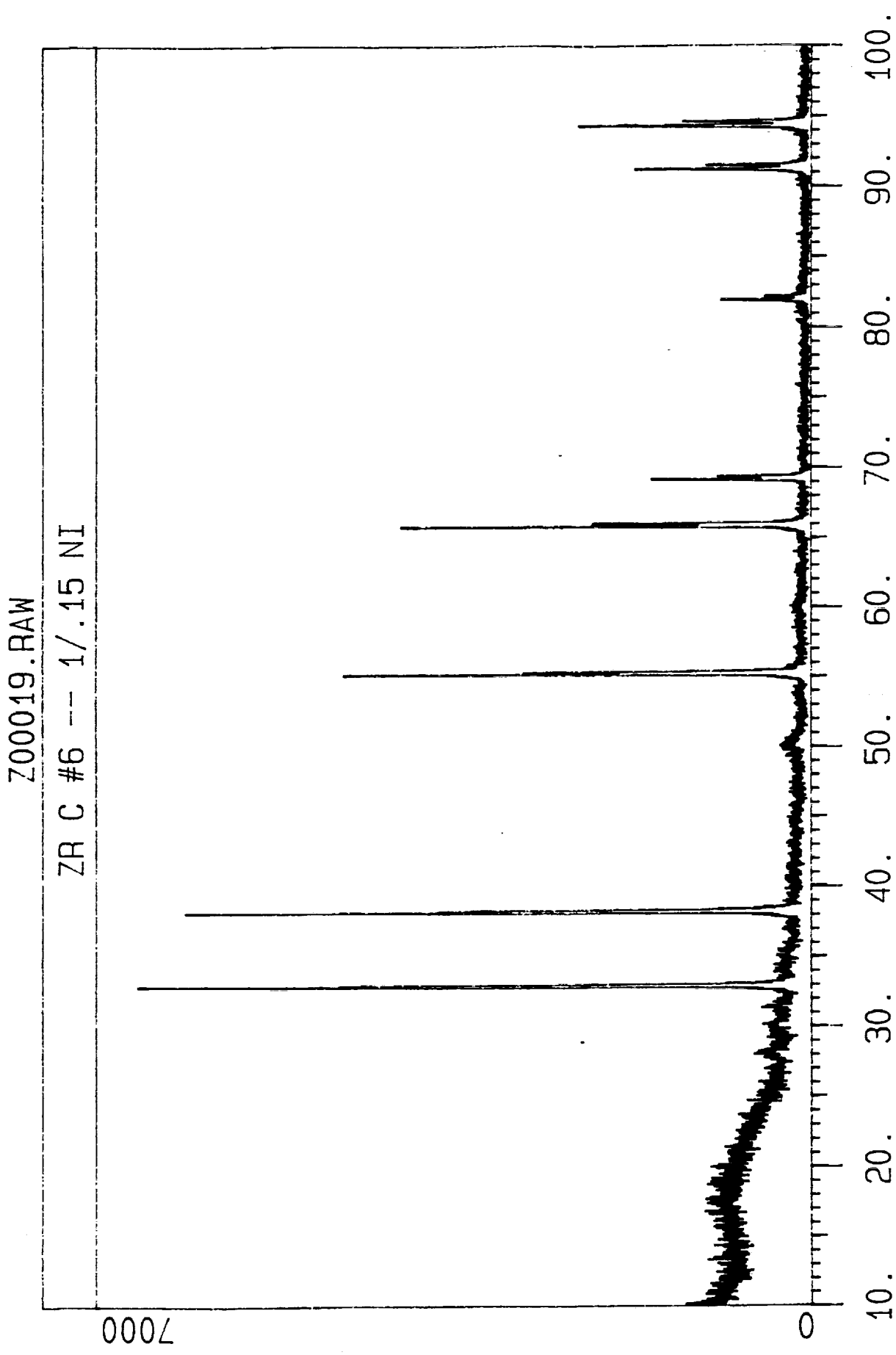
Z00019.RAW
ZR C #6 -- 1/.15 NI
7000
0
10.
20.
30.
40.
50.
60.
70.
80.
90.
100.

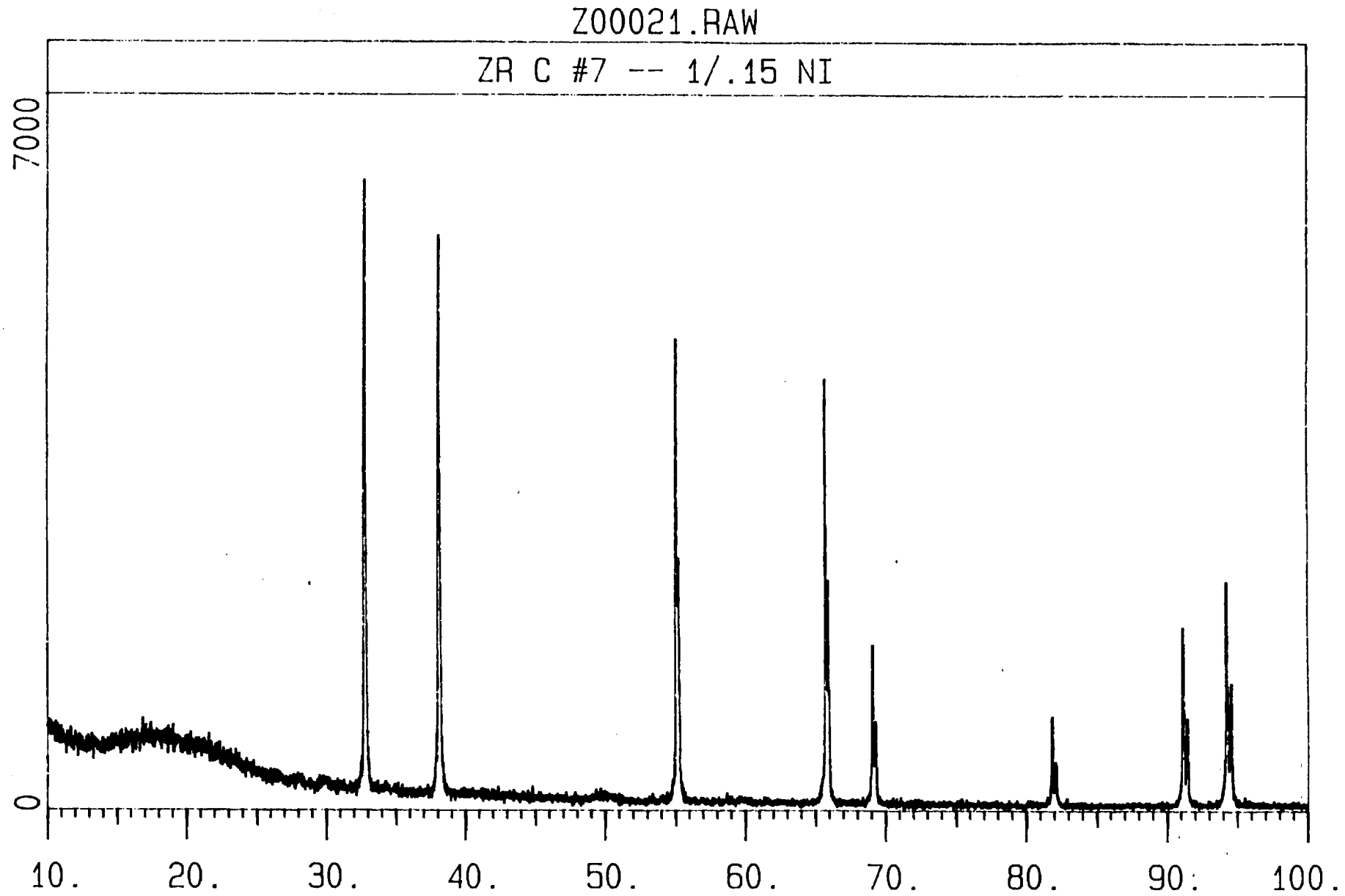
Z00021.RAW
ZR C #7 -- 1/.15 NI
7000
0
10.
20.
30.
40.
50.
60.
70.
80.
90.
100.

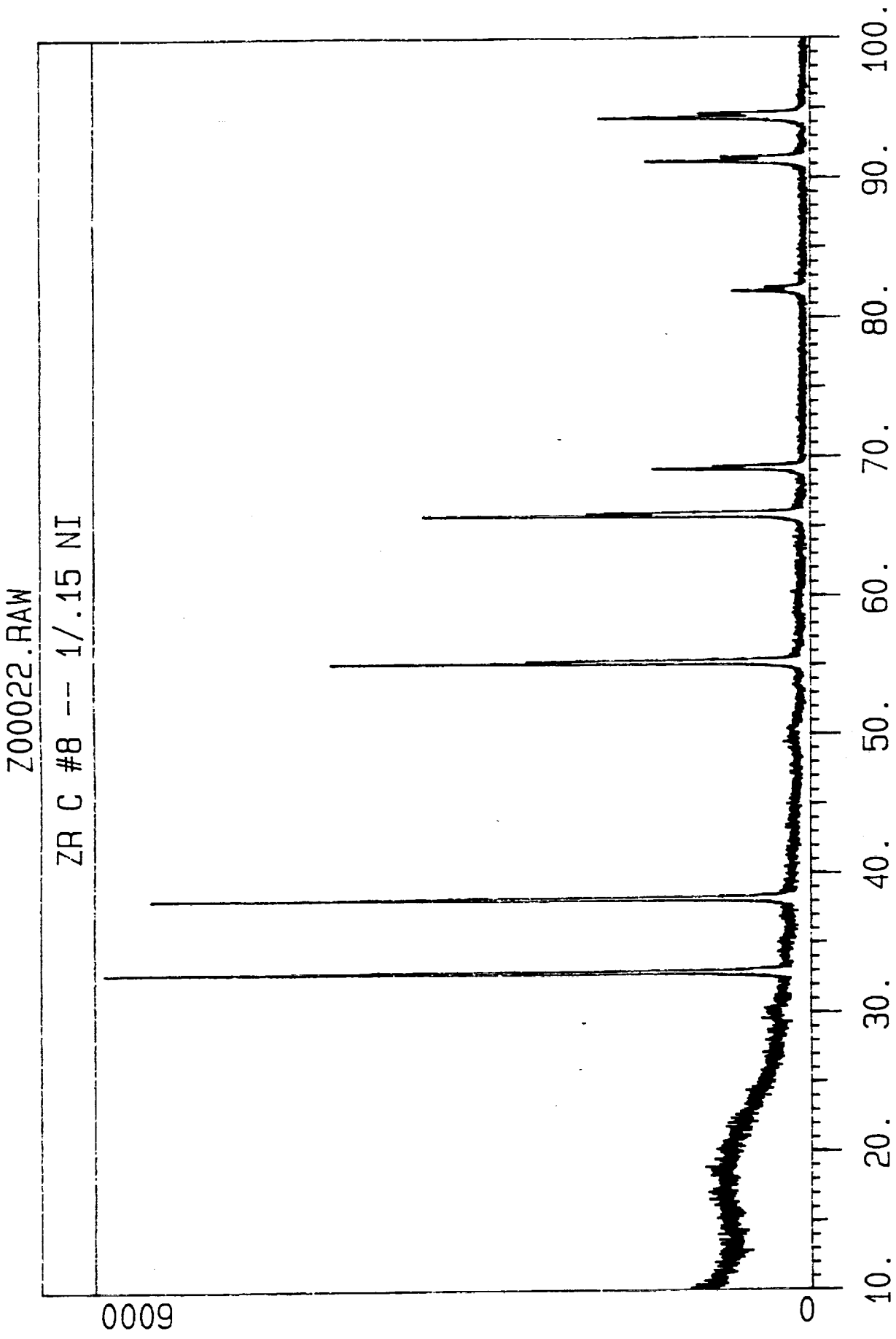
Z00022.RAW
ZR C #8 -- 1/.15 NI
6000
0
10.
20.
30.
40.
50.
60.
70.
80.
90.
100.

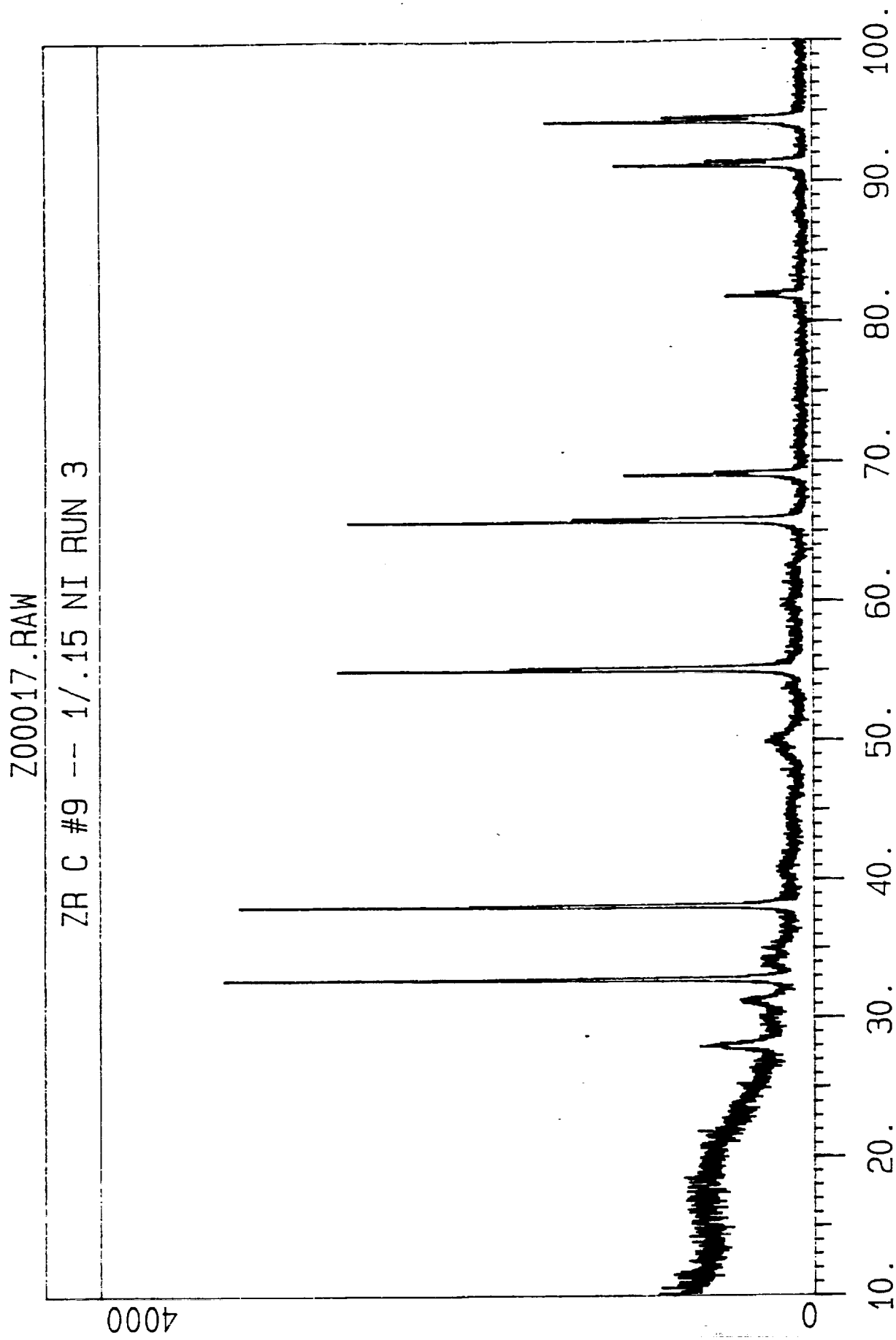
Z00017.RAW
ZR C #9 -- 1/.15 NI RUN 3
4000
0
10.
20.
30.
40.
50.
60.
70.
80.
90.
100.

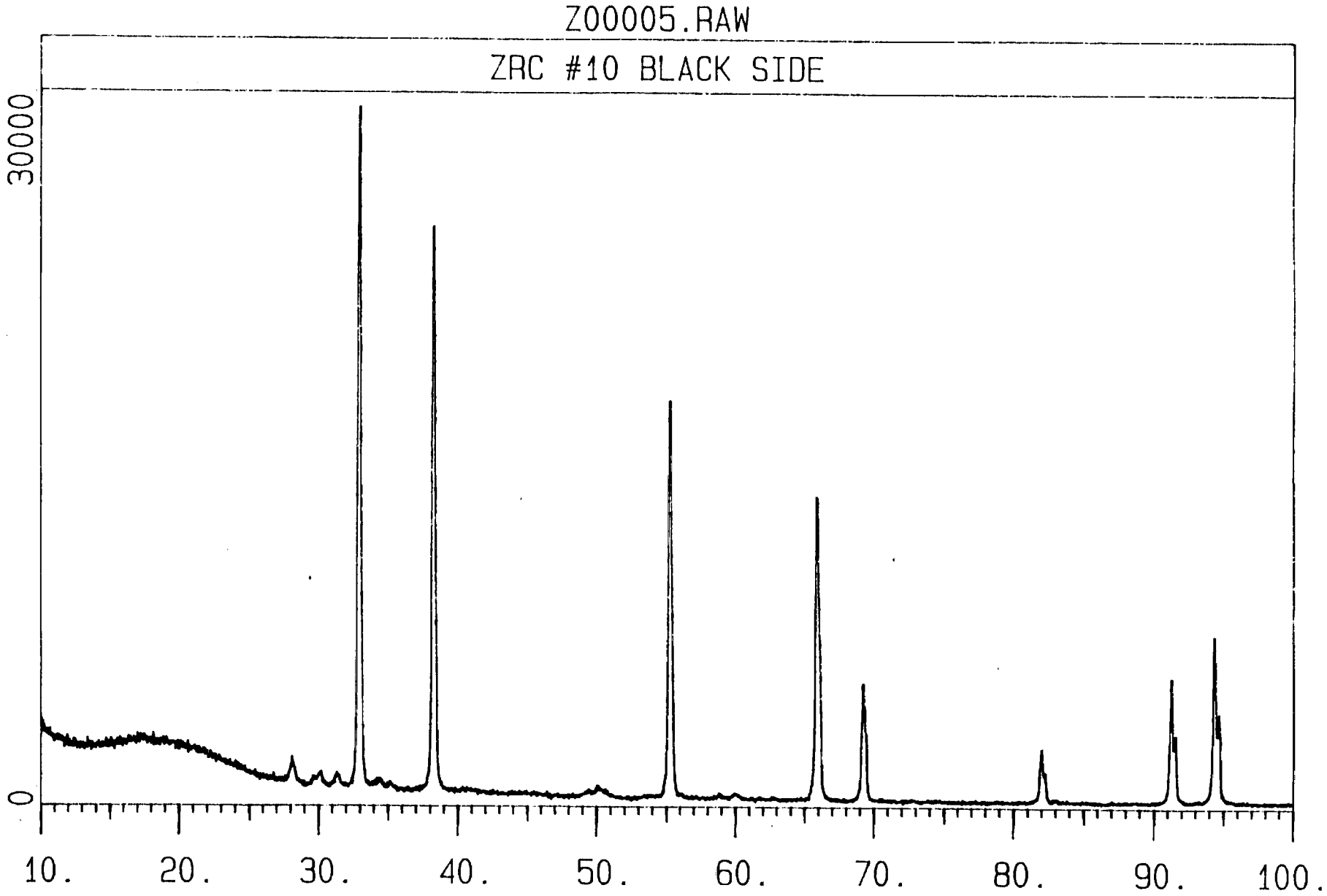
Z00005.RAW
ZRC #10 BLACK SIDE
30000
0
10.
20.
30.
40.
50.
60.
70.
80.
90.
100.

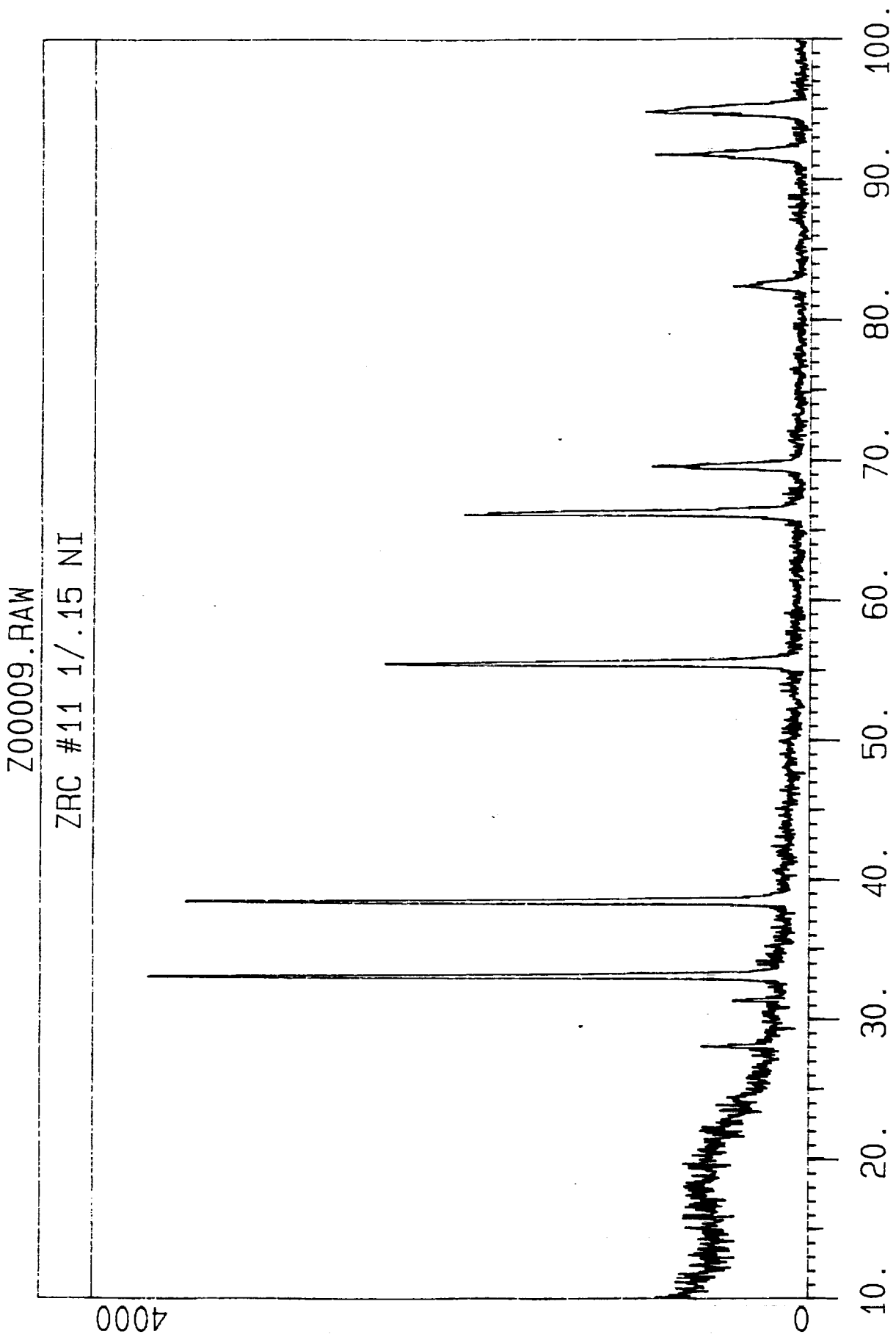
Z00009.RAW
ZRC #11 1/.15 NI
4000
0
10.
20.
30.
40.
50.
60.
70.
80.
90.
100.

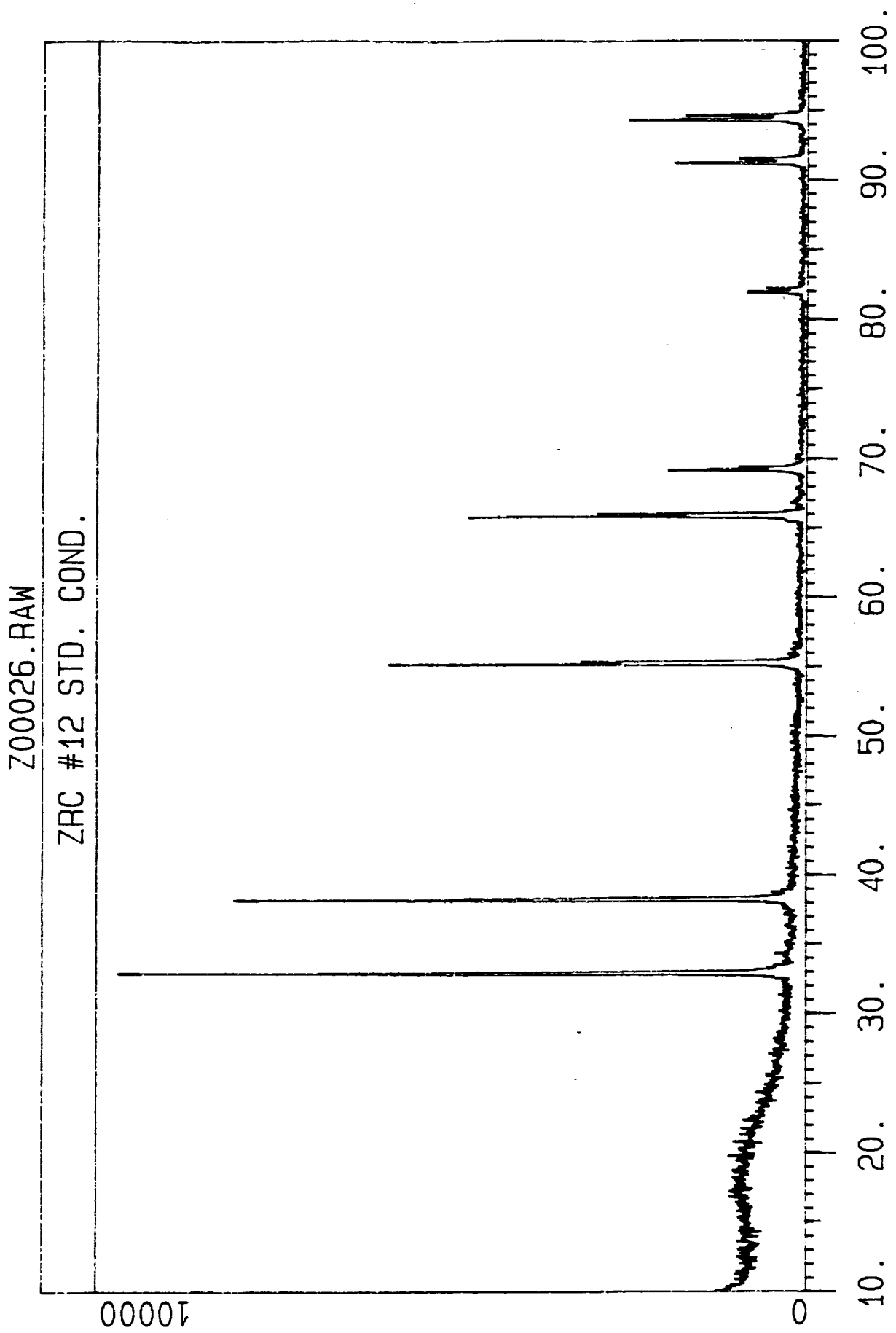
Z00026.RAW
ZRC #12 STD. COND.
10000
0
10.
20.
30.
40.
50.
60.
70.
80.
90.
100.

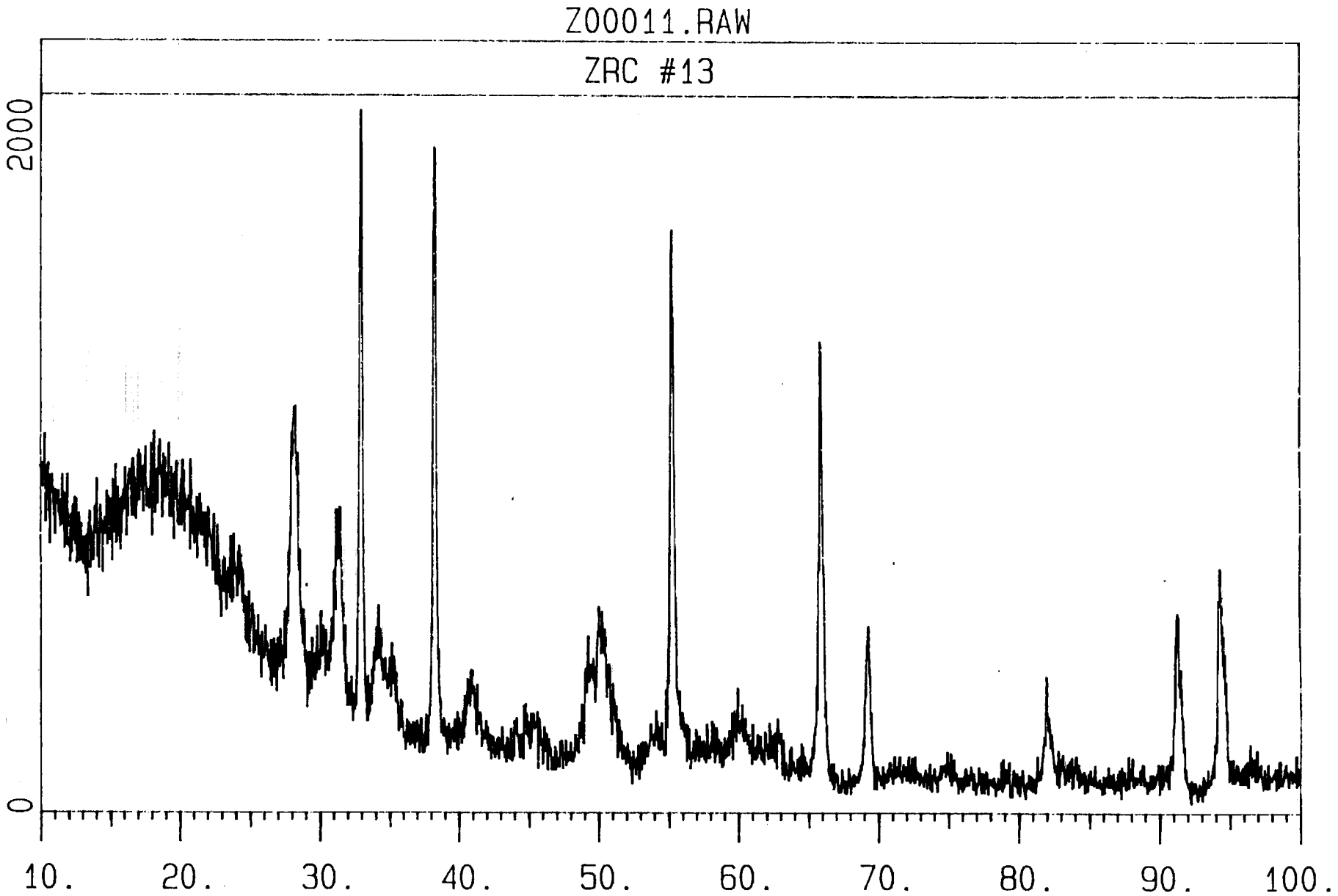
Z00011.RAW
ZRC #13
2000
0
10.
20.
30.
40.
50.
60.
70.
80.
90.
100.

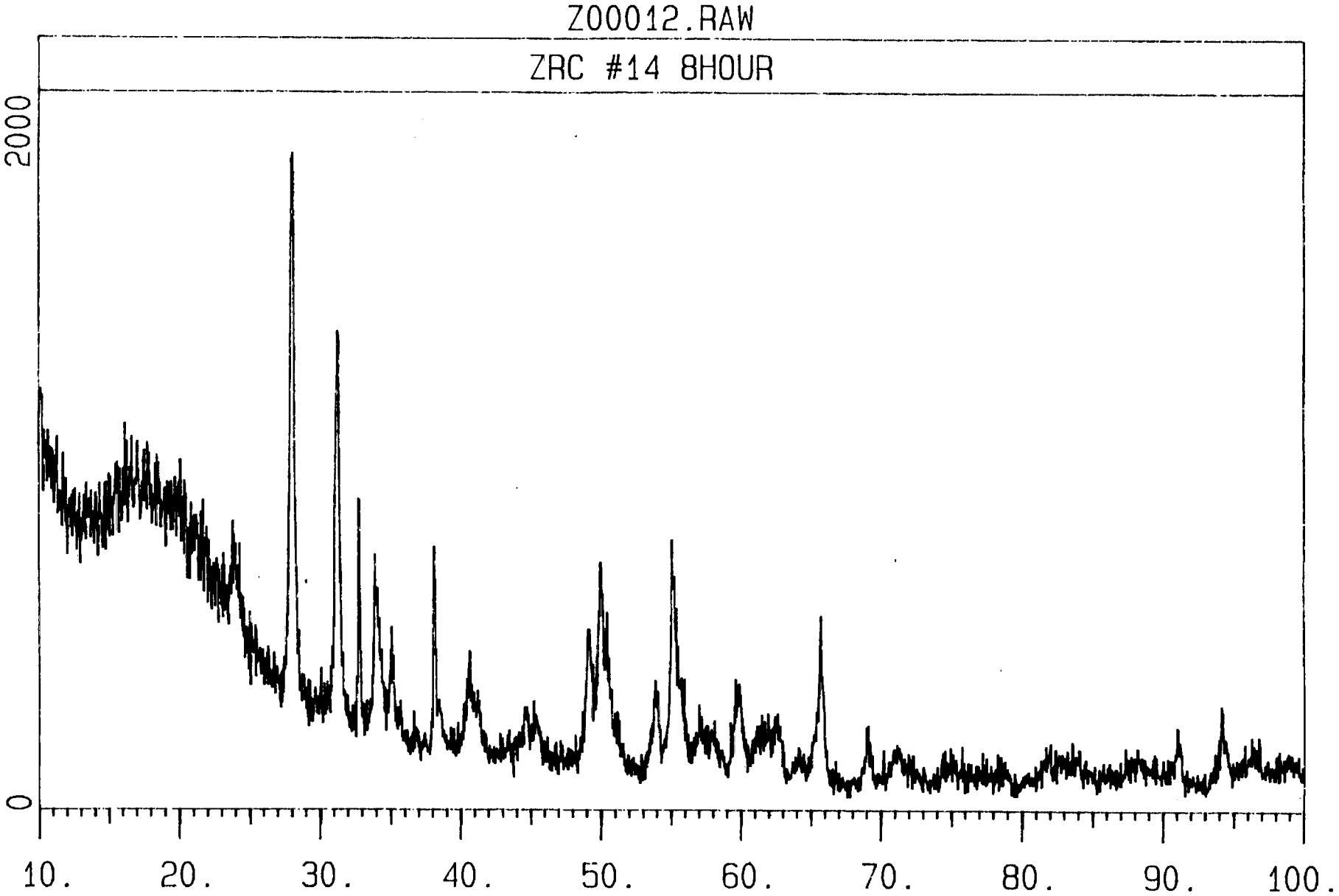
Z00012.RAW
ZRC #14 8HOUR
2000
0
10.
20.
30.
40.
50.
60.
70.
80.
90.
100.

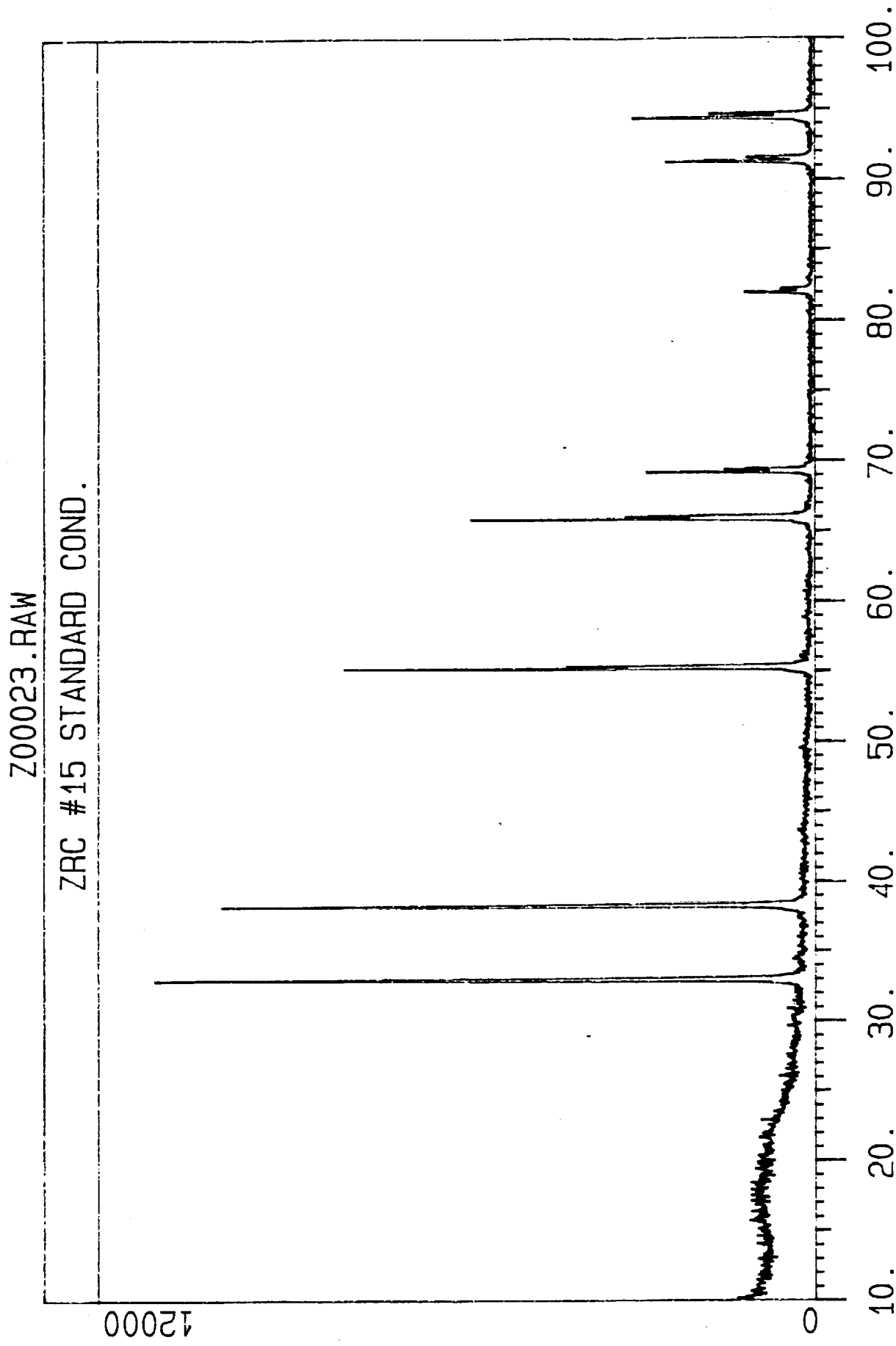
Z00023.RAW
ZRC #15 STANDARD COND.
12000
0
10.
20.
30.
40.
50.
60.
70.
80.
90.
100.

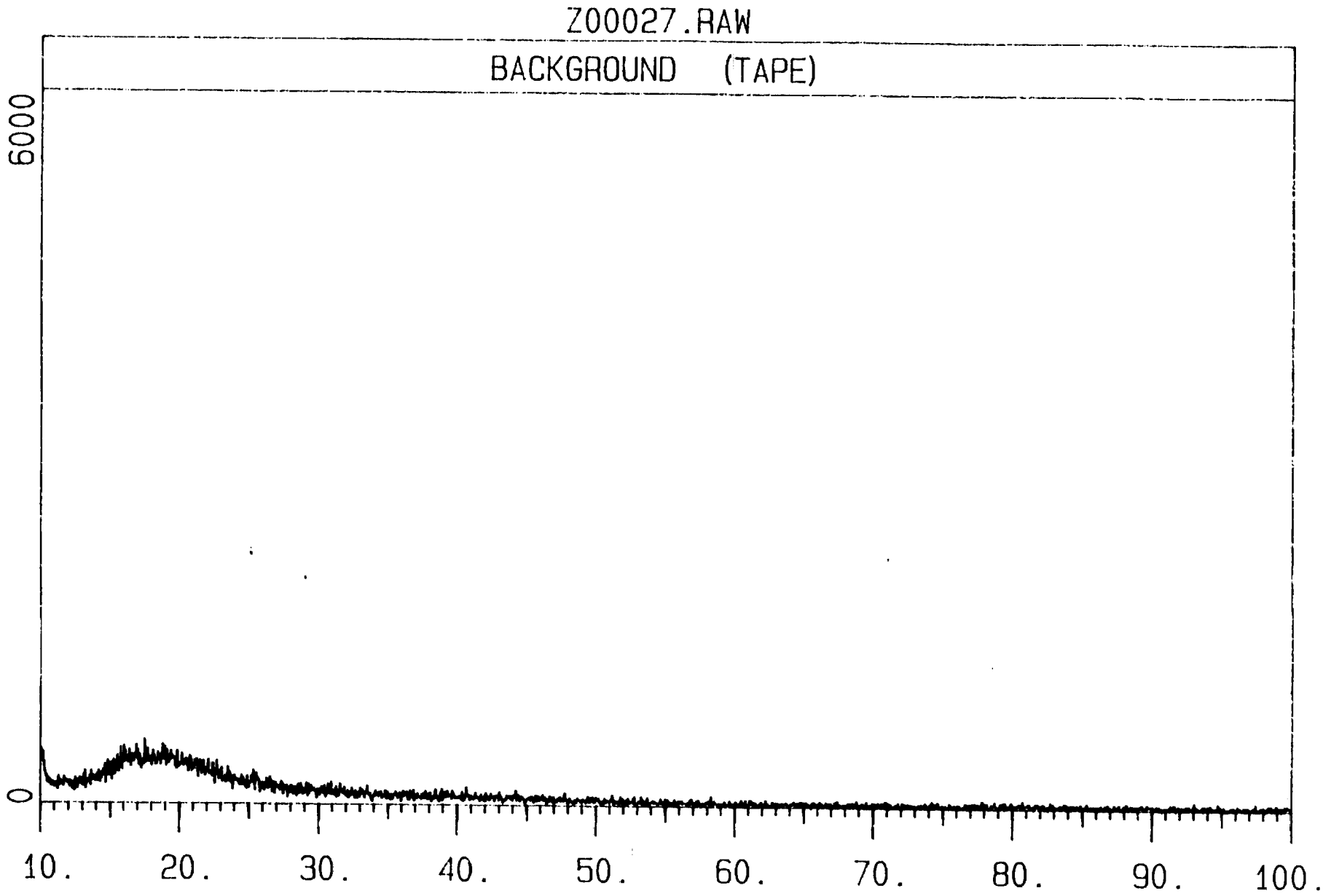
Z00027.RAW
BACKGROUND (TAPE)
6000
0
10.
20.
30.
40.
50.
60.
70.
80.
90.
100.

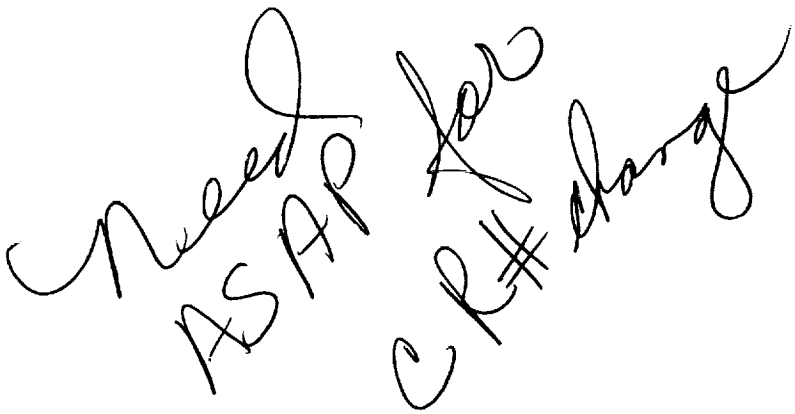

SCREEN IMAGE USER=*TTM SESSION=TF1BL37 6/21/93-11:22:05-AM

QUALITY CONTROL

FID:	1N	TMP:	164781	ISS:	0	AGY:	NASA	QNM:	ABST	ACT:	KCG
CRT:	N	NSF:	Y	HUR:	OK	AQT:	REG	SNM:		EIN:	PNF
RPA:	Y	FST:	MAR	ACR:		FOI:	HC	LNG:	EN	CIN:	KCG
MUR:	OK	PDT:	19930223	LCA:		DCL:	TRP	CAT:	26	DIN:	
MCP:	G	PAG:	119	FRR:		DSC:	NC	CSC:		KIN:	
MCS:	3	DCF:		RVD:	0	TSC:	NC	ALI:	N	AIN:	
				SCC:						QIN:	

COR: US UNITED STATES
CFS: US UNITED STATES

SAP: Avail: CASI HC(en1) A06/MF(en1) A02

1) SRC: a8528793 - Auburn Univ., AL.
CSS: Materials Engineering Program.

UTL: Hot hydrogen testing of refractory materials and c
eramics
TLS: Final Report, 24 Feb. 1992 - 23 Feb. 1993

1) AUT: Zee, Ralph
2) AUT: Chin, Bryan
3) AUT: Cohron, Jon

RPN: NASA-CR-193080
NAS 1.26: 193080
CNT: C\NAS8-39131

OCC: 0_ MNM: ___ DATA: _____

(PF2=RESET; PF3=SIGNON; PF4=RELEASE; PF5=SELECTION; PF6=SUBQUEUE)
(PF14=PRIOR PAGE; PF15=NEXT PAGE; PF19=MODIFY; PF22=ABSTRACT/WORDS NOT FOUND)
(PF23=ANALYTIC NOTE; PF24=RECORD CERTIFICATION)